



EXPLANATORY NOTES

**Department of
Industry and Resources**

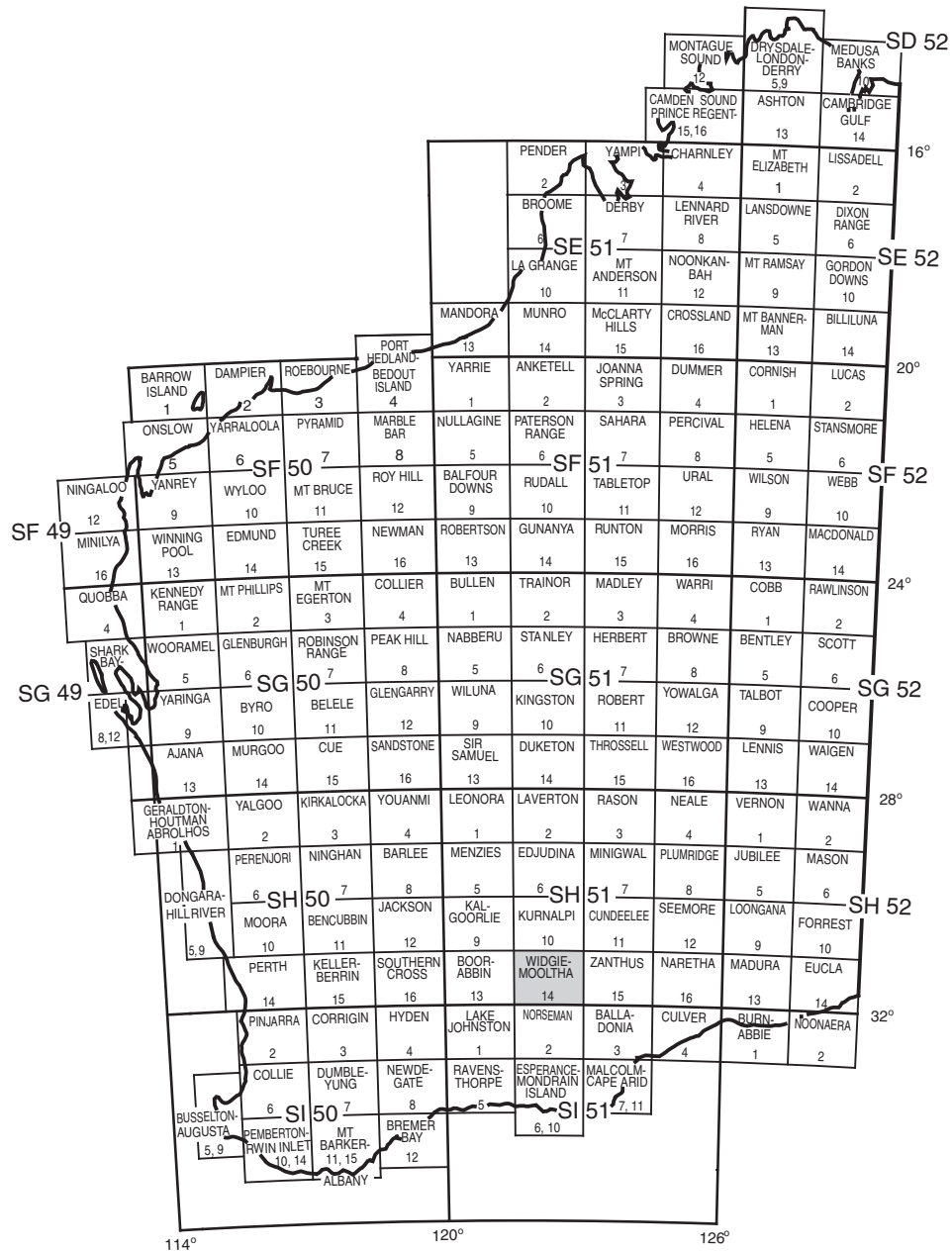
GEOLOGY OF THE YARDINA 1:100 000 SHEET

by CE Hall and SA Jones

1:100 000 GEOLOGICAL SERIES



Geological Survey of Western Australia



LAKE LEFROY 3235	MOUNT BELCHES 3335	ERAYINIA 3435
WIDGIEMOOLTHA SH 51-14		
COWAN 3234	YARDINA 3334	YARDILLA 3434



GEOLOGICAL SURVEY OF WESTERN AUSTRALIA

GEOLOGY OF THE YARDINA 1:100 000 SHEET

by
CE Hall and SA Jones

Perth 2008

MINISTER FOR ENERGY; RESOURCES; INDUSTRY AND ENTERPRISE
Hon. Francis Logan MLA

ACTING DIRECTOR GENERAL, DEPARTMENT OF INDUSTRY AND RESOURCES
Stuart Smith

EXECUTIVE DIRECTOR, GEOLOGICAL SURVEY OF WESTERN AUSTRALIA
Tim Griffin

REFERENCE

The recommended reference for this publication is:

Hall, CE, and Jones, SA, 2008, Geology of the Yardina 1:100 000 sheet: Geological Survey of Western Australia,
1:100 000 Geological Series Explanatory Notes, 41p.

National Library of Australia Card Number and ISBN 978-1-74168-142-0 (PDF)

ISSN 1321-229X

Grid references in this publication refer to the Geocentric Datum of Australia 1994 (GDA94). Locations mentioned in the text are referenced using Map Grid Australia (MGA) coordinates, Zone 50. All locations are quoted to at least the nearest 100 m.

Copy editor: L Day and DP Reddy
Cartography: M Prause
Desktop publishing: KS Noonan

Published 2008 by Geological Survey of Western Australia

This Explanatory Note is published in digital format (PDF) and is available online at www.doir.wa.gov.au/GSWA/publications. Laser-printed copies can be ordered from the Information Centre for the cost of printing and binding.

Further details of geological publications and maps produced by the Geological Survey of Western Australia are available from:

Information Centre
Department of Industry and Resources
100 Plain Street
EAST PERTH, WESTERN AUSTRALIA 6004
Telephone: +61 8 9222 3459 Facsimile: +61 8 9222 3444
www.doir.wa.gov.au/GSWA/publications

Cover photograph:

S-folds in para-amphibolites, southwest YARDINA (MGA 415450E 6459452N)

Contents

Abstract	1
Introduction	1
Access	1
Climate, physiography, and vegetation	3
Previous investigations	4
Current work	4
Nomenclature	6
Regional geology	6
Kalgoorlie Terrane	7
Kurnalpi Terrane	7
Burtville Terrane	7
Regional deformation and metamorphism	7
Archean Yilgarn Craton	9
Rock types	9
Metamorphosed fine-grained mafic rocks (<i>Amw</i> , <i>Ambbr</i> , <i>Ambps</i>)	9
Medium- to coarse-grained mafic rocks (<i>Aod</i> , <i>Aog</i>)	9
Felsic volcanic and volcanoclastic rocks (<i>Afr</i> , <i>Afrp</i>)	10
Metamorphosed felsic volcanic and volcanoclastic rocks (<i>Amfrz</i> , <i>Amyf</i> , <i>Amyfa</i>)	11
Metasedimentary rocks (<i>Aspv</i> , <i>Asxf</i> , <i>Asxs</i> , <i>Acc</i> , <i>Amktq</i> , <i>Amha</i> , <i>Amhel</i> , <i>Amhs</i> , <i>Amlv</i> , <i>Amt</i>)	11
Mount Belches Formation (<i>Abe-mh</i> , <i>Abe-mhe</i> , <i>Abe-mhz</i> , <i>Abe-mls</i>)	15
Granitic rocks (<i>Ag</i> , <i>Agc</i> , <i>Agch</i> , <i>AgchsI</i> , <i>Agm</i> , <i>Agmb</i> , <i>Agmbs</i> , <i>Agmh</i> , <i>Agm</i> , <i>Agycs</i> , <i>Amgss</i> , <i>Amgz</i>)	15
Veins and dykes (<i>g</i> , <i>gp</i> , <i>zq</i>)	18
Archean deformation	18
D ₁ event	19
D ₂ event	19
D ₃ and D ₄ events	20
Archean metamorphism	20
M ₁ event	20
M ₂ event	21
M ₃ event	21
Domain boundaries and major faults on YARDINA	21
Mount Monger Fault	21
Lefroy Fault	22
Proterozoic geology	22
Widgiemooltha Dyke Suite (<i>Pwlji-o</i> , <i>Pwlji-ax</i> , <i>Pwlji-og</i> , <i>Pwlji-oh</i> , <i>Pwlji-ow</i> , <i>Pwlbi-om</i> , <i>Pwlbi-gi</i>)	22
Woodline Formation (<i>Ewo-sl</i> , <i>Ewo-stq</i>)	23
Undivided mafic and ultramafic dykes, including the Fraser dyke swarm (<i>Eod</i>)	24
Albany–Fraser Orogeny	25
Deformation in the Woodline Formation	25
Proterozoic metamorphism	25
Cenozoic geology	25
Eundynie Group (<i>EeEU-s</i> , <i>EeEU-kl</i>)	26
Regolith	28
Residual and relict units (<i>Rc</i> , <i>Rf</i> , <i>Rf_g</i> , <i>Rg</i> , <i>Rgp_g</i> , <i>R_cd_pm</i> , <i>R_cqs</i> , <i>Rk</i> , <i>Rmp</i> , <i>R_s</i> , <i>Rw</i> , <i>Rz</i>)	29
Colluvium and sheetwash (<i>C</i> , <i>Cf</i> , <i>Cg</i> , <i>Ck</i> , <i>Cm</i> , <i>Cq</i> , <i>Cmp_r</i> , <i>Cts</i> , <i>Cz</i> , <i>Czu</i> , <i>W</i> , <i>Wf</i> , <i>Wg</i> , <i>Wk</i> , <i>Wq</i>)	29
Lacustrine units (<i>L_dl</i> , <i>L_d2</i> , <i>L_d2k</i> , <i>L_m</i> , <i>L_p</i> , <i>L_{sgm}</i> , <i>L_{mp}</i>)	29
Sandplain units (<i>S</i> , <i>S_d</i> , <i>S_p</i> , <i>S_{dk}</i>)	30
Alluvial units (<i>A</i> , <i>A_c</i> , <i>A_p</i> , <i>A_r</i> , <i>A_u</i>)	30
Economic geology	30
Vein and hydrothermal mineralization — undivided	30
Precious metal — gold	30
Pegmatitic mineralization	30
Speciality metal — tantalum	30
Orthomagmatic mafic and ultramafic mineralization	31
Base metal and steel industry metals — copper and nickel	31
Stratabound sedimentary — clastic-hosted mineralization	31
Energy mineral — uranium	31
Sedimentary — basin mineralization	31
Energy rock — lignite	31
Industrial rock — limestone	31
Hydrogeology	31
Acknowledgements	31
References	33

Appendices

1. Gazetteer of localities on YARDINA	37
2. Whole-rock geochemistry of metasedimentary, felsic volcanic, and granitic rocks from YARDINA	38

Figures

1. Location and regional geological setting of YARDINA	2
2. Main cultural and physiographic features on YARDINA	3
3. Interpreted Precambrian bedrock geology of YARDINA	5
4. Aeromagnetic map of total magnetic intensity for YARDINA	6
5. Tremolite–actinolite-bearing metabasalt with a strong cleavage, western margin of YARDINA	10
6. Measured sections of a rhyolite and overlying volcanoclastic breccia and sandstone–mudstone succession	12
7. Competent layer of chert boudinaged in less competent carbonaceous mudstone	13
8. Upright chert beds dipping steeply to the west	13
9. Para-amphibolite with preserved graded bedding	13
10. Clast-supported breccia	15
11. Monzogranite with biotite schlieren and crosscutting veins and dykes	17
12. Map showing northwest-plunging F_2 folds, southwest YARDINA	19
13. Northwest-plunging F_2 folds in para-amphibolite units with S-asymmetry	20
14. Stereoplots illustrating the moderately northwest-plunging F_2 folds and stretching lineations, southwest YARDINA	20
15. The axial surface of an F_2 fold is curved, indicating later warping	21
16. Twinned andalusite in a metasandstone of the Mount Belches Formation	21
17. The Binneringie Dyke of the Widgiemooltha Dyke Suite	23
18. The Woodline Formation	24
19. Stereoplots illustrating poles to bedding and faults measured in the Woodline Formation	25
20. The location of YARDINA with respect to the Cenozoic Lefroy and Cowan paleodrainage channels	27
21. Rock types of the Eundynie Group	28
22. Megamottles in saprolite above monzogranite	29

Tables

1. Geological history of the southeastern Eastern Goldfields Superterrane	8
2. Microprobe results of amphiboles from para-amphibolite units, YARDINA	14
3. Characteristics of granite groups in the Eastern Goldfields Superterrane	16
4. SHRIMP geochronological data for emplacement ages of granites on YARDINA	18
5. Stratigraphy of the Eocene Eundynie Group in the Cowan and Lefroy paleodrainage channels on YARDINA	26

Geology of the Yardina 1:100 000 sheet

by

CE Hall and SA Jones

Abstract

The YARDINA 1:100 000 sheet lies within the southern part of the Eastern Goldfields Superterrane of the Archean Yilgarn Craton. Granitic and metasedimentary rocks (volcaniclastic and siliciclastic) are the main bedrock types, with greenstones confined to a small area on the western margin of the map sheet. The Proterozoic Widgiemooltha Dyke Suite includes the well-exposed east-northeasterly trending Binneringie Dyke and the poorly exposed northeasterly trending Jimberlana Dyke in northern and southeastern YARDINA respectively. The Proterozoic Woodline Formation overlies the Archean rocks in a northeasterly trending belt in the eastern part of YARDINA. Flat-lying Cenozoic Eundynie Group sedimentary rocks unconformably overlie the Archean basement and are commonly found on the western margins of playa lakes.

Structural trends in the Archean rocks on YARDINA are similar to the regional structural grain of the Eastern Goldfields Superterrane. Open to tight upright D_2 folds are well developed in metamorphosed sedimentary rocks of the Mount Belches Formation and in the southwestern corner of the map. D_2 folds have a well-developed axial-planar foliation and fold axes plunge moderately to the northwest, and are the result of east-northeast – west-southwest crustal shortening. Regional metamorphism, which probably post-dates D_2 , ranges from greenschist to amphibolite grade and is overprinted by retrograde chlorite replacing garnet and cordierite. Gentle warping of D_2 folds is rare, but is attributed to the collision of the southeastern margin of the Yilgarn Craton with East Antarctica as part of the Mawson Craton during the 1345–1140 Ma Albany–Fraser Orogeny (D_3). D_3 Albany–Fraser Orogeny-related deformation is also observed in the Proterozoic rocks of the Woodline Formation, with fold axes of open upright folds and gentle warps trending northeast and broadly parallel to the Yilgarn Craton–Albany–Fraser Orogen contact.

Archean granitic rocks make up at least 50% of the basement on YARDINA. The granitic rocks are dominated by massive to moderately foliated monzogranites to quartz monzonites (–biotite–hornblende). Minor rock types include syenogranites and a clinopyroxene-bearing syenite.

Eundynie Group sedimentary rocks, deposited during an Eocene marine transgression, include massive siltstone–sandstone with trace fossils and limestone. Deposition of fluviodeltaic to marine sediments was associated with the Cowan paleodrainage channel, remnants of which, such as Lake Cowan, coincide with the present-day drainage system.

The only commodity produced on YARDINA is tantalum from pegmatites intruding metasedimentary rocks of the Mount Belches Formation at the Bald Hill mine in northern YARDINA. The area has been explored for gold, base metals (Cu, Ni), uranium, limestone for smelter flux, and lignite.

KEYWORDS: Yardina, Yilgarn Craton, Eastern Goldfields Superterrane, metasediments, granite, basic igneous rocks, volcanic rocks, Mount Belches Formation, Woodline Formation, Binneringie Dyke, Jimberlana Dyke, Eundynie Group.

Introduction

The YARDINA* 1:100 000 map sheet (SG 51-14, 3334) is on the WIDGIEMOOLTHA 1:250 000-scale map sheet, and is bound by longitudes 122°00' and 122°30'E, and latitudes 31°30' and 32°00'S. The sheet is named after Yardina Soak†, which is situated slightly north of the map centre. The northern part of YARDINA lies in the Coolgardie and

Northeast Coolgardie Mineral Fields, whereas the southern part is in the Dundas Mineral Field. The centre of YARDINA is about 130 km south-southeast of Kalgoorlie–Boulder and 65 km northeast of Norseman (Fig. 1).

Access

Access to the northern areas of YARDINA is via the Binneringie haul road that provides ingress to Binneringie Homestead and the Bald Hill tantalum mine. The Binneringie road exits on to the Esperance–Coolgardie Highway, 5 km south of Widgiemooltha. The southern

* Capitalized names refer to standard 1:100 000 map sheets, unless otherwise indicated.

† MGA coordinates of localities mentioned in the text are listed in Appendix 1.

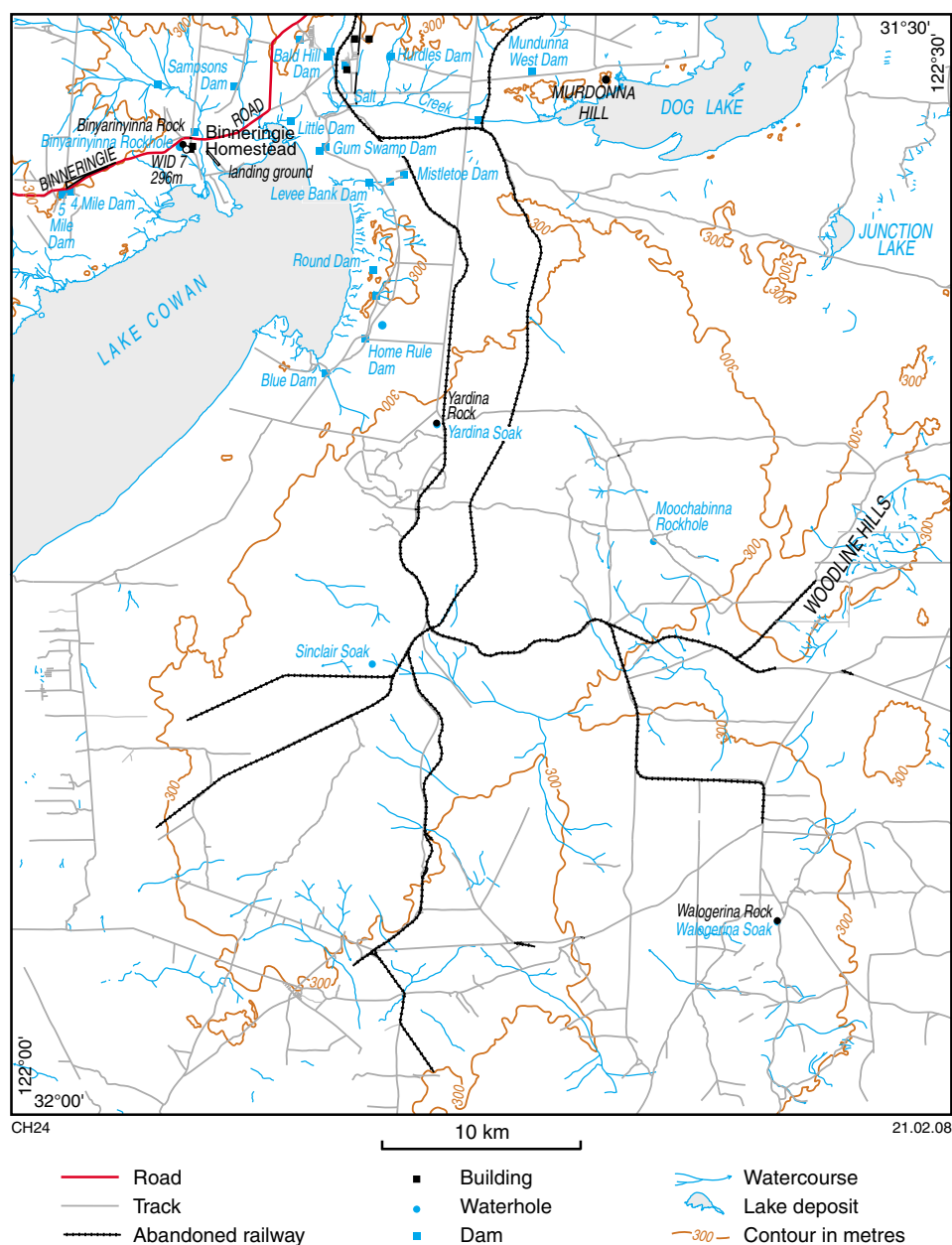


Figure 2. Main cultural and physiographic features on YARDINA

margin of YARDINA is accessible by several well-formed tracks that egress on to the Eyre Highway, which runs 8–12 km south of YARDINA (Fig. 1). There is no direct access to the western margin of YARDINA, much of which is occupied by Lake Cowan, and access to the eastern margin is restricted to minor tracks from the adjacent map sheet (YARDILLA). Many of the tracks on YARDINA follow the historic Woodline railway (Fig. 2) which was built in the earlier part of the 20th Century to haul wood to the mines and smelters.

Climate, physiography, and vegetation

YARDINA has a semi-arid climate, with the closest weather stations at Norseman, Balladonia, and Kalgoorlie–Boulder

recording annual rainfall averages to 2007 of 288, 225, and 261 mm respectively. Rainfall is most consistent during the winter months. However, isolated thunderstorms and remnants of tropical cyclones in the summer months provide sporadic and heavy downfalls that produce substantial runoff. Temperatures in the summer months commonly exceed 35°C, and minimum temperatures during winter commonly drop below 5°C with occasional frosts (climate data from the Commonwealth Bureau of Meteorology website <<http://www.bom.gov.au>>).

The physiography of YARDINA is largely controlled by basement rock types that are overlain by extensive regolith and the Cowan paleodrainage system that was incised during the Jurassic. Although bedrock exposure is poor, structural trends are visible on aerial photos, satellite imagery, and aeromagnetic data. Areas dominated by

granitic rocks, particularly the northwest and southeast corners of YARDINA, form an irregular terrain of gentle undulations interspersed by sheetwash zones and deep regolith cover with claypans and sink holes. In the northeastern and western parts, metasedimentary rocks and minor mafic and ultramafic rocks are overlain by extensive sandplains. These sandplains are adjacent to the northern extent of Lake Cowan, which has an average elevation of about 275 m above Australian Height Datum (AHD), and is part of the south to southwesterly draining Cowan paleodrainage channel (Clarke, 1994). The northern margin of Lake Cowan is dominated by a broad east-northeasterly trending ridge formed by the Paleoproterozoic Binneringie Dyke, which rises from the lake floor to an elevation of about 320 m above sea level (Figs 3 and 4). Smaller isolated paleolakes, with prominent escarpments around the west and northwest margins, are commonly formed by mottled saprolite rocks capped by silcrete, or fluvial to deltaic sedimentary rocks of the Eocene Eundynie Group. The Proterozoic Woodline Formation forms large northeasterly trending, rock-covered ridges and small, isolated conical hills near the central-eastern margin of YARDINA (Fig. 3). Relief is typically low across the map, with the highest point (383 m above AHD) in the southeast corner, and the lowest point (263 m above AHD) on the western margin of Lake Cowan (MGA 407116E 6487800N).

YARDINA lies in the extensive Eremaean Botanical Province of Diels (1906), and locally within the Binneringie System of the Southwest Interzone (Burbidge, 1960; Beard, 1990), which is also known as the Coolgardie Botanical District (Beard, 1990). Detailed reports on the vegetation of Western Australia, which include YARDINA, have been written by Beard (1975, 1981, 1990).

A great deal of the original woodland vegetation was cleared for timber for mining operations in the middle of the last century. However, stands of trees untouched by fire or timber cutters indicate a dominance of mixed woodland to open woodland with saltbush understorey. The broad low ridges and sheetwash plains that dominate YARDINA are mainly covered by mixed eucalypt woodland including *Eucalyptus salmonophloia* (salmon gum), *Eucalyptus salubris* (gimlet), *E. flocktoniae* (merrit) and patches of giant mallee (*E. oleosa*) and black butt (*E. lesouefii*, *E. dundasii*). The eucalypts are intermingled with tall shrubs dominated by broombush (*Eremophila scoparia*), greybush (*Cratystylis concephala*), bluebush (*Maireana sedifolia*), and saltbush (*Atriplex vesicaria*), with a patchy ground layer of grasses and ephemeral herbs (Beard, 1975, 1990).

Wattle, mulga (*Acacia* sp.), and broombush are common on granite-derived soils. Shrubs observed less frequently include *Exocarpos aphyllus*, *Santalum acuminatum* (quandong), and *Santalum spicatum* (sandalwood). In areas where there is a sandy to rubbly outcrop of granitic rock, tall trees are absent and replaced by thickets of broombush (*Eremophila scoparia*). Where there are thick patches of sand overlying granitic rocks, a rich Kwongan* flora grow, including sedges such as *Lepidosperma drummondi*. Patches of spinifex are common on granitic and felsic volcanic rocks.

In and around the playa lake system, vegetation is dominated by samphire (*Halosarcia* sp.), saltbush, bluebush, and greybush (Beard, 1975, 1990). Rounded-leaf pigface (*Disphyma crassifolium*) commonly grows where quartz dykes are exposed in the salt-lake beds and lake edges. The soils are highly calcareous in the southeastern part of YARDINA, and become slightly less calcareous to the north and west (Northcote et al., 1968).

Previous investigations

Sofoulis et al. (1965) recorded the geology of the YARDINA sheet in the first edition WIDGIEMOOLTHA (1:250 000) map and in the accompanying explanatory notes (Sofoulis, 1966). The geology of YARDINA was revised by Griffin and Hickman (1988a) in the second edition of the WIDGIEMOOLTHA (1:250 000) map and the accompanying explanatory notes (Griffin, 1989). Broad tectonic models of the Eastern Goldfields have included parts of YARDINA (e.g. Barley et al., 1989; Swager, 1997; Krapez et al., 1997; Weinberg et al., 2003).

Regional and local studies have included Proterozoic rocks of the Woodline Formation and Phanerozoic rocks of the Eundynie Group (Myers, 1990; Griffin, 1989; Clarke, 1994; Clarke et al., 2003).

Open-file reports, maps, and data for mining and exploration tenements submitted to the Department of Industry and Resources (DoIR) are available on the Western Australian mineral exploration (WAMEX) database at the DoIR library in Perth and at the Geological Survey of Western Australia (GSWA) Kalgoorlie regional office. WAMEX reports are also progressively becoming available online on the DoIR website <<http://www.doir.wa.gov.au>>.

Current work

YARDINA has been included in the East Yilgarn Geological Information Series digital data package covering fifty-nine 1:100 000 map sheets in the Eastern Goldfields (Geological Survey of Western Australia, 2007). An aeromagnetic interpretation of YARDINA and seven adjoining 1:100 000 map sheets is contained in the Southeastern Yilgarn Geological Exploration package (Geological Survey of Western Australia, 2005).

Fieldwork for YARDINA was carried out between August and November 2003, and completed in March 2004. Mapping was based on colour 1:25 000 aerial photographs taken in February 2002. Aeromagnetic data with a line spacing of 200 m, flown by Fugro Airborne Surveys in 2001, was used for geological interpretation. Landsat Thematic Mapper (TM) false colour imagery (using ratios of bands 2, 3, 4, 5 and 7) assisted the interpretation of regolith unit distributions.

* Kwongan: Aboriginal term for the Western Australia sandplain and its vegetation that consists typically of a layer of small ericoid shrubs less than 1 m (Beard, 1990).

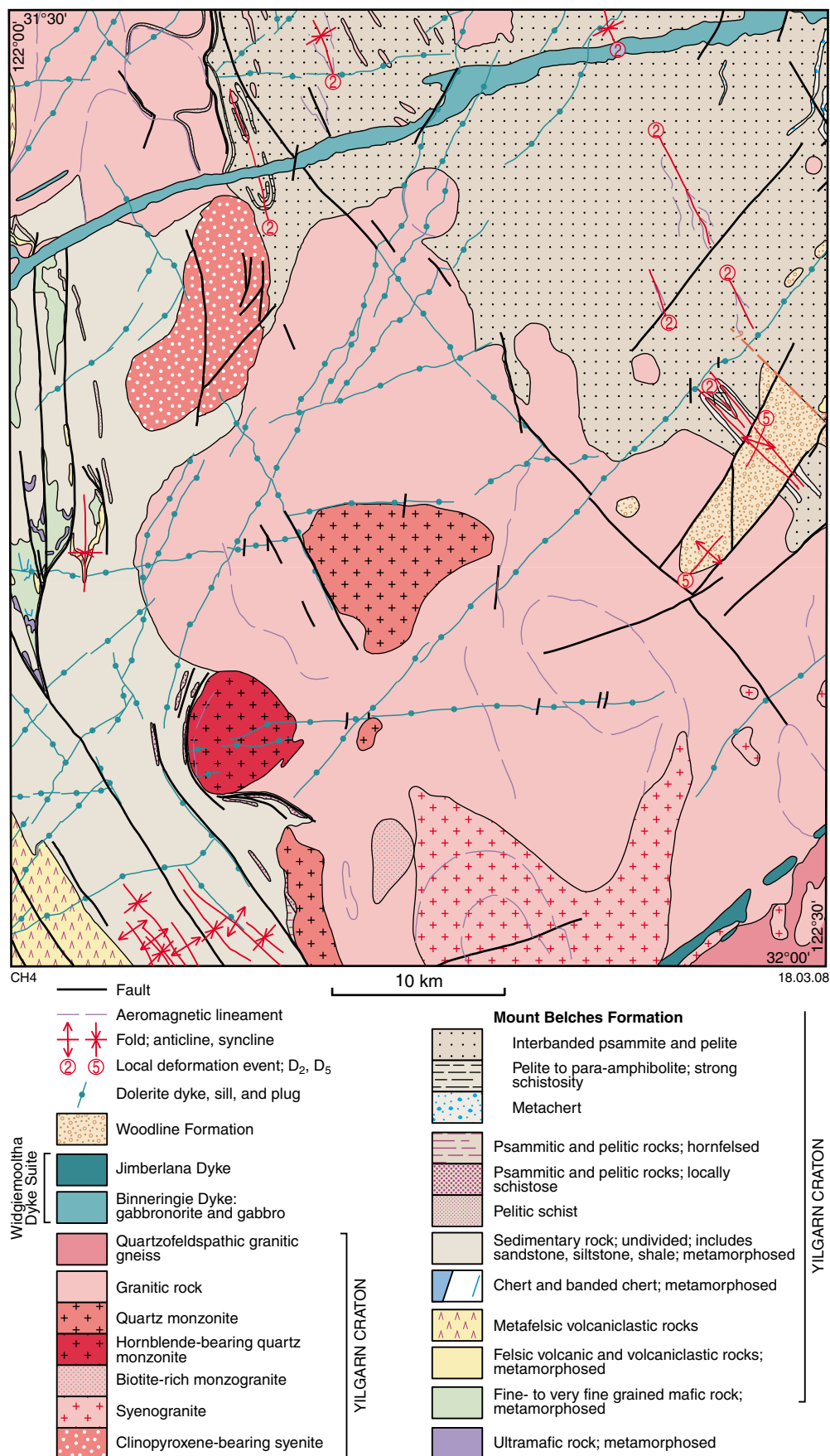


Figure 3. Interpreted Precambrian bedrock geology of YARDINA

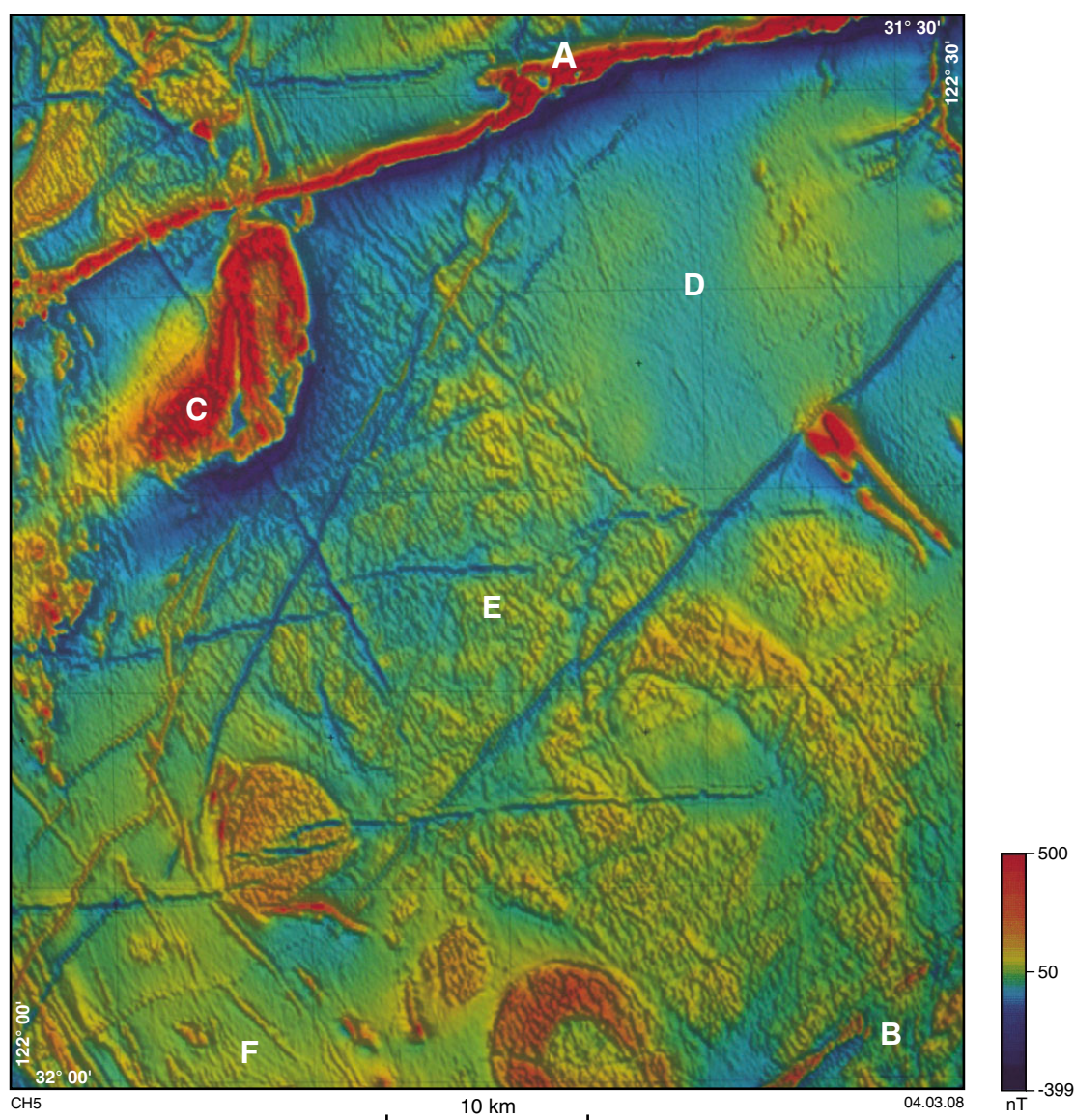


Figure 4. Aeromagnetic map of total magnetic intensity for YARDINA. A = Binneringie Dyke, B = Jimberlana Dyke, C = clinopyroxene-bearing syenite, D = Mount Belches Formation, E = multiple granitic bodies, F = metasedimentary rocks. Image published with the permission of Fugro Airborne Surveys Pty Ltd

Nomenclature

Although all Archean rocks on YARDINA have been metamorphosed, where primary textures are adequately preserved to allow identification of a protolith, the prefix 'meta' is commonly removed for ease of description. Metamorphic terminology is applied to rocks for which protoliths cannot be identified.

Regional geology

YARDINA lies near the southeastern margin of the Eastern Goldfields Superterrane (formerly known as the Eastern Goldfields Granite–Greenstone Terrane) of the Archean Yilgarn Craton and the Proterozoic Albany–Fraser

Orogen (Tyler and Hocking, 2001; Cassidy et al., 2006). The Eastern Goldfields Superterrane is characterized by a pronounced north-northwest structural grain that is defined by a network of anastomosing major faults, shear zones, and linear to arcuate greenstone belts separated by large elongate to oval granitic bodies. The superterrane has been subdivided into a number of terranes, based on differing lithostratigraphic packages separated by major tectonic features. Until recently there was no consensus on precise terrane boundary locations (Myers, 1990, 1997; Swager, 1997; Swager et al., 1995, 1997; Brown et al., 2001; Groenewald et al., 2002; Cassidy et al., 2006). However, recent collaboration between GSWA, Geoscience Australia, and various academic groups in the Predictive Mineral Discovery Cooperative Research Centre (pmd*CR) subdivided the Eastern Goldfields

Superterrane into the Kalgoorlie, Kurnalpi, and Burtville Terranes and component domains that are fault-bound geologically contiguous blocks within terranes (Cassidy et al., 2006; Fig. 1).

Kalgoorlie Terrane

The north-northwesterly trending Kalgoorlie Terrane (Cassidy et al., 2006) is the westernmost terrane of the Eastern Goldfields Superterrane and has a strike length of more than 600 km. The terrane extends from Wiluna, about 500 km north of Kalgoorlie–Boulder, to Norseman in the south. The western margin of the Kalgoorlie Terrane is bound by the Ida and Waroonga Fault Systems, separating it from the Southern Cross Domain of the Youanmi Terrane (formerly Southern Cross Granite–Greenstone Terrane), whereas the eastern margin is marked by the poorly exposed Ockerburry Fault System, including the Mount Monger Fault (Fig. 1).

The Kalgoorlie Terrane is divided into an older lithostratigraphic succession of rocks (>2730 Ma) that are found in the Norseman, Boorara and Wiluna Domains, and a younger (c. 2710–2666 Ma) more-abundant greenstone succession. The younger greenstone succession has been well documented from regional studies and drillcore data (Swager et al., 1995; Swager and Griffin 1990; Krapez et al., 2000). The lowermost part of the succession is the Lunnon Basalt which is more than 1900 m thick, but the base is not exposed (Morris, 1993). The Lunnon Basalt is overlain by a komatiite unit (Kambalda Komatiite) that is 80 m to more than 2000 m thick (Groenewald et al., 2000). The Kambalda Komatiite is overlain by dominantly basaltic units with a total thickness greater than 1000 m. These units are the Paringa Basalt and the Devon Consols Basalt, which are separated by the Kapai Slate (Swager et al., 1995). Above the mafic–ultramafic succession are rocks of the Black Flag Group (>1000 m thick), which comprise felsic volcanic and volcanoclastic rocks with minor mafic units (Morris, 1998).

Kurnalpi Terrane

The Kurnalpi Terrane (Cassidy et al., 2006) is bound by the Kalgoorlie Terrane to the west and the Burtville Terrane to the east (Fig. 1). The terrane comprises c. 2715–2705 Ma calc-alkaline complexes, mafic volcanic rocks, and quartz-poor epiclastic rocks, with subordinate rhyodacite and iron-rich sandstone–siltstone units (locally referred to as banded iron-formation) which are intruded by regionally extensive dolerite and gabbro sills (Barley et al., 2003).

The six domains of the Kurnalpi Terrane include, from east to west, the Linden, Edjudina, Laverton, Murrin, Menangina, and Gindalbie Domains. Differences in volcanic and depositional settings are identified in all domains, but together the components indicate crustal growth from an early volcanic arc, to back-arc ocean-floor volcanism, to intra-arc rifting (Barley et al., 2002; Groenewald et al., 2006).

Burtville Terrane

The Burtville Terrane (Cassidy et al., 2006) is the easternmost terrane, and is bound by the Hootanui

Fault system on the western margin with the Kurnalpi Terrane. This poorly outcropping terrane is broadly divided into three domains — Duketon, Merolia, and Yamarna — which include ultramafic, mafic, volcanic, and sedimentary rocks. Geochronological constraints are poor, but the Duketon Domain includes an intermediate volcanoclastic rock and a porphyritic intrusion from the Famous Blue prospect dated at 2805 ± 5 Ma and 2804 ± 6 Ma respectively (Barley et al., 2003), and a felsic volcanoclastic sandstone in the Merolia Domain with an age of c. 2769 Ma (Wingate and Bodorkos, 2007).

Regional deformation and metamorphism

The Eastern Goldfields Superterrane was affected by four major compressional events, separated by periods of extension (Archibald et al., 1978; Archibald, 1987; Swager et al., 1997; Nelson, 1997; Swager, 1997; Table 1). Most authors recognize an early deformation event (D_1) that involved thrusting and recumbent folding, followed by east-northeast – west-southwest crustal shortening during D_2 that produced major regional-scale upright F_2 folds (2675–2657 Ma; Nelson, 1997). D_3 deformation is characterized by north-northwesterly trending regional sinistral strike-slip faults and associated folding. Continued regional shortening produced conjugate brittle structures (D_4) that overprint all previous structures and most granites (Swager et al. 1997; Nelson, 1997; Swager, 1997).

Regional metamorphic grades in the Eastern Goldfields Superterrane range from prehnite–pumpellyite to amphibolite facies with typically low to moderate pressures, and partly reflect the distribution of granitic bodies (Witt, 1991; Ridley, 1993; Swager, 1997). Metamorphic grades in greenstones are typically higher (amphibolite facies) along the margins with the surrounding granite, whereas lower grade zones (prehnite–pumpellyite and greenschist facies) occupy the central parts of the greenstone belts. Peak metamorphic conditions were typically reached during D_2 deformation, probably contemporaneously with the bulk of granitic emplacement at c. 2660 to 2640 Ma (Witt, 1991; Nelson, 1997; Swager et al., 1997). A metamorphic study of the Kalgoorlie region by Mikucki and Roberts (2003) highlighted the critical role of post- D_2 granitic rocks in controlling the distribution of peak metamorphic isograds. They also demonstrated that gold mineralization occurred during or after peak regional metamorphism, but before the collapse of elevated metamorphic geotherms back to premetamorphic steady-state conditions.

Much of the Yilgarn Craton has been stable since the Archean, with only minor deformation recorded during the Proterozoic and Phanerozoic. The east-northeasterly trending mafic Widgiemooltha Dyke Suite intruded the region at about 2420 Ma (Nemchin and Pidgeon, 1998). Unconformably overlying the Archean basement and dyke suite is the Proterozoic Woodline Formation deposited between 1737 and 1620 Ma (Turek, 1966; Hall and Jones, 2005). Deformation of the Woodline Formation is attributed to the Albany–Fraser Orogeny that records the continent–continent collision of the Yilgarn Craton margin and East Antarctica between 1345 and 1170 Ma (Myers,

Table 1. Geological history of the southeastern Eastern Goldfields Superterrane

Age (Ma)	Features	Timing constraints
<i>D_e — extension</i>		
c. 2705	Low-angle shear on granite–greenstone contacts; synvolcanic ^(a) granites; deposition of komatiite basalt synchronous with intrusion of layered mafic to ultramafic sills; polydirectional extension, local recumbent folding ^(b)	Felsic tuff interbedded with komatiites c. 2705 Ma ^(b)
>2666	Subsequent deposition of Black Flag Group ^(c) ; Mount Belches Formation ^(d)	Black Flag Group (Kalgoorlie Sequence maximum deposit age 2666 Ma ^(c)) (Spargoville Sequence 2698–2686 Ma ^(c))
<i>D₁ N–S compression (?diachronous)</i>		
2683–<?2672	N–S-directed thrusting and local recumbent folding ^(e,f,g) M ₁ associated with development of layer-parallel foliation	Felsic volcanic rocks 2681 ± 5 Ma, 2675 ± 3 Ma ^(h) maximum age; 2674 ± 6 Ma post-D ₁ felsic porphyry dyke ⁽ⁱ⁾ between Kalgoorlie and Democrat
<i>Post-D₁ and pre-D₂ extension</i>		
<2672–>2655	Follows D ₁ with rollover anticlines and E–W extension leading to clastic infill of local synclinal basins ^(j)	Post-D ₁ and pre-D ₂ felsic porphyry 2674 ± 6 Ma ⁽ⁱ⁾ predates Kurrawang and Merougil Conglomerates
<i>D₂ (Wangkathaa Orogeny^(k)) — E–W compression (?diachronous)</i>		
c.2675–2655	E–W shortening with upright folds and shallow NNW-plunging fold axes ^(e,l,m) ; folding and doming of granite bodies driven by granite buoyancy regional stresses ⁽ⁿ⁾ M ₂ peak metamorphic conditions during D ₂ (–?D ₃) lower- to mid-greenschist to amphibolite facies	Minimum: 2660 ± 3 Ma ^(o) post-D ₂ monzogranite Maximum: 2675 ± 2 Ma ^(h) post-D ₁ monzogranite Kambalda Anticline; syn- or late-deposition of the Kurrawang Sequence at 2655 Ma ^(h) Voluminous granitic intrusions at 2675–2657 Ma ^(h)
<i>D₃ — transpression</i>		
c. 2663–2645 ^(j,h)	Tightening of F ₂ folds ^(p,q) Contemporaneous with and outlasting D ₂	Minimum: 2658 ± 13 Ma (Brady Well Monzogranite) Boulder–Lefroy Fault ^(q,e) , Butchers Flat Fault ^(e)
<i>D_e post-orogenic collapse</i>		
c. 2640	Post-metamorphic orogenic collapse ^(i,r)	Late-tectonic granite c. 2640 Ma; Ida Fault ^(s)
<i>D₄ — transpression</i>		
<?2640	W to WNW oblique sinistral faults ^(t,u) ; NE to ENE oblique dextral/reverse faults ^(l,g) ; low-Ca granitoid intrusion throughout D ₂ –D ₄ ^(u)	2638 ± 26 Ma ^(u) ; 2651 ± 5 Ma ^(s) post-tectonic alkaline granites; Paddington area, Mount Charlotte, Black Flag Fault
<i>Dyke intrusion</i>		
c. 2420	Intrusion of Widgemooltha dyke swarm	c. 2418 Ma ^(v) Binneringie Dyke; c. 2411 Ma Jimberlana Dyke ^(w)
<i>Deposition of Woodline Formation</i>		
<1620	Deposition of Woodline Formation; NW to SE flow direction	<c. 1737 Ma ^(x) quartz arenite, NW Y ^{ARDILLA}
<i>D₅ — Albany–Fraser Orogeny</i>		
c. 1345–1260	Deformation of Archean rocks (and Woodline Formation) related to dextral transpression probably during late Stage I phase ^(y) of the Albany–Fraser Orogeny M ₃ lower greenschist- to amphibolite-facies metamorphism of Archean and Proterozoic rocks (Woodline Formation) during the Albany–Fraser Orogeny; peak thermal metamorphism post-dates main collisional event (Stage I) ^(z)	Southeast Y ^{ARDILLA} 1205 ± 10 Ma ^(za) random mineral growth overprinting compressive fabrics; Mount Barren Group
<i>Dyke intrusion</i>		
c. 1210	Intrusion of Fraser dyke swarm	c. 1210 Ma ^(z) dolerite dyke; Kambalda
<i>Marine transgressions</i>		
50–38	Deposition of Eundynie Group — Cowan and Lefroy paleodrainage channels; ?laterite formation;	50–38 Ma ^(zb) ; southeastern Eastern Goldfields
<38	Uplift, erosion, laterite development	38 Ma–present; southeastern Eastern Goldfields
<div><div><div>(a) Hammond and Nisbet (1992)</div><div>(b) Passchier (1994)</div><div>(c) Krapez et al. (2000)</div><div>(d) Painter and Groenewald (2001)</div><div>(e) Swager and Griffin (1990)</div><div>(f) Gresham and Loftus-Hills (1981)</div><div>(g) Archibald et al. (1981)</div></div><div><div>(h) Nelson (1997)</div><div>(i) Kent and McDougall (1995)</div><div>(j) Swager (1997)</div><div>(k) Blewett et al. (2004)</div><div>(l) Witt (1994)</div><div>(m) Hunter (1993)</div><div>(n) Weinberg et al. (2003)</div></div><div><div>(o) Swager and Nelson (1997)</div><div>(p) Swager et al. (1995)</div><div>(q) Swager (1989)</div><div>(r) Goleby et al. (1993)</div><div>(s) Nelson (1995)</div><div>(t) Chen et al. (2001)</div><div>(u) Hill et al. (1992)</div></div><div><div>(v) Nemchin and Pidgeon (1998)</div><div>(w) Fletcher et al. (1987)</div><div>(x) Hall and Jones (2005)</div><div>(y) Clark et al. (2000)</div><div>(z) Wingate et al. (2000)</div><div>(za) Dawson et al. (2003)</div><div>(zb) Clarke (1994)</div></div></div>		

1990, 1995; Nelson et al., 1995; Clark et al., 1999, 2000). Based on lithological grounds, Myers (1990) and Tyler and Hocking (2001) divided the orogen into the Northern Foreland and the Biranup and Nornalup Complexes. During the collision, high-grade quartzofeldspathic gneisses and layered mafic intrusions of the Fraser Complex (part of the Biranup Complex) were juxtaposed against the southern margin of the Yilgarn Craton. At about 1210 Ma the northeasterly to north-northeasterly trending Fraser dyke swarm intruded an area within 100 km of the Yilgarn Craton – Albany–Fraser Orogen suture (Wingate et al., 2000).

Large paleodrainage channels formed during pre-Jurassic glaciation events and were flooded during the Paleocene by marine transgressions, resulting in widespread deposition of the largely fluviodeltaic to estuarine Eundynie Group (Clarke, 1994; Clarke et al., 2003). Subsequent development of extensive laterite profiles resulted from prolonged deep weathering. Semi-arid conditions throughout most of the Neogene and Quaternary enhanced development of playa lakes and their associated dune systems in the lowlands defined by the paleodrainage channels (Griffin, 1989; Clarke, 1994; Clarke et al., 2003).

Archean Yilgarn Craton

The Yilgarn Craton on YARDINA is dominated by Archean granites and greenstones. Variably deformed granitic rocks make up at least half of the map area, and are dominant across the northwestern, central and southeastern parts of the map sheet.

The northeastern and southwestern corners of YARDINA are dominated by Archean metasedimentary rocks, with minor mafic, ultramafic, and felsic volcanic and volcanoclastic rocks. The Archean rocks are typically deeply weathered, with a thick cover of regolith that results in very poor exposure on most of YARDINA. The best outcrops of Archean rocks are on the edges of the playa lake systems.

The Archean rocks of the Yilgarn Craton are intruded by the large Proterozoic mafic Binneringie and Jemberlana Dykes, and the unexposed Fraser dyke swarm. Along the eastern margin of YARDINA the Archean Yilgarn Craton rocks are overlain by the Proterozoic Woodline Formation, which forms a northeast-trending belt of sandstones and quartzites, with subordinate quartz conglomerates and shale (Fig. 3).

Rock types

Poor exposure and the deeply weathered nature of most Archean outcrops on YARDINA limit the correlation of units and identification of a coherent stratigraphy. However, aeromagnetic imagery (Fig. 4) combined with outcrop geology can be used to correlate greenstone units in the northern part of YARDINA with those on adjacent map sheets (COWAN, LAKE LEFROY, MOUNT BELCHES, and YARDILLA).

Metamorphosed fine-grained mafic rocks (*Amw*, *Ambbr*, *Ambps*)

Fine-grained mafic rocks form a minor component of YARDINA and are only exposed along the western margin. They are typically metamorphosed at lower- to middle-greenschist facies. Rock types commonly associated with the mafic rocks include chert, felsic volcanic rocks, and carbonate-rich mudstones interbedded with minor chert.

The mafic units for which the protolith cannot be identified (*Amw*) are predominantly massive and fine grained, extremely weathered, and commonly form small, isolated outcrops.

Strongly altered pyroxene-spinifex-textured mafic rocks (*Ambps*) and tremolite–actinolite-rich metabasalts (*Ambbr*) are only found along the central-western edge of the map (MGA 406000E 6482000N; MGA 410500E 6486000N), and are likely to be a continuation of the mafic–ultramafic succession exposed on LAKE COWAN and LAKE LEFROY (Griffin, 1988, 1990; Griffin and Hickman, 1988b) to the northwest. Both units are interlayered with thin (decimetre- to metre-scale) chert bands and well-indurated, carbonate-rich mudstones.

Although all pyroxene spinifex-textured mafic units (*Ambps*) are strongly altered, relict pyroxene-spinifex texture is common in hand specimens and thin sections, with acicular amphibole (possibly tremolite) replacing pyroxene. The groundmass is typically recrystallized and composed of chlorite, epidote, plagioclase, carbonate, and quartz(–mica). Tremolite–actinolite-rich metabasalts (*Ambbr*) are typically strongly cleaved (Fig. 5), with the strike of the cleavage planes parallel to regional F_2 fold axes. Despite the alteration and cleavage development, interlayered sedimentary units, abundant varioles, and a weak variation in grain size allow individual flow units to be recognized in places. In thin section the metabasalts are dominated by the ubiquitous secondary growth of tremolite–actinolite, with subordinate feldspar, epidote, and quartz. Griffin (1990) provided a summary of similar rock units along strike that are less altered and better exposed on LAKE COWAN and LAKE LEFROY, and included a summary of collated geochemical data.

Medium- to coarse-grained mafic rocks (*Aod*, *Aog*)

Dolerite (*Aod*) is a medium-grained mafic rock metamorphosed at lower- to middle-greenschist facies that is only exposed on the western margin of YARDINA. The unit is typically massive to weakly foliated with ophitic to subophitic textures preserved. Dolerite is typically associated with finer grained mafic rocks and may represent the coarser grained zones of differentiated mafic flows.

Gabbro (*Aog*) outcrops in a few scattered, poorly exposed locations along the western margin of YARDINA. These rocks are typically deeply weathered and are commonly associated with finer grained mafic rocks such as metabasalt (e.g. MGA 406749E 6499446N). At this location the gabbro has a strong northwest-trending

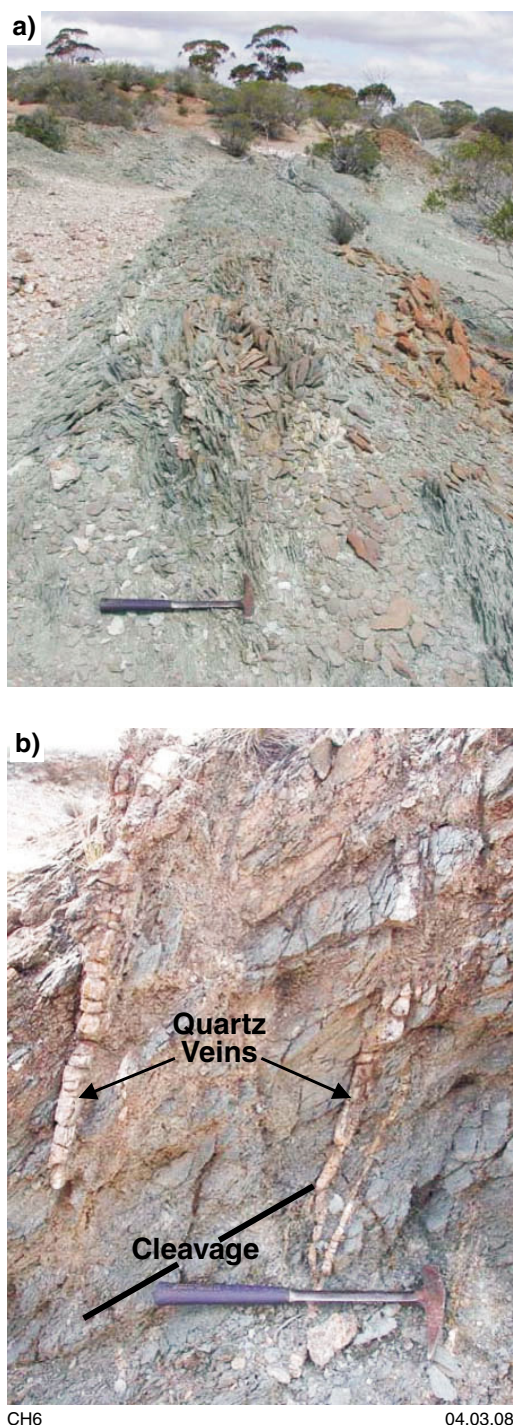


Figure 5. Tremolite–actinolite-bearing metabasalt (*Ambbr*) from the western margin of YARDINA (MGA 406411E 6482173N): a) showing the strong cleavage; b) quartz veins crosscutting the cleavage

cleavage and jointing perpendicular to the cleavage. In thin section the gabbro is characterized by a strong alteration assemblage, the composition of which depends on the grade of metamorphism (e.g. may contain epidote, chlorite, and amphibole). Plagioclase is saussuritized and secondary quartz trains are commonly parallel to the dominant cleavage plane.

Felsic volcanic and volcanoclastic rocks (*Afr*, *Afrp*)

Felsic volcanic rocks (*Afr*, *Afrp*) are restricted to several isolated outcrops along the central-western margin of YARDINA and a small outcrop along the eastern margin adjacent to YARDILLA. Outcrops of rhyolite (*Afr*) on the western margin (MGA 407278E 6482050N) are closely associated with fine- to coarse-grained mafic and felsic volcanoclastic rocks, and commonly have a blocky appearance due to pervasive jointing perpendicular to the regional northwesterly trending foliation. In hand specimen, fine (≤ 1 mm) flecks of biotite are uniformly dispersed throughout, and minor sulfides are found on joint surfaces. In thin section the rhyolite is composed of abundant euhedral to subhedral feldspar microphenocrysts in a holocrystalline groundmass of quartz, feldspar, magnetite, and minor biotite. In comparison, a rhyolite of 3 m minimum thickness, exposed at the base of a volcanoclastic breccia to sandstone succession (MGA 410428E 6485559N), is recognized by the presence of small, rounded quartz eyes (1–2 mm) in a massive, dark blue-grey, fine-grained rock. In thin section this rhyolite is characterized by rounded quartz grains with resorption textures, and euhedral to subhedral feldspar in a quartzofeldspathic groundmass with a trachytic texture. Major- and trace-element analysis results for this rhyolite (GSWA 179051; Appendix 2) show a SiO_2 wt% of 75.17, and Nb, Y and Zr values similar to Black Flag Group rhyolites in the Kambalda region (Morris, 1998)

There is no exposure of the contact relationship between the rhyolitic unit (*Afr*) along the eastern margin of YARDINA (MGA 452596E 6491826N) and other rock types. The rhyolite is massive, with crosscutting quartz veinlets and red-stained joints and fractures. The rock comprises 1–2% euhedral to subhedral feldspar phenocrysts in a recrystallized groundmass of quartz, feldspar, and accessory magnetite. Chlorite and sericite are common along fracture planes and as selvages to quartz veins. The interpretative bedrock geology map (Fig. 3) indicates contact with metasedimentary rocks of the Mount Belches Formation. However, it is unclear whether the rhyolite is older and the Mount Belches Formation unconformably overlies the rhyolite, or if the rhyolite is a member of the Mount Belches Formation. In the latter case previous descriptions of the Mount Belches Formation have not identified any contemporaneous volcanic activity during deposition of the formation (Painter and Groenewald, 2001). Major oxide and trace element data of the rhyolite (GSWA 179028; Appendix 2) show a very different $\text{Na}_2\text{O}:\text{K}_2\text{O}$ ratio and enrichment in Nb, Y, and Zr with respect to the rhyolite on the western margin of YARDINA. However, there are similarities in both major oxide and trace element data with felsic volcanic rocks from Perkollilli near Kanowna, which have been dated at 2675 ± 3 Ma (Morris, 1998).

A porphyritic rhyolite unit (*Afrp*) has been identified at a single location (MGA 406868E 6481400N) on the western margin of YARDINA, where it is in sharp contact with a strongly cleaved tremolite–actinolite-bearing metabasalt. Phenocrysts of feldspar are up to 8 mm long, and are

euhedral to subhedral. In thin section the rock comprises alkali-feldspar phenocrysts with Carlsbad twinning and quartz with resorption features, in a groundmass of quartz, feldspar, carbonate, chlorite, magnetite, and mica.

Metamorphosed felsic volcanic and volcanoclastic rocks (*Amfrz*, *Amvf*, *Amvfa*)

A metasomatized, strongly foliated metarhyolitic rock (*Amfrz*; MGA 406400E 6500450N), exposed along the northwestern margin of Lake Cowan, is in direct contact with the Proterozoic Binneringie Dyke and is likely to be a large xenolith within the dyke. The outcrop has a distinctive pinkish tinge, with elongate quartz eyes and feldspar phenocrysts parallel to a strong foliation.

Scattered outcrops of felsic volcanoclastic rocks (*Amvf*, *Amvfa*), metamorphosed at greenschist to amphibolite facies, were mapped along the western margin of YARDINA. Rocks with abundant amphibole (*Amvfa*) are typically well indurated and are commonly exposed as rounded boulders within the regolith profile, or along scarps at lake edges. In the southwestern corner of YARDINA, outcrops can be identified on aerial photographs by a sharp increase in the vegetation density, which is dominated by *Eremophila* sp. and *Melaleuca* sp. The growth pattern of metamorphic amphibole in outcrop is either parallel to the regional foliation (S_2) or in a stellate pattern. In thin section (GSWA 179012) the rock is composed of porphyroclasts of euhedral to subhedral feldspar and rounded quartz in a recrystallized mosaic (granoblastic texture) of quartz and minor feldspar and amphibole. Larger grains of subhedral amphibole (0.5–1 mm), with a deep-green to light-green-blue pleochroism, are aligned parallel to S_2 . There is a second stage of amphibole growth that is at a random angle to the S_2 fabric, and with no obvious crenulation of the S_2 fabric, suggesting that the amphibole growth was probably during the latter stages of D_2 deformation. Accessory minerals include opaque minerals, epidote, and zircon.

Elsewhere, felsic volcanoclastic rocks (*Amvf*) are commonly weathered and strongly foliated, with the foliation defined by the growth of red-brown mica or chlorite. Porphyroclasts of feldspar lie within a fine-grained quartz-rich groundmass. Subordinate minerals include epidote, chlorite, zircon, and opaque minerals.

Metasedimentary rocks (*Aspv*, *Asxf*, *Asxs*, *Acc*, *Amktq*, *Amha*, *Amhel*, *Amhs*, *Amlv*, *Amt*)

The majority of metasedimentary rocks exposed on YARDINA are deeply weathered, but retain features indicating a sedimentary origin. These units are among the most abundant lithologies on YARDINA, and are best exposed in the west and southwest, particularly on the edges of the playa lake systems. Because much of the Archean rock lies under cover, the remains of numerous exploration drillholes have been used to determine the distribution of these rocks.

On the western margin of a small lake (MGA 410428E 6485559N) a succession of previously unrecognized, well-bedded, moderately well sorted to very well sorted sandstone (*Aspv*) conformably overlies a very thickly bedded monomict breccia (*Asxf*) that is in turn concordant with an underlying rhyolite (Fig. 6). The 2–3 m-thick breccia is moderately to poorly sorted, and clast supported (Fig. 6a). The rhyolite clasts are partially flattened in a direction parallel to the regional foliation and the bedding of the overlying sandstones. In thin section, a weakly developed schistosity closely parallels the long axes of the clasts. The interstitial matrix is dominated by clay minerals, with a fine mosaic of quartz and feldspar and subordinate relic microphenocrysts of feldspar and rounded quartz that show embayment textures.

Above and concordant with the breccia and rhyolite is a 76 m-thick succession of moderately bedded volcanoclastic sandstones and siltstones. Normal grading, planar lamination, and cross-bedding are difficult to see in the outcrop, but are visible in cut hand specimens (Fig. 6b). The sandstone is dominated by subrounded quartz and volcanogenic lithic fragments (Fig. 6c). Overall, the succession is a fining-upward package. At the top of the succession a pyroxene-spinifex-textured basalt (*Ambps*) with a strong foliation is inferred to be concordant with the sedimentary package. There are no overprinting fabrics to conclusively assign the strong foliation seen in the volcanic to volcanoclastic succession to a particular deformation event. However, the fabric is parallel to regional D_2 fold axes, and the bedding in the felsic units is not repeated or reversed to suggest D_1 folding, thus indicating that the foliation is likely to be a S_2 fabric.

Along strike from the rhyolite–sandstone succession are isolated outcrops of locally silicified, grey to black slate (*Amlv*; MGA 410349E 6486434N). Interlayered chert within silicified portions of the slate is commonly boudinaged parallel to the regional S_2 foliation. Boudin development is also found in units interlayered with massive, well-indurated, grey, carbonate-rich mudstones (*Amktq*; MGA 405965E 6482344N) associated with mafic and felsic rocks (Fig. 7).

Banded chert (*Acc*) has only been mapped along the central-western margin of YARDINA where it is associated with mafic rocks and carbonate-rich mudstones. The chert bands form pronounced ridges and wall-like barriers in lake floors, marginal lake deposits, sand dunes, and weathered mafic rocks (Fig. 8) and are typically the only units that are distinctive and laterally continuous enough to clearly trace out regional folds. The cherts range from strongly laminated, white, pale-, and dark-grey-blue chert to massive chert.

Strongly foliated and metamorphosed sedimentary rocks (*Amha*, *Amhs*, *Amt*, and *Amhel*) are particularly abundant and well exposed around playa lake edges in the southwestern corner of YARDINA. A series of folds at lake edges expose para-amphibolite (*Amha*), metamorphosed sandstone and mudstone couplets (*Amhs*), and metamorphosed sandstone (*Amt*). Sandstone and interbedded mudstone are predominantly metamorphosed at lower greenschist facies, but the metamorphic grade increases markedly to amphibolite facies in the exposed

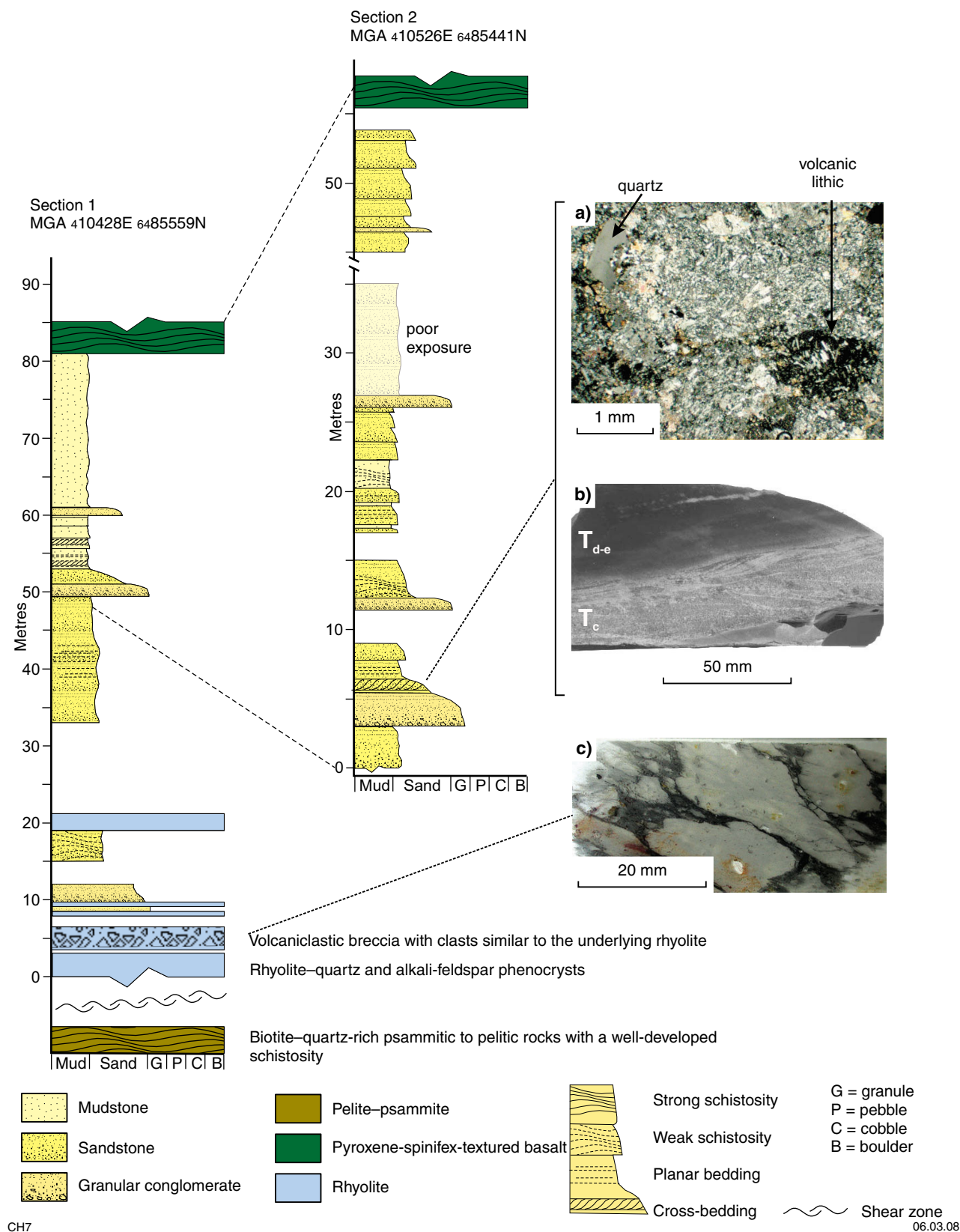


Figure 6. Measured sections of a rhyolite (*Afr*) and overlying volcaniclastic breccia (*Asxf*) and sandstone-mudstone (*Aspv*) succession: a) volcaniclastic sandstone (GSA 179053); b) graded bedding with low-angle cross-bedding; c) photograph of thin section (GSA 179052) of volcaniclastic breccia

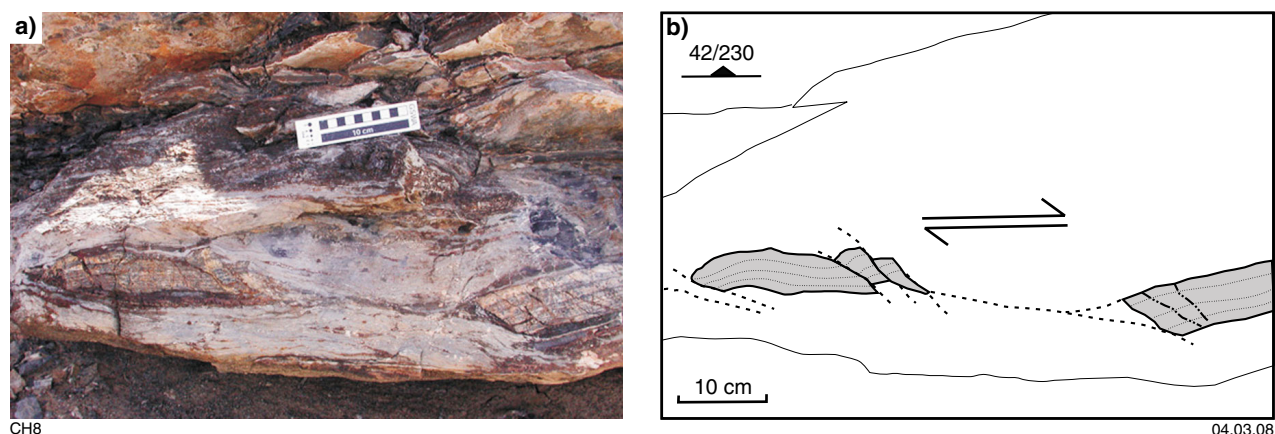


Figure 7. Competent layer of chert (*Acc*) boudinaged in less competent carbonaceous mudstone (*Amktq*): a and b) boudinaged blocks suggest a 'shearband' geometry (after Goscombe et al., 2004) with an extensional dextral displacement. View is to the southwest and S_0 is subparallel to the foliation dipping 42° towards 230° (MGA 405965E 6482344N)

cores of anticlinal folds, and also increases to the east. The increase in metamorphic grade to the east may represent the contact metamorphic effect of a large quartz-monzonite body (MGA 422100E 6462000N). Nearer to the contact with granitic bodies, exploration-drillhole chip samples of the metasediments commonly include sillimanite, biotite, or garnet (*Amhel*).

Graded bedding and scoured bases to tabular sandstone units delineate anticlines and synclines with a northwest plunge. Para-amphibolites derived from graded sandstone and interbedded mudstone show a pattern of abundant amphibole in the finer grained mud-rich portions of a bed, and a lack of amphibole in the quartz-rich sandstone portions of a bed (Fig. 9). Microprobe analysis of amphiboles from two para-amphibolite units (*Amha*; GSWA 179086 and 179016) indicates that the amphiboles would be classified as actinolite to actinolitic hornblende using the classification system of Leake (1978; Table 2).

A breccia unit (*Asxs*) associated with the para-amphibolites in the southwest of YARDINA is a clast-supported, moderately indurated unit that is either massive or shows

a weak normal grading. A poorly sorted, angular to subangular, monomict clast assemblage is composed of recrystallized sandstone and siltstone, with clast sizes ranging from sand size to about 0.3 m (Fig. 10). At the top of the breccia a weak, normally graded pebble breccia

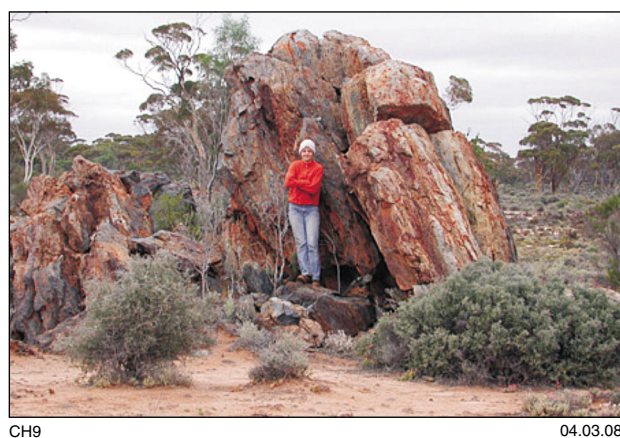


Figure 8. Upright chert beds (*Acc*) dipping steeply to the west (right of picture; MGA 405968E 6481816N)

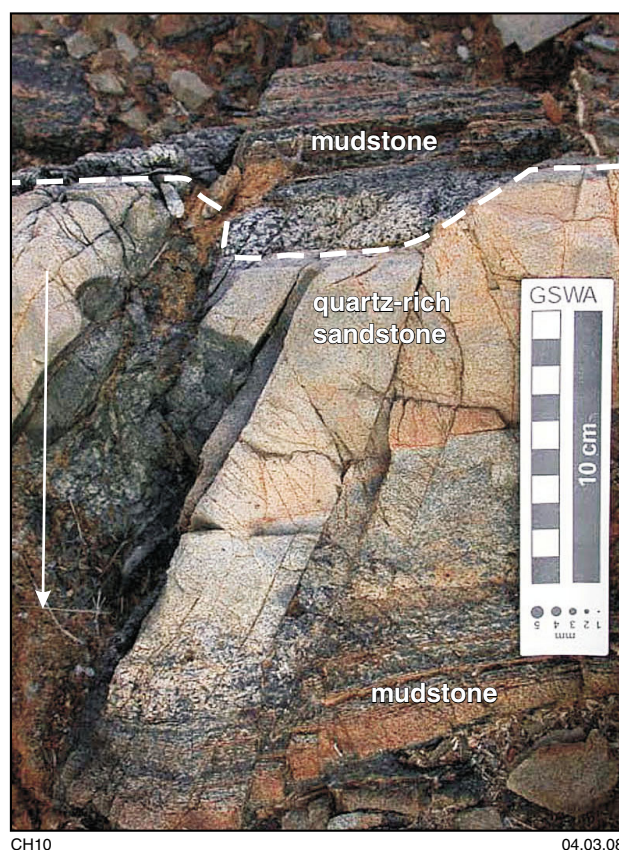


Figure 9. Para-amphibolite (*Amha*) with preserved graded bedding. From the base (dashed white line) the bed grades from quartz-rich, amphibole-poor metasandstone to amphibole-rich metamudstone, indicating a younging direction (solid arrow) from the top to the bottom of the picture

Table 2. Microprobe results of amphiboles from para-amphibolite units (*Amha*), YARDINA

Standard	Point	SiO ₂	TiO ₂	Al ₂ O ₃	Cr ₂ O ₃	FeO	V ₂ O ₃	MnO	MgO	CaO	Na ₂ O	ZnO	K ₂ O	Total
USNM 143965	HORN A26 STD PT1	40.04	4.64	14.36	0.00	10.57	0.00	0.00	12.85	9.93	2.86	0.00	2.22	97.47
USNM 143965	HORN A26 STD PT2	40.10	4.61	14.36	0.00	10.81	0.00	0.08	12.54	9.95	2.72	0.00	2.12	97.29
USNM 143965	HORN A26 STD PT3	39.87	4.59	14.26	0.00	10.90	0.00	0.12	12.47	9.88	2.74	0.00	2.14	96.96
	Known composition*	40.37	4.72	14.90	0.00	10.92	-	0.09	12.80	10.30	2.60	-	2.05	98.75
USNM 111356	HORN A15 STD PT1	41.33	1.25	14.12	0.00	11.10	0.12	0.20	14.66	11.47	2.27	0.00	0.26	96.77
USNM 111356	HORN A15 STD PT2	41.54	1.32	14.37	0.00	11.25	0.09	0.12	14.66	11.34	2.35	0.00	0.24	97.28
USNM 111356	HORN A15 STD PT3	41.18	1.33	14.45	0.00	11.22	0.12	0.17	14.47	11.26	2.29	0.00	0.22	96.73
	Known composition*	41.46	1.41	15.47	0.00	11.47	0.15	-	14.24	11.55	1.91	-	0.21	97.87
GSWA no.														
179086	AMPH 1 PT 1	48.97	0.30	7.00	0.08	11.96	0.17	0.22	14.83	12.02	1.06	0.00	0.13	96.74
179086	AMPH 1 PT 2	50.70	0.25	4.95	0.10	11.41	0.12	0.23	15.33	12.33	0.66	0.00	0.15	96.22
179086	AMPH 1 PT 3	52.01	0.00	2.49	0.00	13.32	0.00	0.26	14.65	12.58	0.14	0.00	0.04	95.49
179086	AMPH 2 PT 1	48.91	0.33	6.31	0.07	13.48	0.00	0.24	14.00	12.36	0.71	0.00	0.36	96.78
179086	AMPH 2 PT 2	53.28	0.05	1.54	0.07	10.50	0.00	0.31	16.97	12.53	0.18	0.00	0.07	95.51
179086	AMPH 2 PT 3	53.19	0.05	1.74	0.07	10.54	0.00	0.24	16.67	12.72	0.19	0.00	0.09	95.51
179086	AMPH 3 PT 1	52.40	0.17	1.99	0.00	12.14	0.00	0.25	16.19	12.25	0.34	0.00	0.17	95.89
179086	AMPH 3 PT 2	51.37	0.15	2.61	0.07	12.31	0.00	0.26	15.64	12.24	0.42	0.00	0.20	95.28
179086	AMPH 3 PT 3	52.75	0.30	2.86	0.05	12.32	0.00	0.27	15.82	12.04	0.49	0.00	0.21	97.10
179016	AMPH 1 PT 1	46.91	0.21	8.65	0.00	15.68	0.11	0.24	12.50	11.51	1.41	0.00	0.15	97.36
179016	AMPH 1 PT 2	46.24	0.26	8.81	0.04	15.98	0.00	0.14	12.20	11.64	1.46	0.00	0.18	96.96
179016	AMPH 1 PT 3	46.13	0.24	9.36	0.05	16.00	0.08	0.13	12.21	11.72	1.30	0.00	0.27	97.49
179016	AMPH 2 PT 1	52.77	0.13	2.54	0.00	12.51	0.07	0.20	16.21	12.26	0.36	0.00	0.16	97.21
179016	AMPH 2 PT 2	53.10	0.16	2.81	0.00	12.64	0.00	0.15	16.12	11.99	0.46	0.10	0.19	97.70
179016	AMPH 2 PT 3	52.46	0.15	3.29	0.07	13.07	0.00	0.17	15.69	12.01	0.45	0.00	0.19	97.55
179016	AMPH 3 PT 1	47.82	0.21	7.44	0.00	16.36	0.00	0.16	12.38	11.87	1.15	0.00	0.29	97.70
179016	AMPH 3 PT 2	47.75	0.27	7.48	0.05	15.27	0.00	0.16	12.99	11.65	1.00	0.00	0.21	96.82
179016	AMPH 3 PT3	45.88	0.35	8.46	0.00	16.31	0.06	0.20	12.04	11.89	1.22	0.11	0.21	96.72

NOTE: * Known amphibole standards are from Jarosewich et al. (1980). Analysed on a Cameca SX50 series microprobe at CSIRO, Kensington, Perth, 2005

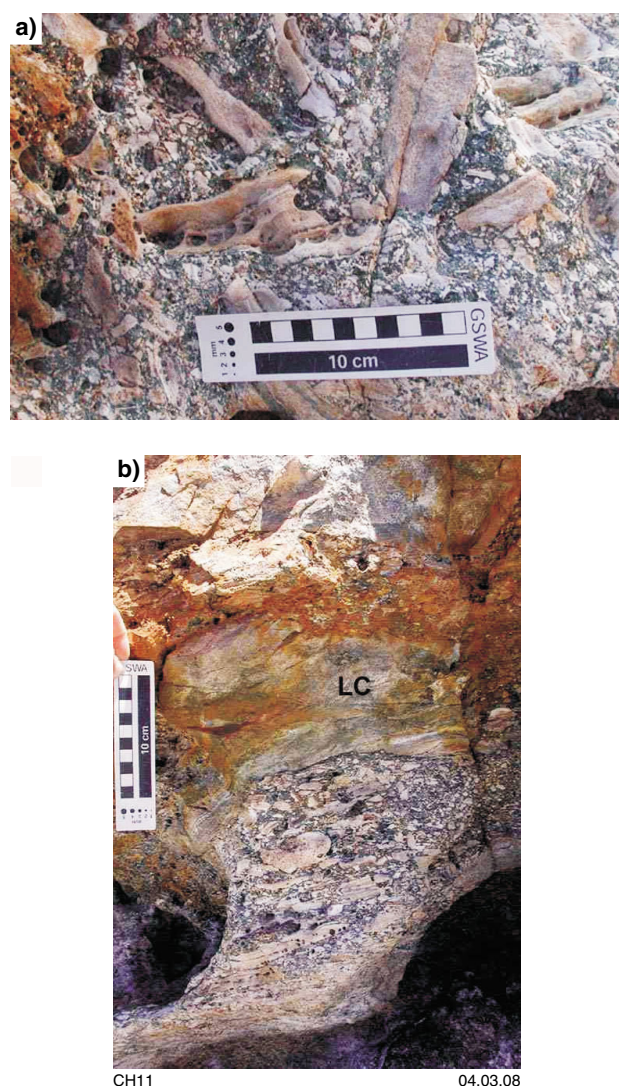


Figure 10. Clast-supported breccia (Asxs) showing:
a) metasedimentary clasts randomly orientated;
b) poorly sorted, bedding-parallel clasts (LC = large clast)

is in planar contact with overlying well-bedded para-amphibolite. The orientation of the clasts ranges from a random orientation to parallel to the bedding in the overlying para-amphibolite. The matrix comprises a fine mosaic of recrystallized quartz with secondary amphibole, similar to the overlying para-amphibolite, suggesting an intraformational provenance. The breccia is interpreted to have been deposited from a sediment gravity flow prior to deposition of overlying sandstone–mudstone couplets that are now preserved as para-amphibolites.

Mount Belches Formation (*Abe-mh*, *Abe-mhe*, *Abe-mhz*, *Abe-mls*)

The Mount Belches Formation is a thick sequence of metamorphosed turbiditic rocks that covers much of MOUNT BELCHES (Painter and Groenewald, 2001) and extends on to YARDINA, ERAYINIA, and YARDILLA (Fig. 1). The Mount Belches Formation has been included in

either the Gindalbie Terrane (Swager et al., 1997; Krapez et al., 2000; Brown et al., 2001) or in an area called the Randall Dome in the Kurnalpi Terrane as a large fault-bound block of metasedimentary rocks that forms a dome above a series of large granitic bodies (fig. 3 of Painter and Groenewald, 2001). Sensitive high-resolution ion microprobe (SHRIMP) U–Pb zircon ages on detrital zircons from Mount Belches Formation sandstone indicate maximum depositional ages of 2666 ± 5 Ma (Krapez et al., 2000) or c. 2667 Ma (Bodorkos et al., 2006). The sequence probably represents deposition by mass-flow traction and turbidity currents in a submarine environment (Painter and Groenewald, 2001). Regional mapping has enlarged the known extent of the Mount Belches Formation and, with outcrops on either side of the Kalgoorlie–Kurnalpi terrane boundary (Fig. 1), indicates that the Kalgoorlie and Kurnalpi Terranes amalgamated before c. 2666 Ma (Hall, 2007).

Mount Belches Formation rocks on YARDINA are dominated by metamorphosed steeply dipping, fine- to coarse-grained sandstone, siltstone, and mudstone, with minor conglomerate. Banded iron-formation and chert, as seen to the north on MOUNT BELCHES, do not outcrop. However, aeromagnetic data suggest folded chert at depth beneath Proterozoic rocks of the Woodline Formation and Cenozoic sediments (Figs 3 and 4). The sandstone–siltstone sequences (*Abe-mh*) commonly display graded bedding, parallel and cross-laminations, scours, Bouma sequences, and soft-sediment deformation. Many beds have mudstone as the uppermost interval (now dominated by medium-grained metamorphic biotite or amphibole). In thin section the coarse-grained sandstones and granular conglomerates contain relict detrital-quartz grains (up to 5 mm) interspersed with biotite clots and poikiloblastic plagioclase crystals, with subordinate hornblende, chlorite, muscovite and carbonate, and accessory magnetite, zircon, titanite, tourmaline, pinitized cordierite and apatite. A similar mineral assemblage is found in the mudstone layers, but staurolite, andalusite, and garnet are present where the metamorphic grade is higher and there is a strong schistosity (*Abe-mls*).

Hornfelsed (*Abe-mhe*) and metasomatized (*Abe-mhz*) units of the Mount Belches Formation are most common in the northwestern corner of YARDINA, where metasedimentary rocks are intruded by granitic plutons and dykes, pegmatite veins, quartz veins, and the Binneringie Dyke. Similar metasedimentary rocks also outcrop along the contact with the large granitic domain to the west that includes Binyarinyinna Rock.

Granitic rocks (*Ag*, *Agc*, *Agch*, *Agchsl*, *Agm*, *Agmb*, *Agmbs*, *Agmh*, *Ag*, *Agycs*, *Amgss*, *Amgz*)

The dominance and lithological variation of granitic rocks on YARDINA reflects the regional distribution of granite and granitic gneiss in the Eastern Goldfields, and accounts for about 70% of the surface area. Regionally, the dominant rock types are biotite(–amphibole) monzogranite, trondhjemite, and sodic granodiorite, commonly forming extensive composite batholiths. Minor granitic rocks

include syenite, tonalite, and quartz diorite, commonly forming small, isolated plutons, and dykes and pods.

Several classification schemes have been used to subdivide the granitic rocks of the Eastern Goldfields. These schemes include using structural characteristics and deformation events (Bettenay, 1977; Witt and Davy, 1993); and relationships to greenstone belts, with ‘internal’ granites found within or marginal to the greenstone belts and ‘external’ granites outside of the belts (Sofoulis and Bock, 1963; Perring et al., 1989). However, recently acquired radiometric ages of granites have shown that the age of granite emplacement cannot be correlated to structural features. Thus, recent classification systems have adopted a multidisciplinary approach using conventional and isotopic geochemistry, geochronology (U–Pb SHRIMP studies) and petrological characteristics (Wyborn, 1993; Champion and Sheraton, 1993, 1997; Cassidy and Champion, 2002). In particular, the work by Champion and Sheraton (1993, 1997) has resulted in the broad classification of granite and granitic gneiss into two major groups (high Ca and low Ca) and three minor groups (high HFSE, mafic, and syenitic granites). Table 3 outlines the characteristics of these groups. Recent granite studies have shown a pronounced change in type and style of magmatism at c. 2665 Ma, from abundant high-Ca granites to less voluminous low-Ca granites (Cassidy and Champion, 2002).

Granite comprises a significant part of the exposed rock on YARDINA and aeromagnetic data suggest that at least

half of the YARDINA basement is granitic. Where there has been deep weathering of granitic rocks, but the protolith is still recognizable, the classification is undivided granitic rock (Ag). Where the protolith is altered to kaolinized saprolite, the rock has been classified as deeply weathered rock (Rw). Much of the area in the granite terrain is dominated by granite-derived sand and soils interspersed with silcrete, calcrete, and scattered loose boulders of strongly weathered granite, which has been mapped as relict material over granite (Rg, Rpgg, or Rs).

Strongly foliated granite (Amgss) outcrops in the southwestern and northwestern parts of YARDINA. Outcrops in the northwestern area (MGA 412550E 6513888N) are poorly exposed but, when traced along strike on aeromagnetic images (Fig. 4), form an arcuate pattern that coincides with a thin zone of interpreted metasedimentary rocks (Amls on Fig. 3).

Metasomatized granitic rocks (Amgz) are along the margins of the Paleoproterozoic Binneringie Dyke. In thin section the original coarse-grained texture of the granite is readily identifiable, with subhedral feldspar partially altered to sericite. Interstitial quartz and feldspar display a granophyric texture with abundant secondary minerals including chlorite, epidote, and sericite. Accessory minerals include opaque minerals, zircon, and mica.

Where granite is less weathered, it consists predominantly of medium- to coarse-grained equigranular monzo-

Table 3. Characteristics of granite groups in the Eastern Goldfields Superterrane

Group	Percentage of total granite area	Age range (Ga)	Lithologies	Geochemistry	Petrogenesis
High Ca	>60	>2.70 – 2.66	Monzogranite, granodiorite, trondhjemitic	High Na ₂ O; low Th, LREE, Zr; Rb/Sr low; mostly Y-depleted 68–77 wt% SiO ₂	Deep crustal (garnet stable) or slab melting with assimilation of crust and fractionation; older crust essential
Low Ca	>20	2.66 – 2.63	Syenogranite, monzogranite, minor granodiorite	Low Al ₂ O ₃ , CaO, Na ₂ O and Sr; higher HFSE and LILE than high-Ca group 70–76 wt% SiO ₂	Reworked crustal source — Archean TTG; variable partial melts by dehydration; high temperatures at moderate crustal depth
High-HFSE	5–10	2.71 – 2.65	Syenogranite, monzogranite, minor granodiorite; associated with felsic volcanic centre	Enriched in TiO ₂ , MgO, total FeO, Y, Zr, and Nb; CaO, K ₂ O contents similar to the low-Ca group; LILE moderate to low >74 wt% SiO ₂	Pre-existing crustal rocks at moderate depth; possible partial melt of tholeiitic source or crustally contaminated fractionated tholeiitic magmas
Mafic	5–10	2.69 – 2.64 Cluster at 2.66	Diorite, granodiorite, tonalite; monzogranite, trondhjemitic	Variable silica content, subdivided by variations in the LILE and LREE contents 50–70 wt% SiO ₂	Crustal- and mantle-derived sources required
Syenite	<5	2.66 – 2.64	Syenite, monzonite, quartz syenite, alkali-feldspar syenite	High alkali content, abundance of other elements varies; negative Nb, Ti anomalies 55–73 wt% SiO ₂	?Dominantly crustal origin Possible metasomatized mantle source with crustal contribution

SOURCES: Champion and Sheraton (1997); Champion and Cassidy (2002). Table modified from Groenewald et al. (2003)

granite (*Agm*) or quartz monzonite (*Agc*) with minor biotite(–hornblende; <3% mica), and may contain large, zoned feldspar megacrysts up to 3 cm. Monzogranites with abundant biotite (>3%; *Agmb*) are scattered over most of YARDINA, but the best exposure is in the northwestern corner. In the centre of YARDINA, monzogranites are rich in elongate biotite schlieren (*Agmbs*) that frequently show an alignment, commonly at a high angle to the regional tectonic fabric. The schlieren are typically 1–5 cm long (Fig. 11a), but the largest biotite-rich enclave observed was more than 2 m in length and crosscut by late-stage granite and pegmatite veins (Fig. 11b; MGA 421944E 6485328N). At this locality, crosscutting relationships suggest a magmatic evolution of:

- intrusion of equigranular medium-grained biotite-rich (5–8%) monzogranite with mafic schlieren and enclaves;
- intrusion of leucocratic, biotite-poor veins (1–10 cm thick);
- intrusion of fine-grained, mesocratic equigranular, biotite-rich (>8%) monzogranite; followed by
- muscovite–feldspar–quartz pegmatite veins (Fig. 11c).

Quartz monzonite is restricted to a pluton in the centre of the map sheet and smaller bodies in the southwest that are in contact with Archean metasedimentary rocks (Fig. 3). One such smaller, roughly circular body (6–7 km diameter) is more mafic, with biotite (1–2%), hornblende (3–10%; *Agch*), and hornblende–biotite schlieren (*Agchs*). This pluton (Toil and Trouble; Table 4) has been dated at 2649 ± 9 Ma (Fletcher and McNaughton, 2002). In thin section the rock comprises quartz, feldspar, biotite, hornblende, titanite, and opaque minerals, with an alteration assemblage of sericite, epidote, and chlorite. Unlike the biotite-rich quartz monzonite, the hornblende-bearing quartz monzonite is not crosscut by leucocratic veins and pegmatite.

Syenogranite (*Agr*) is found in the south of YARDINA, particularly along a 12 km-long, north-trending low ridge in the southeastern corner. Elsewhere, outcrops of the syenogranite are poorly exposed and weathered to residual clasts in a soft red soil with sinkholes. Syenogranite typically comprises quartz–microcline–albite with subordinate muscovite and biotite. A small syenogranite at a lake edge along the eastern margin of the map (MGA 448510E 6475300N) contains abundant magnetite. Individual grains are up to 5 mm in size and slightly augen-shaped due to a pervasive northwest-trending foliation (S_2).

A clinopyroxene-bearing syenite (*Agycs*) with mafic schlieren outcrops on a peninsular on the eastern margin of Lake Cowan, near Blue Dam. The syenite is very well exposed, has a shallow-dipping (5–20°) foliation, abundant

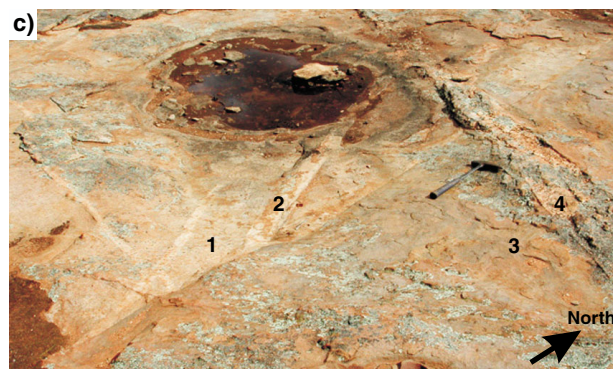


Figure 11. Monzogranite with biotite schlieren and crosscutting veins and dykes: a) monzogranite with centimetre-scale biotite schlieren aligned east-southeast; b) large north-trending biotite-rich enclave with two leucocratic crosscutting veins, hosted by a biotite monzogranite; c) crosscutting relationships in a monzogranite. From oldest to youngest the intrusive relationships are: 1 = equigranular medium-grained biotite-rich (5–8%) monzogranite with mafic schlieren and enclaves; 2 = leucocratic biotite-poor veins (1–10 cm thick); 3 = fine-grained mesocratic equigranular biotite-rich (>8%) monzogranite; and 4 = muscovite–feldspar–quartz pegmatite dykes

CH12

30.05.07

Table 4. SHRIMP geochronological data for emplacement ages of granites on YARDINA

Site/rock name	Rock type classification ^(a)	MGA coordinates	Zircon age	Titanite age	Interpreted magmatic age
Talbot (Yardina Rock)	Monzogranite biotite bearing low Ca	426706E 6493675N	High discordance 19 analyses c. 2600–2685 Ma	–	c. 2625 Ma
Sinclair	Monzogranite biotite bearing high Ca	422751E 6478254N	High discordance 12 analyses xenocrystic	Concordant 22 of 26 analyses 2655 ± 20 Ma	2655 ± 20 Ma
Toil and Trouble	Quartz monzonite (–hornblende) high Ca	419738E 6472063N	Wide scatter 10 of 19 analyses 2648 ± 11 Ma	Concordant 17 of 20 analyses 2652 ± 14 Ma	2649 ± 9 Ma (weighted mean)
End of Day	Granodiorite mafic	444041E 6460881N	Discordant 8 of 31 analyses 2663 ± 11 Ma	Concordant 12 of 21 analyses 2658 ± 20 Ma	2660 ± 15 Ma (weighted mean)

SOURCE: Fletcher and McNaughton (2002); Cassidy and Champion (2002)

NOTES: (a) Classification (high, low Ca, mafic) after Cassidy and Champion (2002); see Table 3

mafic schlieren, and enclaves ranging in size from less than 1 cm to 50 cm. It is coarse grained, with alkali feldspar with micropertthitic textures partially enclosed by green pleochroic clinopyroxene, and contains quartz, titanite, and minor biotite and muscovite. The syenite on YARDINA has not been dated. However, Cassidy and Champion (2002) placed it within the Gilgarna Clan that range in age from c. 2664 to 2644 Ma. Syenites and other felsic alkaline rocks of the Eastern Goldfields Superterrane make up 5–10% of all granitic rocks in the southeastern Yilgarn Craton, and are typically found at the margins of greenstone belts or along major crustal lineaments (Smithies and Champion, 1999; Cassidy and Champion, 2002).

The geochemistry of the various granitic rocks in the Eastern Goldfields has been described by Johnson (1991), Champion and Sheraton (1997), Witt and Davy (1997), Smithies and Champion (1999), and Cassidy and Champion (2002). Geochronological data for granites on YARDINA are presented in Table 4.

Veins and dykes (*g*, *gp*, *zq*)

Small, fine-grained granitic dykes (*g*) intrude metasedimentary rocks in the southwest of YARDINA, and sedimentary rocks of the Mount Belches Formation. The dykes range from less than 1 up to 4 m wide, are typically steeply dipping with a north-northwesterly trend, and are massive to weakly foliated.

Pegmatite dykes and pods (*gp*) are common in the northern part of YARDINA, where they intrude metasedimentary rocks of the Mount Belches Formation and granitic rocks. The pegmatite dykes typically comprise very coarse feldspar, books of muscovite, and interstitial quartz. Pegmatite dykes 1–8 m thick that intrude the Mount Belches Formation are mined at the Bald Hill mine for tantalum from tantalite. Pegmatites in granitic rocks are particularly abundant in granites that are near outcrops of the Mount Belches Formation and also near north-northwesterly

trending lineaments, faults, or granitic dykes (e.g. MGA 433800E 6491800N).

Quartz veins (*q*) are common on YARDINA and typically contain massive milky white quartz, with rare laminated and crystalline quartz veins. The veins contain rare carbonate, and display a range of morphologies including foliation- and bedding-parallel tension-gash arrays, and conjugate sets. Foliation-parallel (*S*₂) quartz veins, from less than 1 up to 1.5 m wide, are very common in rocks of the Mount Belches Formation around the edges of Dog Lake, and can form massive, irregular pods of milky white quartz with minor muscovite (MGA 440007E 6514521N). Extensive quartz stockwork outcrops in the southwest corner of YARDINA, where veins crosscut tightly folded northwesterly trending sandstones and siltstone (MGA 412050E 6462400N).

Archean deformation

Two Archean deformation events have been recognized on YARDINA. The best source of structural data from the Archean rocks is found in outcrops along the western and northern edges of the playa lakes in the northeast (particularly in the lake pavements), and in the west and southwest. These areas, together with the Proterozoic Woodline Formation and structural data from adjoining maps such as YARDILLA and MOUNT BELCHES (Jones, 2005; Jones and Ross, 2005; Painter and Groenewald, 2001), provided much of the data for the deformation history on YARDINA. Five deformation events (*D*₁ to *D*₅) are recognized regionally in the Archean rocks. For completeness, these events are listed in Table 1 and are summarized below:

- *D*₁: recumbent folding and thrusting;
- *D*₂: tight upright folding from east-northeast–west-southwest crustal shortening;
- regional-scale *D*₃–*D*₄ faults and shear zones (only recognized on aeromagnetic images);
- *D*₅: Albany–Fraser Orogen-related warping and drag folds of *D*₂ structures (Jones, 2006).

D₁ event

The earliest regional deformation event (D₁) is not recognized on YARDINA. However, on adjacent ERAYINIA and YARDILLA, D₁ is characterized by a penetrative S₁ foliation that is near-parallel to bedding and commonly overprinted by a second foliation (S₂). The Archean rocks are typically of greenschist-facies grade with a metamorphic mineral assemblage of muscovite, feldspar, chlorite, and biotite, with the chlorite–biotite transition used to separate lower and higher greenschist facies in metasedimentary rock. Recognition of D₁ structures is difficult due to subsequent upright folding (D₂) and shearing that has rotated structures (Swager and Griffin, 1990). Regionally, rocks that tend to preserve folds related to this early deformation event are banded cherts and bedding-parallel quartz veins that are strongly deformed and rodded parallel to L₁ and F₁ fold hinges (Jones 2005, 2007).

D₂ event

D₂ is the earliest deformation event recognized on YARDINA and is characterized by open to tight, upright, north-northwesterly–northwesterly trending folds with a well-developed axial-planar foliation (S₂) that was produced during east-northeast–west-southwest shortening. F₂ fold hinges are particularly well developed in metasedimentary rocks of the Mount Belches Formation and para-amphibolites in the southwestern part of YARDINA. In the southwestern area, a series of northwesterly trending anticlines and synclines (F₂ folds) in Archean

para-amphibolites are well exposed along a lake edge (Fig. 12). Graded bedding and scoured bases to tabular metasandstone units delineate a series of anticlines and synclines. The folds are open to tight and plunge gently to moderately to the northwest, with a well-developed stretching lineation defined in places by quartz stringers and rodded sandstone units with the long axes parallel to the fold hinges. These folds are characteristic of the regional F₂ fold style and display S-, M-, and Z-asymmetry (Fig. 13). Disharmonic folding is also common between the interbedded mudstone and sandstone layers as a result of competency contrast.

Stereoplots of D₂ structural elements (Fig. 14) illustrate a northwest trend of the S₂ foliation and show that it is axial planar to upright to moderately northwest-plunging folds. Although there is a large spread in the bedding measurements, they provide a beta axis that lies on the average S₂ foliation plane. The F₂ fold axes display a broad scatter on the stereoplot (Fig. 14) and this may reflect later rotation and warping of F₂ folds (Fig. 15), possibly as a result of northwest–southeast compression during the Albany–Fraser Orogeny. Throughout this southwest area, felsic porphyry dykes commonly strike parallel to the regional northwest-trending foliation.

Similar structural trends and folds are also observed in the Mount Belches Formation along the northern margin of YARDINA. Although outcrops are less well exposed and commonly restricted to the floors of playa lakes, changes in the facing direction of well-bedded metasandstones help define the position of northwesterly trending D₂ fold axes.

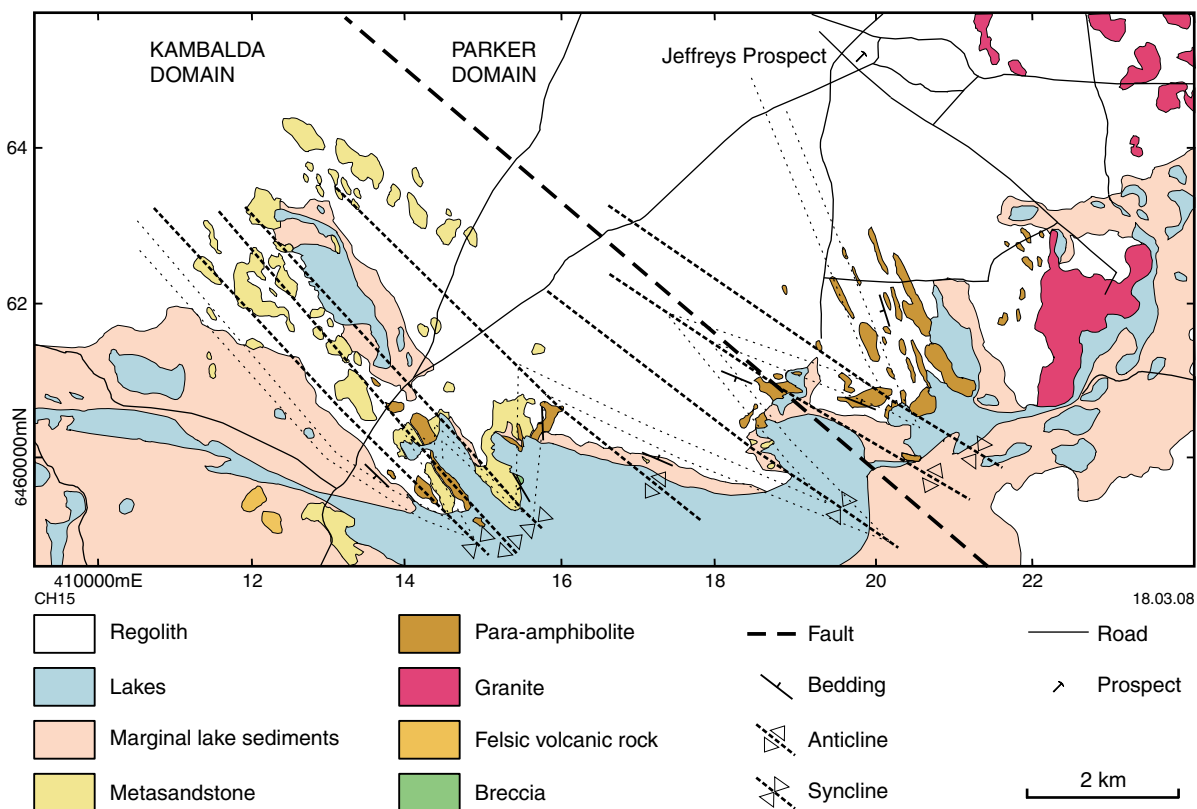


Figure 12. Map showing northwest-plunging F₂ folds, southwest YARDINA



Figure 13. Northwest-plunging F_2 folds in para-amphibolite units with S-asymmetry

Granite dykes commonly strike parallel to the regional northwest-trending foliation.

A package of mafic and felsic rocks and chert along the western margin of YARDINA (MGA 406000E 6482000N) contain good examples of F_2 folds, but at the local scale the trend of the fold axes are more northerly than the regional northwesterly trend. The change in the orientation of the fold axes may be the result of deformation-related intrusion of multiple syn- to post- D_2 granites to the east

(Fig. 3). Mafic rocks near fold hinges are strongly cleaved and quartz veins have intruded subparallel to northwesterly trending fold axial planes (Fig. 5). Chert bands have asymmetric boudin trains parallel to the main foliation (Fig. 7), with shear-band and domino boudin geometries (Goscombe et al., 2004).

D_3 and D_4 events

Transpression during D_3 and D_4 resulted in largely reverse-vertical and sinistral-lateral movement on regional faults (Nelson, 1997; Swager, 1997). Aeromagnetic data, which often provide the best means of identifying structures related to these events, do not provide any unequivocal evidence for D_3 - and D_4 -related structures on YARDINA. On MOUNT BELCHES to the north of YARDINA, Painter and Groenewald (2001) recorded minor fault offsets of D_2 structures and warping of the S_2 foliation in the Mount Belches Formation, and attributed this to D_3 - and D_4 -related transpression.

Archean metamorphism

M_1 event

M_1 is not recorded on YARDINA. However, regionally, the M_1 event is characterized by lower greenschist-facies mineral assemblages of muscovite, quartz, chlorite, and feldspar in Archean metasedimentary rocks. These minerals define the bedding-parallel penetrative S_1 foliation. The alignment of the metamorphic mineral assemblage, parallel to S_1 , suggests that peak M_1 metamorphic conditions were most likely contemporaneous with deformation during the D_1 event. The precise timing of D_1 is uncertain, with various authors giving ages that range from 2675 to 2700 Ma in the Kalgoorlie region (Kent and McDougall, 1995; Nelson, 1997; Swager, 1997).

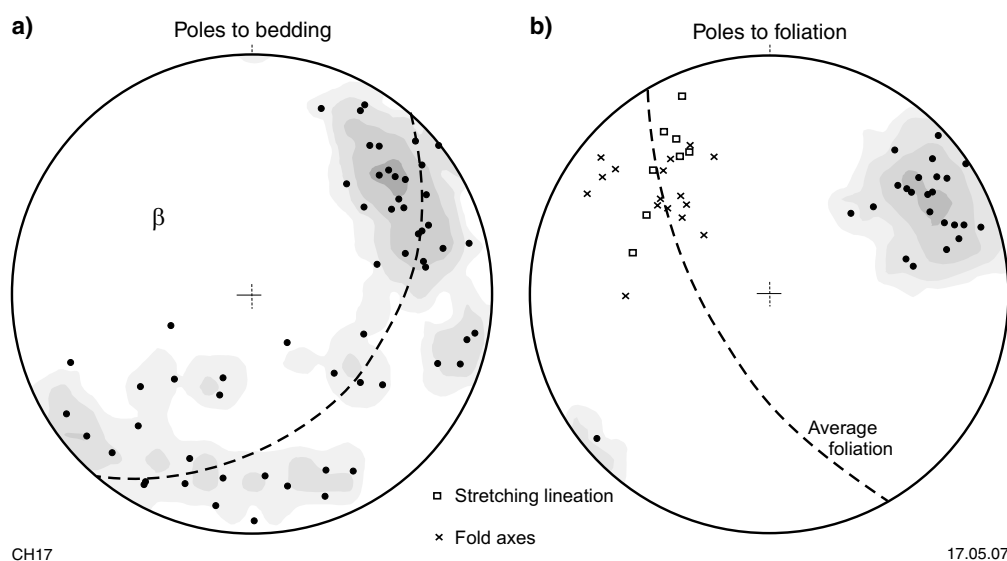


Figure 14. Stereoplots illustrating: a) the moderately northwest-plunging F_2 folds; b) stretching lineations, southwest YARDINA

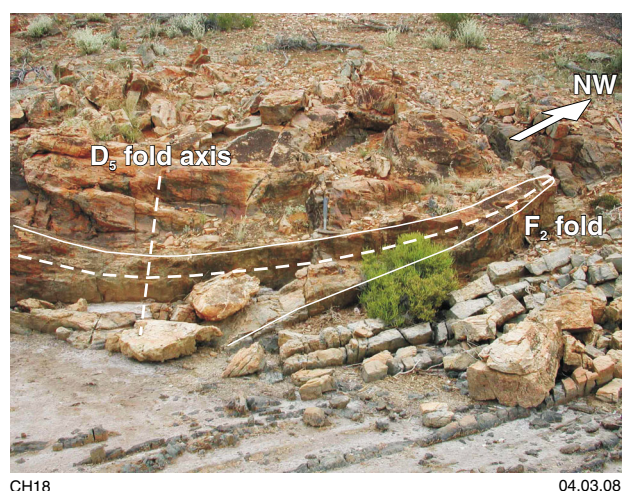


Figure 15. The axial surface of an F_2 fold is curved, indicating later warping

M_2 event

The M_2 event is recognized across YARDINA and the Eastern Goldfields Superterrane. It is characterized by mid-greenschist to amphibolite facies rocks with a mineral assemblage of quartz–muscovite–chlorite–feldspar–biotite and quartz–feldspar–biotite–amphibole–garnet (–staurolite–andalusite) in metasedimentary rocks (Fig. 16), and chlorite–feldspar–biotite–amphibole in metabasalts. Peak M_2 metamorphic conditions were most likely coeval with deformation during the D_2 event, as there is commonly an alignment of muscovite, quartz, chlorite, and amphibole parallel to the S_2 crenulation cleavage. This regional low- to medium-grade event is common throughout the Eastern Goldfields Superterrane and is thought to broadly reflect the distribution of granitic rocks (Witt, 1991; Ridley, 1993; Swager, 1997; Mikucki and Roberts, 2003). Deformation during the D_2 event was most likely contemporaneous with the widespread granite emplacement (Witt, 1991; Nelson, 1997; Swager et al., 1997).

In the southwestern part of YARDINA, strongly folded sandstone and interbedded mudstone units are predominantly metamorphosed at lower greenschist facies, but the metamorphic grade increases to amphibolite facies in the exposed cores of district-scale anticlines. A further increase in the metamorphic grade is observed towards the east, in the area adjacent to a large granite body (MGA 422500E 6462000N; Fig. 12) where sillimanite appears in muscovite schist, and most likely represents contact metamorphism during granite emplacement.

M_3 event

The M_3 event on YARDINA is a contact metamorphism of Archean country rocks at the margin of the Proterozoic Binneringie Dyke and of large granitic xenoliths with the body of the dyke. At the local scale the granitic rocks have a weak to moderate pinkish tinge and in thin section there is a strong saussuritization of feldspar and subordinate

minerals other than quartz. Contact metamorphism of the Mount Belches Formation, as noted by Painter and Groenewald (2001) on MOUNT BELCHES, was not observed on YARDINA.

Domain boundaries and major faults on YARDINA

Major faults and shear zones throughout the southern Eastern Goldfields region are typically covered by regolith or playa lake deposits, and are mainly identified by geophysical datasets, drilling, and mining operations (Goleby et al., 1993; Swager et al., 1997; House et al., 1999). Most faults and fault systems are poorly constrained in detail, but some larger fault systems are interpreted to be tens to hundreds of kilometres long. Some of these faults define the boundaries of the terranes and domains of the Eastern Goldfields Superterrane (Fig. 1). On YARDINA no major faults have been identified in outcrop. However, two major northwesterly trending faults (Lefroy and Mount Monger Faults) have been interpreted on YARDINA, and currently define boundaries of the Kambalda, Parker, and Bulong Domains (Fig. 1; Swager et al., 1995; Cassidy et al., 2006). These domains were largely defined by Swager et al., (1995) on the basis that firstly major structures such as D_1 thrust faults and F_2 folds could not be traced across the domain-bounding faults, and secondly that mafic units were either thin or absent in some domains when compared to the well-established regional stratigraphy in the Ora Banda and Kambalda Domains of Swager et al. (1995; see **Regional geology, Kalgoorlie Terrane** — younger greenstone succession).

Mount Monger Fault

The Mount Monger Fault is the terrane-bounding fault between the Kalgoorlie Terrane (<2710–2666 Ma) and the Kurnalpi Terrane (c. 2715–2680 Ma; Swager et al.,

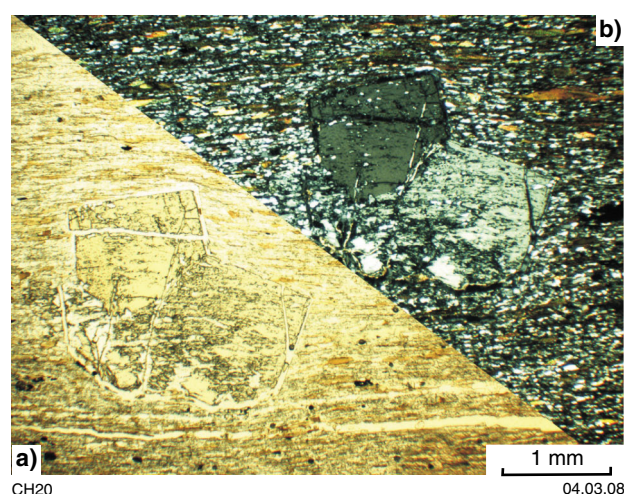


Figure 16. Twinned andalusite in a metasandstone of the Mount Belches Formation: a) plane-polarized light; b) cross-polarized light

1995, 1997; Cassidy et al., 2006). The fault, as interpreted from aeromagnetic data, extends southwards from MOUNT BELCHES through the centre of YARDINA (Fig. 1).

Aeromagnetic data indicate several lineaments on YARDINA that could be interpreted as a continuation of the fault, but these could also be related to the multiple granitic intrusions and dykes in northwest YARDINA. Furthermore, amphibolite-facies rocks of the Mount Belches Formation are mapped on either side of the possible fault extension on YARDINA (Hall et al., 2006), suggesting that either the position of the terrane boundary is incorrect, or that the Mount Belches Formation (<2666 Ma) was deposited after the amalgamation of the Kalgoorlie and Kurnalpi Terranes (Hall, 2007).

Lefroy Fault

The Lefroy Fault is a north-northwesterly trending fault that extends south from Kalgoorlie–Boulder and passes to the east of Kambalda (Fig. 1). The Lefroy Fault has been mapped truncating the eastern limb of the D₂ Kambalda anticline (Griffin, 1990) and was interpreted by Swager and Griffin (1990) as a left-lateral D₃ fault. Alternatively, Swager (1997) modelled the Lefroy Fault as a normal west-dipping fault above which a rollover anticline formed during extension between D₁ and D₂. Surface continuity of the fault is lost south of St Ives (Fig. 1) due to granitic intrusions and the vast expanse of Lake Cowan. However, aeromagnetic data and regional mapping (plate 2 in Griffin, 1990) across COWAN has been used to extend the fault to the southeast, and it is interpreted to cut across the southwest corner of YARDINA (Fig. 1). Cassidy et al (2006) considered it to be the boundary between the Kambalda and the Parker Domains in this area (Fig. 1).

Detailed mapping around lake margins in southwest YARDINA, where the Lefroy Fault is interpreted to extend, does not provide any evidence for a major shear zone, faulting, structural unconformity or significant change in lithofacies. From southwest to northeast, across the 'Lefroy Fault', rocks are tightly folded (see **D₂ event**), but do not appear to be truncated by transcurrent faulting or to be structurally repeated. Rather, the sequence appears to be continuous and is laterally consistent with rocks of the Black Flag Group of the Kambalda Domain, suggesting that the subdivision into the Parker Domain and Kambalda Domain is not warranted on YARDINA.

Proterozoic geology

On YARDINA exposed Proterozoic rocks are restricted to mafic rocks of the Widgiemooltha Dyke Suite (*PWl*) and siliciclastic rocks of the Woodline Formation (*Pwo*). Exposure of the east-northeast–west-southwesterly trending Widgiemooltha Dyke Suite (c. 2420 Ma) is restricted to the Binneringie and Jimberlana Dykes, which intrude both granitic and greenstone rocks. Aeromagnetic data of YARDINA reveal numerous magnetic lineaments with trends that parallel the Binneringie and Jimberlana Dykes, suggesting that similar dykes are more abundant than indicated by surface exposure.

Aeromagnetic images of YARDINA (Fig. 4) also show several magnetic lineaments with a northeasterly trend similar to that of the Fraser dyke swarm which has been dated at 1212 ± 10 Ma (Wingate et al., 2000). The Fraser dyke swarm is an extensive suite of dolerite dykes that is evident on aeromagnetic images of the southeast Yilgarn Craton, but is exposed in only a few working mines. The swarm is broadly parallel to the Yilgarn Craton–Albany–Fraser Orogen margin. Wingate et al. (2000) suggested that they were emplaced during a period of crustal relaxation during the Mesoproterozoic. The Fraser dyke swarm does not outcrop on YARDINA, but northeast-trending dykes that probably form part of the swarm are interpreted from aeromagnetic images.

The latest deformation and metamorphism that is recognizable on YARDINA is that attributed to the Albany–Fraser Orogeny.

Widgiemooltha Dyke Suite (*PWiji-o*, *PWiji-ax*, *PWiji-og*, *PWiji-oh*, *PWiji-ow*, *PWlbi-om*, *PWlbi-gi*)

Two examples of the east-northeasterly trending Paleoproterozoic Widgiemooltha Dyke Suite (Sofoulis, 1966) exposed on YARDINA are the Binneringie and Jimberlana Dykes. The largest of these dykes, the Binneringie Dyke (*PWlbi*) can be traced discontinuously for 600 km across the Yilgarn Craton, and has a maximum width of 3.5 km near the northern margin of Lake Cowan. The dyke forms a prominent east to northeasterly trending ridge on YARDINA, with abundant exposure along the north margin of Lake Cowan. The Jimberlana Dyke (*PWlji*) is 180 km long, and up to 2.5 km wide. Exposure of the Jimberlana Dyke on YARDINA is limited to a few outcrops in the southeast corner.

The dykes are typically vertical to subvertical with sharp contacts and narrow chilled margins (Hallberg, 1987). Granitic rocks in contact with the dykes typically show the effects of thermal metamorphism 1–2 m from the contact, but these effects can be seen as much as 50 m into the granitic body. At a regional scale the trend of the contact with host rocks are typically east northeast, but embayments and apophyses do extend into adjacent country rocks locally. An aeromagnetic image of the Binneringie Dyke (Fig. 4) indicates that the maximum dyke width is about 2.5 km (Fig. 4). Vertical magmatic layering with both cryptic and rhythmic layering is reported from marginal zones in the Binneringie Dyke (McCall and Peers, 1971), but true phase layering with cumulate textures has only been reported from the Jimberlana Dyke (Campbell et al., 1970).

The Binneringie Dyke is predominantly gabbroic, but more intermediate and granophyric phases are locally observed. Marginal phases of the dyke are dominated by magnesium-rich pyroxenes (bronzite), whereas gabbroic rocks towards the centre of the dyke become more progressively iron-rich with augite–pigeonite the common pyroxene (McCall and Peers, 1971). Smaller internal and finer grained mafic

dykes crosscut the larger body (Fig. 17). At the western margin of YARDINA, where the Binneringie Dyke extends onto the adjacent COWAN map sheet, the dyke encloses a granite body (about 1.6 km at its widest point). The granite was originally interpreted by McCall and Peers (1971) to represent a granophyric phase within the dyke, however, Griffin (1989) has, on the basis of composition and field relationships interpreted it to be a hornfelsed granite.

On YARDINA exposures of the Jimberlana Dyke are restricted to small outcrops in the southeast corner. Outcrops are predominantly rubbly with only minor in situ exposure, but units identified include: undivided Jimberlana Dyke (*PWlji-o*) comprising dolerite, gabbro, gabbro-norite and norite in areas with poor exposure; pyroxenite (*PWlji-ax*); gabbro (*PWlji-og*); hornblende gabbro (*PWlji-oh*) and minor norite (*PWlji-ow*).

The Jimberlana Dyke is interpreted to be funnel shaped (in cross section), with an internal lopolitic structure, similar to the Great Dyke of Zimbabwe (Campbell et al., 1970; Campbell, 1991). In the Norseman area nine separate canoe-shaped complexes are recognized which delineate a three-layered series along a strike length of 150 km (Keays and Campbell, 1981; Campbell, 1991). The marginal layered series in the lower part of the dyke consists of gabbroic to ultramafic rocks with adcumulate to orthocumulate textures. The lower layered series is a repeated sequence of olivine and bronzite cumulates overlain by plagioclase–augite–hypersthene cumulates. Unconformably overlying the lower layered series is an upper layered series that represents a fresh pulse of magma (Campbell, 1977). The upper layered series has similar rhythmic layering and composition to the lower layered series, but is capped by a granophyric layer (Campbell et al., 1970; Campbell, 1977; Keays and Campbell, 1981).

Nemchin and Pidgeon (1998) obtained an age of 2418 ± 3 Ma for the Binneringie Dyke, based on the concordia intercept of three conventional baddeleyite U–Pb ages from a granophyric phase of the dyke near Narrogin. Six baddeleyite grains from the same sample were analysed by the U–Pb SHRIMP technique and gave a Pb/Pb age of 2420 ± 7 Ma. Fletcher et al. (1987) obtained a Sm–Nd isochron age of 2411 ± 55 Ma on Jimberlana Dyke using samples from drillcore at Bronzite Ridge near Norseman. This age is within error of the 2411 ± 52 Ma Rb–Sr result on mineral separates from the Celebration and Jimberlana dykes by Turek (1966).

Woodline Formation (*Ewo-sl*, *Ewo-stq*)

The Woodline Formation, originally named the Woodline Beds by Sofoulis and Bock (1963), forms prominent northeasterly trending hills and ridges with scattered outcrops along the central eastern margin of YARDINA. The formation continues onto YARDILLA and ERAYINIA in a northeasterly trending belt more than 50 km long (Jones, 2005; Jones and Ross, 2006). Based on drillhole data (Asarco Ltd, 1971; Western Mining Corp Ltd, 1992a) the

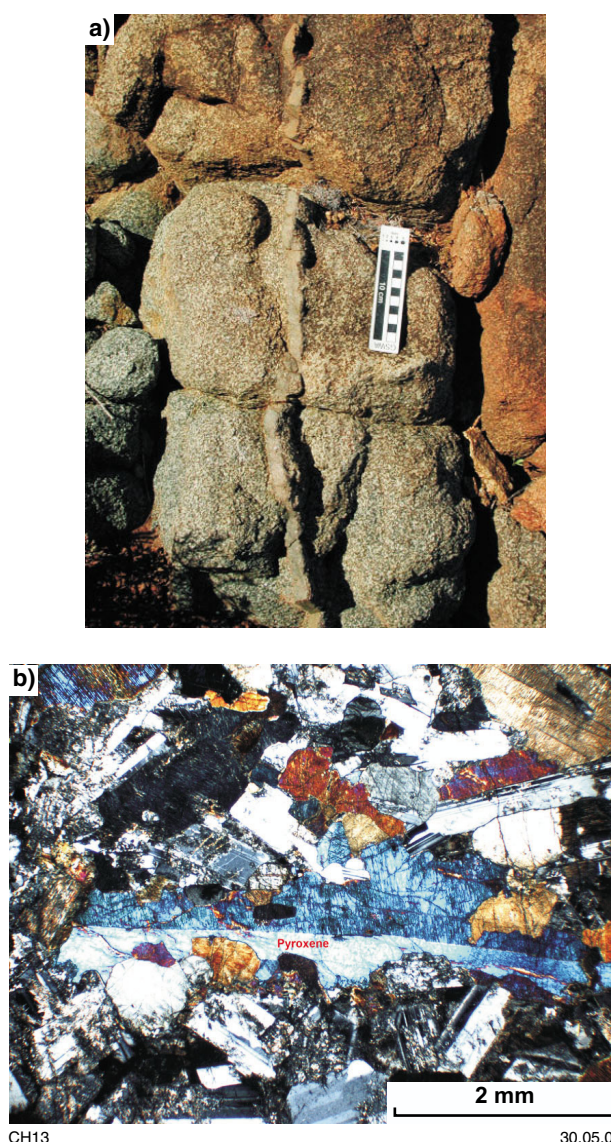
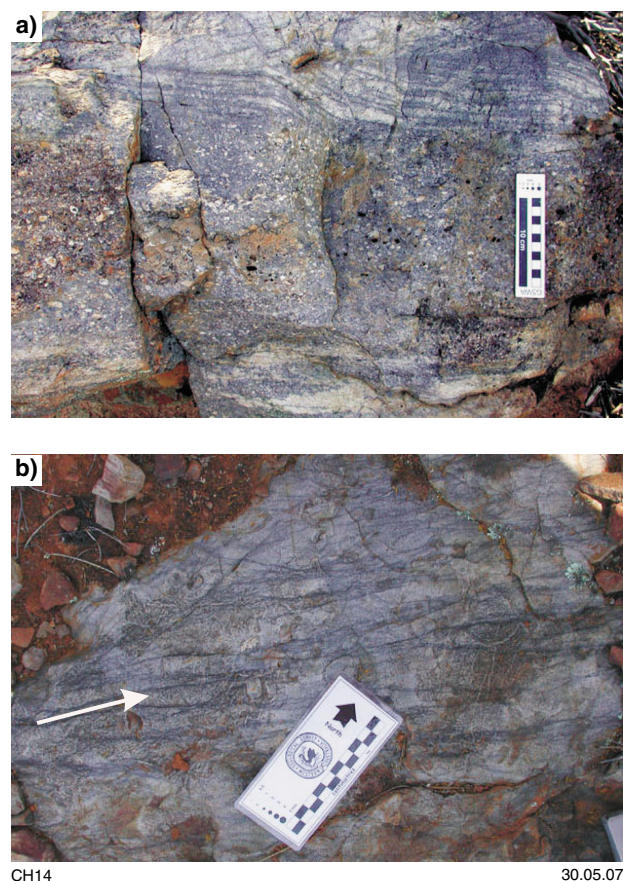


Figure 17. The Binneringie Dyke of the Widgiemoooltha Dyke Suite: a) gabbro–norite crosscut by a 1–2 cm-wide fine-grained mafic vein; b) cross-polarized photomicrograph of gabbro-norite with 4 mm-long, twinned clinopyroxene in the centre

unit is about 250 m thick and consists predominantly of quartz-rich sandstone and minor conglomerate (*Ewo-stq*) and siltstone (*Ewo-sl*; Fig. 18). On YARDILLA matrix- to clast-supported monomict chert breccias with clasts up to 20 cm are interbedded with quartz-rich sandstones and siltstones (Jones, 2005). Although the base of the Woodline Formation is poorly exposed, there is an angular unconformity between the formation and the underlying Archean rocks on ERAYINIA to the north (Jones, 2007; Hall and Jones, 2005). A similar relationship was reported by Griffin (1989) on YARDINA (MGA 450627E 6499528N), but is no longer exposed.

Woodline Formation rocks are gently folded with a weak to moderately developed spaced cleavage (Fig. 18), and are metamorphosed at lower greenschist facies. Although weakly deformed, outcrops are relatively fresh and



CH14

30.05.07

Figure 18. The Woodline Formation: a) pebbly conglomerate grading up to a cross-bedded sandstone (top of picture); b) pressure-solution cleavage (dark-grey streaks as indicated by the arrow) trending 045–060°, which is subparallel to the Albany–Fraser Orogen at the Yilgarn Craton margin

sedimentary structures such as tabular bedding, trough cross-bedding, rip-up clasts, ripple marks, sole marks, scours, and graded beds are well preserved. Graded bedding, scoured bases, and truncated cross-bedding indicate upright bedding.

Sandstones of the Woodline Formation contain grains of chert, monocrystalline quartz grains with straight or weak undulose extinction, and rare quartz grains with deformation lamellae. The rock contains no feldspar, and accessory minerals (zircon, tourmaline, amphibole, and mica) are rare. The well-sorted, well-rounded, and quartz-rich nature of the sandstone units of the Woodline Formation indicates deposition distal from the source. Conglomerates, cross-bedded sandstones, ripple marks, and sole marks indicate a relatively high-energy, possibly fluvial, depositional environment such as a braided stream system. Trough cross-beds and ripple crests in Woodline Formation rocks on ERAYINIA and YARDINA indicate paleoflow directions from the northwest and northeast (Hall et al., 2008). Up section, ripple crests in the quartz-rich sandstone units become symmetrical and siltstone to mudstone units increase in thickness, which suggests a change from fluvial to fluvial deltaic deposition.

Sofoulis (1966) interpreted the Woodline Beds as shallow-water sediments resting unconformably on Archean sedimentary rocks and Middle Proterozoic granite. Griffin (1989) recorded a broadly upward-coarsening package, from minor conglomerates and sandstones at the base to slate and pelitic schists to quartzites with trough cross-bedding, pebbly sandstones, and minor breccia (<1 m thick) at the top. Griffin (1989) inferred depositional settings ranging from shallow-marine or fluvial for coarse-grained metasedimentary rocks (e.g. quartzites) to a low-energy aqueous setting for the mudstones.

Turek (1966) obtained a whole-rock Rb–Sr isochron date of 1620 ± 100 Ma for eight siltstone samples from the Woodline Beds and interpreted this date as a maximum depositional age. SHRIMP U–Pb data from detrital zircons of the Woodline Formation yielded concordant ages ranging from c. 3747 to c. 1737 Ma, giving a maximum depositional age and indicating a provenance that extends back to the Paleoarchean Era (Hall and Jones, 2005). These ages are similar to the maximum depositional age of 1696 ± 7 Ma obtained for the Mount Barren Group, 400 km to the southwest (Dawson et al., 2002), which may be a lateral equivalent of the Woodline Formation.

The Woodline Formation was interpreted by Myers (1995) to represent an allochthonous sequence thrust onto the Yilgarn Craton during the Albany–Fraser Orogeny between 1300 and 1100 Ma. However, the unconformable basal contact, deformation patterns, and detrital zircon geochronology indicate that the Woodline Formation was sourced from several provenances, including granitic rocks of the Eastern Goldfields Superterrane and metasedimentary rocks of the Yilgarn Craton (Hall and Jones, 2005). The Woodline Formation was deposited after 1737 Ma, but prior to the Albany–Fraser Orogeny.

Undivided mafic and ultramafic dykes, including the Fraser dyke swarm (*Pod*)

Aeromagnetic images of the southeastern Yilgarn Craton margin, including YARDINA, highlight numerous magnetic lineaments crosscutting the Archean rocks (Fig. 4). The lineaments are inferred to be Proterozoic mafic and ultramafic dykes (*Pod*). However, no dykes have been recognized in outcrop on YARDINA. Dykes with a northeasterly trend are likely to be part of the Fraser dyke swarm that intrudes the southeastern Yilgarn Craton, parallel to the Albany–Fraser Orogen. These dykes are predominantly composed of undeformed dolerite (Wingate et al., 2000).

Wingate et al. (2000) obtained a mean $^{207}\text{Pb}/^{206}\text{Pb}$ age of 1212 ± 10 Ma from baddeleyite extracted from a northeasterly trending dyke in an opencut mine at Kambalda, 100 km to the northwest. This age is similar to SHRIMP zircon ages reported by Evans (1999) for east-trending dolerite and quartz–diorite dykes (1202 to 1216 Ma) in the southern (Gnowangerup dyke swarm)

and central (Wheatbelt dyke swarm) parts of the Yilgarn Craton adjacent to the western Albany–Fraser Orogen. Wingate et al. (2000) suggested that the Fraser dyke swarm was emplaced coevally with the 1345–1140 Ma Albany–Fraser Orogen, subparallel to the suture in a zone of flexure formed by crustal loading during orogenesis.

Albany–Fraser Orogeny

The last major deformation event (D_5) in the region is related to the Mesoproterozoic collision of East Antarctica forming part of the Mawson Craton with the southern and southeastern margin of the Yilgarn Craton (Jones, 2006). On YARDINA D_5 deformation has resulted in gentle warping of F_2 folds (Fig. 15).

Deformation in the Woodline Formation

The Woodline Formation is typically only weakly deformed, with open upright folding and warping. A weak to moderately developed axial-planar cleavage is defined by a fine anastomosing pressure-solution fabric in the quartz sandstones (Fig. 18b) and fine-grained aligned muscovite defines the foliation in the siltstone. Bedding (S_0) is well preserved, with shallow to moderate dips, and younging indicators show that beds are not overturned.

Abundant small northeast-oriented thrust faults are also observed throughout the Woodline Formation. The faults are predominantly shallow northwest- and southeast-dipping structures, with quartz slickenfibres indicating dominantly reverse or oblique reverse displacement (Fig. 19). Offset on these structures is typically less than a metre, and the faults have little effect on the stratigraphy. The small thrust faults most likely developed during the Albany–Fraser Orogen-related deformation (D_5).

Proterozoic metamorphism

Metamorphic effects related to the Albany–Fraser Orogen (M_5) are recognized in the Proterozoic Woodline Formation and underlying Archean metasedimentary rocks in eastern YARDINA. The metamorphic facies assemblage in the sandstones and siltstones of the Woodline Formation is consistent with lower greenschist-facies metamorphism. Fine-grained muscovite is common in the siltstone, with rare fine muscovite in the matrix of the quartz-rich sandstone. In drillcore samples (DDH1; Asarco Limited, 1971), there is a sharp change in metamorphic grade from lower greenschist facies (M_5) in the Woodline Formation to amphibolite facies (M_2) in underlying Archean metasedimentary rocks that contain garnet and biotite. These Archean metasedimentary rocks also display retrograde minerals with chlorite replacing garnet and cordierite, suggesting a greenschist-facies metamorphic overprint (M_5) in the amphibolite-facies metasedimentary rocks.

Cenozoic geology

The Cenozoic geology of YARDINA is characterized by deposits of deltaic to marine sedimentary rocks associated with paleodrainage channels incised during the Mesozoic (Clarke, 1994), and by deep weathering profiles and lateritization. The deposition of deltaic to marine sediments was the result of extensive marine transgressions during the Eocene across the Eucla Basin (Clarke, 1994; Clarke et al., 2003). Early reports on the marine to non-marine Eocene sediments assigned the sediments found in the southeastern parts of the Yilgarn Craton to the onshore Bremer Basin (Cockbain, 1968; Hocking 1994). However, Clarke et al. (2003) have demonstrated a similar stratigraphy between the Eocene sediments of the onshore Bremer and Eucla Basins and have proposed

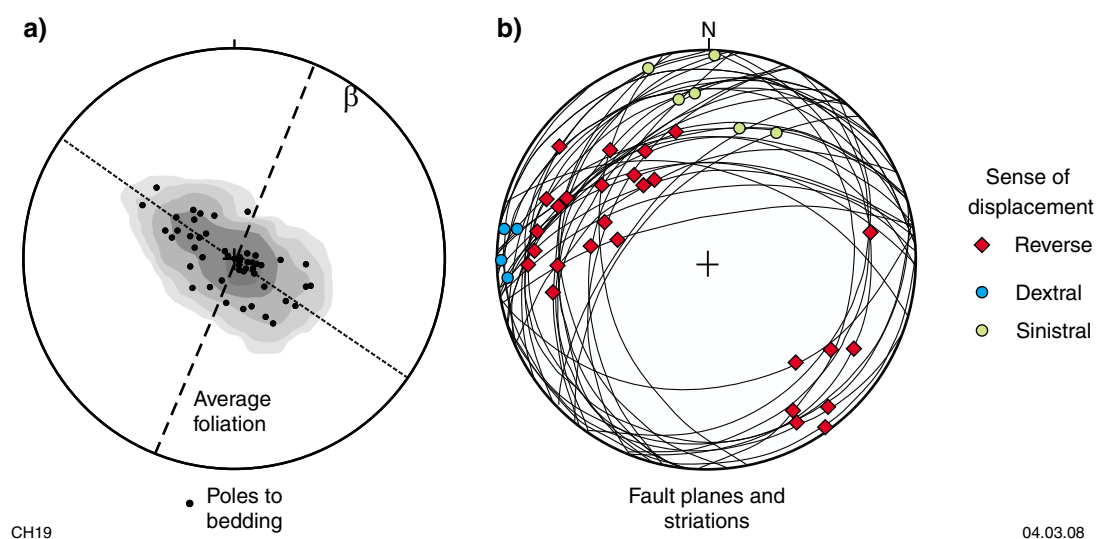


Figure 19. Stereoplots illustrating: a) poles to bedding and the open upright style of folding; b) faults measured in the Woodline Formation, which are predominantly shallow northwest- and southeast-dipping, oblique thrust faults

Table 5. Stratigraphy of the Eocene Eundynie Group in the Cowan and Lefroy paleodrainage channels on YARDINA

Epoch	Marine trans- gression	Group	Existing stratigraphy		Proposed stratigraphy (Clarke et al., 2003)	
			Cowan Paleovalley	Lefroy Paleovalley	Cowan Paleovalley	Lefroy Paleovalley
Oligocene to Holocene		Redmine Group				
Late Eocene	Tuketja	Eundynie Group	Princess Royal Spongolite	Princess Royal Spongolite and Hampton Sandstone	Pallinup Formation (Princess Royal Member)	Pallinup Formation (Princess Royal Member)
Mid–Upper Eocene	Tortachilla		Upper Werrillup Formation	Pidinga Formation	Werrillup Formation	Werrillup Formation
			Norseman Formation	Pidinga Formation	Norseman Formation	No unit recognized
Middle Eocene			Lower Werrillup Formation	Pidinga Formation	North Royal Formation	North Royal Formation

Source: Clarke et al., 2003
CH26

06.03.08

that the term Bremer Basin be abandoned for the onshore Eocene succession. The Cenozoic stratigraphy of the Eucla Basin presented by Clarke et al. (2003) is summarized in Table 5.

Two major transgressions recognized across the Eucla Basin are known as the Tortachilla and Tuketja transgressions. The earliest preserved sedimentary rocks deposited during these transgressions, commonly found within the paleochannels (Fig. 20), are the Eundynie Group (Cockbain, 1968) and the post-Eocene Redmine Group. Only the Eundynie Group is recorded on YARDINA.

Eundynie Group (*EeEU-s*, *EeEU-kl*)

The Eocene Eundynie Group contains fluviodeltaic, estuarine, and marine sediments, and is exposed throughout the southern Eastern Goldfields, predominantly within large dendritic paleodrainage channels such as the Cowan and Lefroy paleodrainages that formed at the margins of the Eucla Basin. On YARDINA the paleodrainage channels are spatially associated with the present-day drainage system of Lake Cowan. This drainage system is also described in the hydrogeology report of the WIDGIEMOOLTHA 1:250 000 sheet (Kern, 1996). Although the Cowan system now flows south towards the offshore Bremer Basin, it is thought to have originally flowed to the northeast, based on the acute angle of convergence with the Lefroy system (Hocking and Cockbain, 1990; Clarke, 1994). Reversal of the Cowan channel, as a result of uplift along the Jarrahwood Axis between the Cowan and Lefroy paleodrainage channels (Fig. 20), occurred during post-Eocene warping of the area. Dips up to 8° are recorded in some of the large tabular bedded sandstone units of the Eundynie Group in northern YARDILLA (Jones, 2005) and on the MOUNT BELCHES (Painter and Groenewald, 2001).

Outcrops of undivided Eundynie Group (*EeEU-s*) are common in the northern, eastern and southwestern parts of YARDINA, and are spatially associated with the present-day drainage channels and playa lakes. Undivided Eundynie Group consists of a range of facies including poorly sorted fine- to medium-grained sandstone, interbedded siltstone and mudstone, granular conglomerate, and spongolite. The outcrops are typically deeply weathered, with ubiquitous iron staining and silicification obscuring many original features. The sediments are only weakly to moderately consolidated, and silcrete, calcrete or ferricrete commonly forms a cap over the outcrops. Massive, variably spongolitic, fine-grained sandstone to siltstone is the most common Eocene unit observed on YARDINA. Bedding is poorly defined, but rare graded bedding, flaser bedding, and bioturbation textures dip up to 11°. The flat-lying nature of the Eundynie Group and the presence of silcrete and calcrete caps results in the formation of breakaway and ‘mesa-type’ outcrops, which form scarps up to 8–10 m high beside the playa lakes, particularly on the western and northwestern margins of the lakes, with Eocene rocks resting unconformably above Precambrian basement rocks (e.g. Junction Lake).

Sponge spicule-rich outcrops are generally massive, limonite stained, and commonly disintegrate to cobble- to pebble-sized fragments. Fine, irregular burrows in white- to cream-coloured siltstone to very fine sandstone and fine- to medium-grained quartz-rich sandstone with shelly fragments are also observed in this unit. Similar rock units are found on ERAYINIA, including bivalve fragments in semiconsolidated sandstone (Jones, 2007).

Trace fossil burrows up to 150 mm long and 12–14 mm wide are found in well-sorted siltstone in the northern regions of YARDINA. The burrows are most similar to *Rhizocorallium* sp. (Fig. 21a) and are most commonly horizontal to bedding, although vertical burrows are

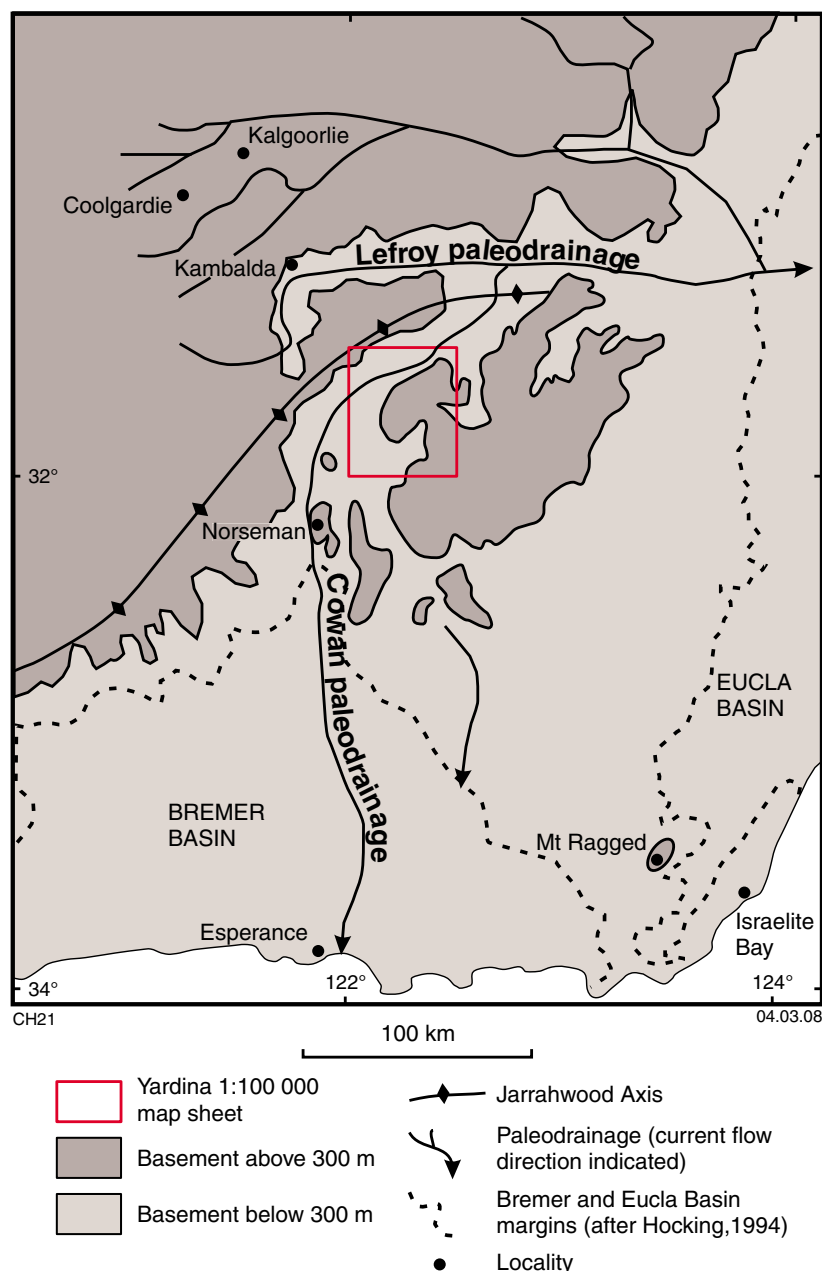


Figure 20. The location of YARDINA (red box) with respect to the Cenozoic Lefroy and Cowan paleodrainage channels (modified from Clarke, 1994)

also present. *Rhizocorallium* trace fossils are part of the *Cruziana* ichnofacies commonly associated with depositional environments such as estuaries, lagoons, and continental shelves (Frey and Pemberton, 1984).

Fossil-rich limestone (*EeEU-kl*) outcrops along the eastern and northern shore of Lake Cowan in the northern part of YARDINA. A macrofossiliferous unit adjacent to the southern margin of the Binneringie Dyke and exposed beneath sand dunes at the edge of Dog Lake (MGA 434683E 6510558N) has abundant shelly fragments of bivalves, brachiopods, echinoderms, and bryozoa in a sandy calcite-rich matrix (Fig. 21b).

A second limestone unit, found on the eastern margin of Lake Cowan (MGA 420300E 6497000N), unconformably overlies Archean rocks including granite, clinopyroxene-bearing syenite, and well-bedded metasedimentary rocks. The limestone is very well indurated, with abundant microfossils and shelly fragments. Microscopically, the rock comprises fragmental and complete foraminifera tests, fragmental shelly detritus, 1–2% subangular monocrystalline quartz, and 2–4% iron-stained glauconite in a sparry calcite cement (Fig. 21c). Bedding is poorly defined to massive, and weathered surfaces have a karren-like appearance. Western Mining Corporation Ltd (1976) reviewed the potential of this unit for use as a nickel-

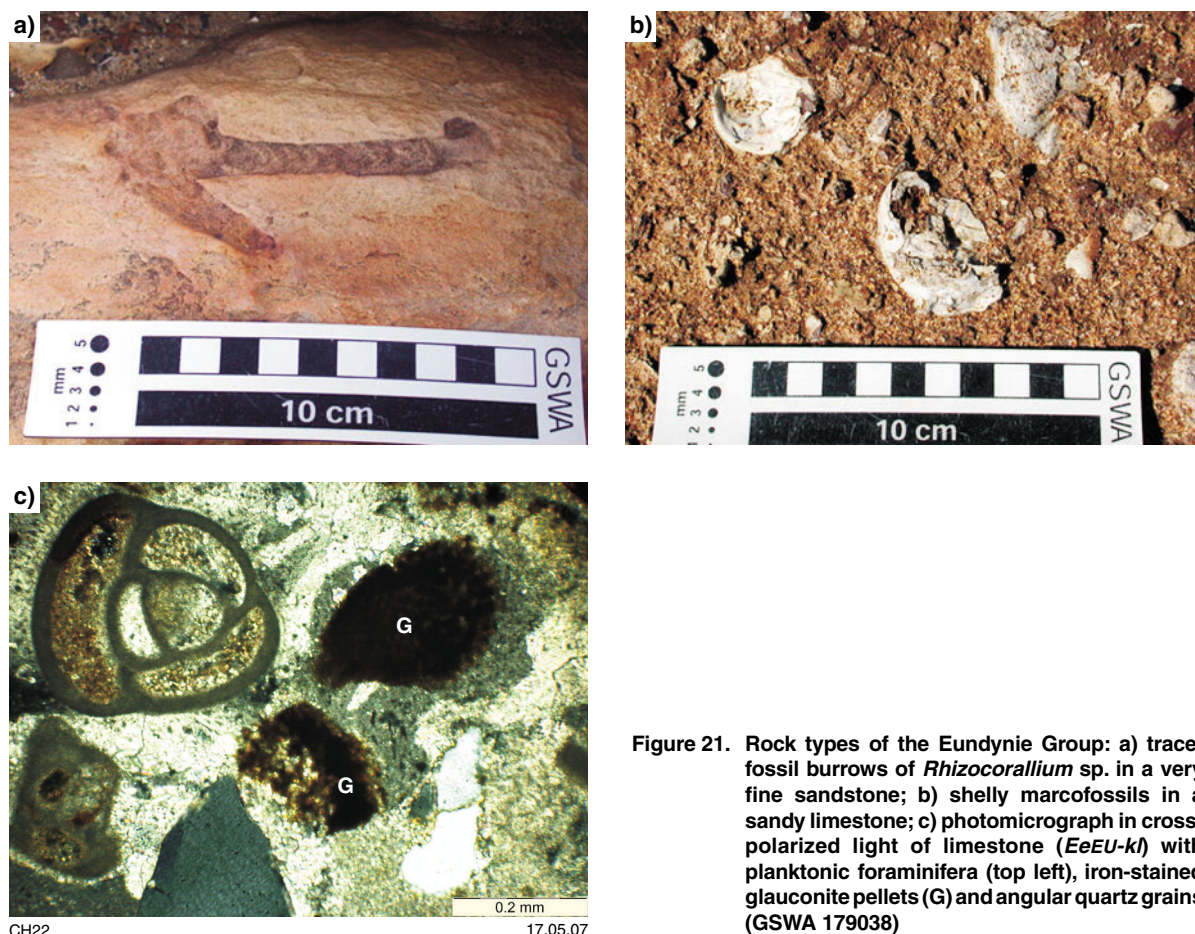


Figure 21. Rock types of the Eundynie Group: a) trace-fossil burrows of *Rhizocorallium* sp. in a very fine sandstone; b) shelly macrofossils in a sandy limestone; c) photomicrograph in cross-polarized light of limestone (*EeEU-kl*) with planktonic foraminifera (top left), iron-stained glauconite pellets (G) and angular quartz grains (GSWA 179038)

smelter flux in their Binyaryinyinna limestone exploration program. Nine percussion and three diamond holes were drilled in late 1973, which encountered limestone, clays, and ferruginous silcrete in the top 6–10 m that overlay 10–20 m of coquina in a muddy matrix. Geochemical sampling indicated an ore grade in the coquina in the top 2.63 m with an average CaO value of 27% (Western Mining Corporation Ltd, 1976). No further work on the limestone has been undertaken since 1976.

On YARDINA the majority of outcrops of undivided Eundynie Group comprise spongolitic sandstone and associated sedimentary rocks that most likely correlate with the Late Eocene Pallinup Formation (Cowan Paleochannel; Clarke et al., 2003). The limestone units can be correlated to the Norseman Formation (Clarke, 1994; Clarke et al., 2003), a highstand system tract of the Tortchilla transgression. Clarke et al. (2003) suggested that the bryozoan–mollusc-rich limestone was deposited at a maximum depth of between 15 and 110 m in a drowned estuary of the Cowan paleodrainage channel.

The quartz sandstone and siltstone units that are observed in vertical sections adjacent to the playa lakes are difficult to correlate to the Norseman Formation. These units may be part of the non-marine to marginal-marine Middle Eocene North Royal Formation, or unconformably above the Norseman Formation, and associated with Late

Eocene Werillup Formation (Table 5). On YARDILLA, east of YARDINA, Jones (2005) reported spongolitic sandstone (Pallinup Formation) unconformably overlying clay, cross-bedded and channelized sandstones with plant rootlets and carbonized wood, siltstone, and lignite, suggesting that the basal sediments are part of the non-marine to marine North Royal Formation.

The Cenozoic sedimentary sequence reflects two marine transgressions during the Middle to Late Eocene (Clarke, 1994; Clarke et al., 2003). The first transgression, the Tortachilla, resulted in the deposition of fluviodeltaic to estuarine sediments (North Royal Formation) that were in turn overlain by fossiliferous limestone of the Norseman Formation. The second transgression, the Tuketja, was more extensive and during a highstand the spongolitic Princess Royal Formation was deposited in an estuarine environment.

Regolith

The prolonged stability of the Yilgarn Craton, combined with marked climate change from wet, humid conditions in the Paleogene to semi-arid conditions that have prevailed from the Neogene, has resulted in deep weathering and development of complex regolith profiles (Anand and Paine, 2002). On YARDINA thick sheetwash or eolian deposits, or both, cover much of the area.

Residual and relict units (*Rc*, *Rf*, *Rf_g*, *Rg*, *Rgp_g*, *R_ic_kp_m*, *R_iqs*, *Rk*, *Rmp*, *R_s*, *Rw*, *Rz*)

On YARDINA residual lateritic profiles are best preserved along the trend of the Cowan paleodrainage channel and around small playa lakes. In these areas the deeply weathered bedrock grades upward into kaolinitic saprolite and a mottled zone that is variably kaolinitic and ferruginous, and typically capped by a variably siliceous and ferruginous duricrust or lag. At most localities only duricrust or lag is observed.

Siliceous duricrust (*Rz*) and ferruginous duricrust (*Rf*) overlie a range of rock types, from Archean metasedimentary rocks and granites to Tertiary sedimentary rocks. Ferruginous duricrust typically comprises hematite and lesser goethite, with minor siliceous lenses. The duricrust predominantly forms low ridges of massive to rubbly outcrops over volcanoclastic and siliciclastic rock in the north.

Residual units over granite (*Rg*, *Rgp_g*) are predominantly composed of clay- and quartz-sand-rich soil with minor silcrete, calcrete, and poorly exposed weathered granite. These deposits are common over the extensive granitic domain from the northwestern to the southeastern part of YARDINA. Mottled to saprolitic zones (*R_ic_kp_m*) above monzogranites, with deeply incised channels or metre-high breakaways, are common at the western ends of small paleolakes, and at the northern end of Lake Cowan. These sites typically have a megamottled zone within which there is a clear transition from a hematite-stained mottled section to white kaolinitic clay (Fig. 22). Quartz-rich residual sand (*R_s*) and clay (*Rc*) are mainly above granitic units.

Residual calcrete (*Rk*) is common in the south and southeastern corner of YARDINA. Low ridges and rubbly outcrops are commonly surrounded by colluvium with abundant loose calcrete nodules and fragments (*Ck*).



CH23

17.05.07

Figure 22. Megamottles in saprolite above monzogranite. Haematite-stained megamottle (deep red) changes to kaolinitic clay (white areas)

Deep-red unconsolidated soil overlying mafic and ultramafic Proterozoic rocks (*Rmp*) is restricted to areas overlying the Binneringie Dyke in the northeast corner of YARDINA. Three small gossans (*Rf_g*) overlie the Jimberlana Dyke in the southeast.

Quartz-rich sand- to pebble-sized clasts of quartzite and sandstone (*R_iqs*) are common on flat-topped ridges of the Woodline Formation, which are commonly surrounded by colluvium with a similar composition.

Deeply weathered bedrock (*Rw*) for which the protolith cannot be determined is restricted to small outcrops, commonly at lake margins, scattered over YARDINA.

Colluvium and sheetwash (*C*, *Cf*, *Cg*, *Ck*, *Cm*, *Cq*, *C_imp_r*, *Cts*, *Cz*, *Czu*, *W*, *Wf*, *Wg*, *Wk*, *Wq*)

The distinction between colluvium and sheetwash is based on slope, where colluvium (*C*) is classified as mass wasting deposits on significant to perceptible slope, and sheetwash deposits (*W*) are found on ground with a minimal gradient and are adjacent to Quaternary alluvial channels (Hocking et al., 2001). Undivided colluvium (*C*) and sheetwash (*W*) are predominantly composed of clay, silt, and sand; calcrete and silcrete fragments; lithic clasts; and minor ferruginous granules and nodules. Iron-rich colluvium (*Cf*) and sheetwash (*Wf*) consist of fine ferruginous granules and lateritic gravel, and are most common adjacent to the Proterozoic mafic dykes where they are associated with a colluvium dominated by pebble- and cobble-sized mafic lithic rocks (*C_imp_r*).

Quartzofeldspathic colluvium (*Cg*) and sheetwash (*Wg*) are present above and adjacent to granitic rocks in western YARDINA. They consist mainly of clay, quartz sand, and lithic fragments of granitic composition. Calcrete-rich colluvium (*Ck*) and sheetwash (*Wk*) deposits have significant proportions of calcrete nodules and fragments. The calcrete-rich colluvial deposits commonly form low ridges and are found over most of YARDINA.

Colluvium derived from ferromagnesian rocks (*Cm*) and colluvium from siliceous caprocks (*Czu*) overlie, and are adjacent to, outcrops of the Binneringie and Jimberlana Dykes respectively. Quartz-rich colluvium (*Cq*) and sheetwash (*Wq*) are composed of angular vein-quartz fragments, and are common on the edges of the playa lakes and around large quartz blows. Silcrete-dominant colluvium (*Cz*) is a small component of the regolith, and is typically found at the margins of granitic rocks.

Lithic-rich colluvium (*Cts*) lies on slopes immediately adjacent to outcrops of the Woodline Formation, forming a distinct apron around these quartz-rich outcrops.

Lacustrine units (*L_d1*, *L_d2*, *L_d2k*, *L_m*, *L_p*, *L_xgm_m*, *L_xmp_r*)

The playa lake systems on YARDINA are dominated by the present-day forms of Lake Cowan and Dog Lake, which

are remnants of the larger Cowan Paleochannels (Clarke, 1994). Away from the larger lakes the playa-lake systems are made up of chains of small lakes separated by sand dunes, sandplain deposits, alluvial deposits, and small channels. The lakes form flat expanses of clay, mud, and sand with abundant gypsum, halite, and carbonate (L_p).

Active dunes (L_{d1}) are variably composed of orange-yellow eolian sand and gypsum, and are typically non-vegetated or have only minor vegetation predominantly of samphire and saltbush. Stabilized dunes (L_{d2}) consist of eolian sand and clay and are vegetated predominantly by eucalypts, and locally by *Casuarina* sp. and *Cypress* sp., particularly near rocks of the Widgiemooltha Dyke Suite.

Sand dunes with calcrete nodules (L_{d2k}) are most common in the southeastern corner of YARDINA where there are extensive residual and colluvial deposits of calcrete (Rk and Ck respectively). Fringing lacustrine deposits (L_m) are located on broad plains adjacent to the playa lakes and consist of closely interspersed dunes, small lakes, and alluvial and sheetwash deposits.

Bedrock subcropping in the floor of small playa lakes, commonly at the periphery of larger lakes such as Dog Lake, includes metasedimentary rocks (L_{sgm}) and rocks of the Widgiemooltha Dyke Suite (L_{spm}). The trend of the subcropping basement in the playa lakes is commonly clearly seen on aerial photographs and gives a good indication of the strike of the sedimentary rocks.

Sandplain units (S , S_d , S_p , S_u , k)

Sandplain deposits (S) on YARDINA are extensively developed adjacent to major present-day drainage systems such as Lake Cowan and Dog Lake. Sand and playa terrain (S_p) with stabilized dunes (S_d) forms an undulating region east of Lake Cowan and between the Binneringie Dyke and the granite-dominated area in the centre of the sheet.

Sand dunes with abundant calcrete nodules and fragments (S_{uk}) border the eastern margins of Lake Cowan.

Alluvial units (A , A_e , A_p , A_r , A_u)

Quaternary alluvium (A) on YARDINA includes ephemeral, incised stream-channel deposits with stream bars (A_r) and overbank deposits. Alluvium consists of clay, silt, sand, and gravel of mixed composition.

Deltaic deposits (A_e) are commonly found at the mouths of streams that discharge into Lake Cowan, and are best seen on aerial and satellite imagery.

Non-vegetated to semi-vegetated clay and silt-filled claypans (A_p) are relatively common along the drainage systems throughout YARDINA. Superficial, narrow ephemeral streams (A_u) that run off granite-dominated and sandplain areas in the centre of YARDINA typically only develop during very heavy precipitation, and terminate at a sheetwash zone (W).

Economic geology

The only commodity produced on YARDINA is tantalum from pegmatites intruding metasedimentary rocks of the Mount Belches Formation at the Bald Hill mine. Surface and near-surface exploration has been carried out for many commodities such as gold, nickel, uranium, and tantalum. Various techniques have been employed including aircore (AR), rotary air blast (RAB), reverse circulation (RC) and diamond drilling, geological mapping, geophysics, and rock-chip and soil sampling.

Vein and hydrothermal mineralization — undivided

Precious metal — gold

Although gold deposits and prospects have been reported on the adjacent sheets of MOUNT BELCHES to the north (Randalls and Karnilbinia mining centres), ERAYINIA to the northeast (French Kiss prospect), and at numerous workings to the west on COWAN (west of the Lefroy Fault), no economic finds have been reported on YARDINA.

The most extensive mineral exploration, consisting of RAB drilling programs and limited diamond drilling, has been carried out along the central-western margin and southwestern corner of YARDINA. This exploration followed up gold anomalies in soil or rock-chip samples, and tested structural targets identified by geophysical surveys. The only open-file data from this area is from the Jeffreys Gold project (MGA 419880E 6465305N), where Red Back Mining NL (1998) estimated an indicated resource of 0.347 Mt at an average grade of 2.260 g/t Au.

Minor drilling for gold in northeastern YARDINA was a part of much larger drilling programs on MOUNT BELCHES, ERAYINIA, and YARDILLA.

Pegmatitic mineralization

Speciality metal — tantalum

Tantalite is mined from pegmatites in the openpit at the Bald Hill tantalum mine operated by Haddington Resources Limited. The mine is near the northern edge of YARDINA (MGA 421898E 6512948N) where tantalum-rich pegmatites, 1–8 m thick and with a shallow dip, have intruded steeply dipping sandstones and siltstones of the Mount Belches Formation. In December 2002 the (non-JORC) resource at the Bald Hill mine was 2.09 Mt at 375 ppm tantalum pentoxide containing 1.5 Mt tantalite (Resource Information Unit, 2007).

Ongoing exploration drilling programs by Haddington Resources Limited on YARDINA, near the mine at the 'Creekside project' estimated an initial resource of 136 000 t at 390 ppm tantalite (Haddington Resources Limited, 2005).

Additional information on the Bald Hill deposit is provided in Fetherston (2004).

Orthomagmatic mafic and ultramafic mineralization

Base metal and steel industry metals — copper and nickel

Exploration for nickel on YARDINA has been minor, and only in conjunction with gold exploration. Western Mining Corporation Ltd (1992a) reported on a soil-sampling program and a 34-hole RAB drilling program that tested for gold and nickel at 'Lake Carmine' (MGA 410678E 6486430N), but no significant results were returned.

Exploration for nickel–copper sulfides in the Proterozoic Kimberlana Dyke and surrounding areas has been carried out by a number of companies, with the most significant exploration programs by WMC and Pan Australia Exploration in the late 1960s to early 1970s and in the 1990s respectively (Western Mining Corporation Ltd, 1972; Pan Australia Exploration Pty Ltd, 1997). However, sampling programs and aeromagnetic studies did not identify targets on YARDINA that were of sufficient interest to prompt further exploration and the tenements were relinquished.

Stratabound sedimentary — clastic-hosted mineralization

Energy mineral — uranium

Exploration for fossil placer-type uranium or gold, or both, in the Proterozoic Woodline Formation was carried out from 1969 to 1971 by Asarco Australia Ltd (1971) based on geological mapping, rock-chip sampling, radiometrics, SP logging, and RC and diamond drilling, but no significant radioactivity was reported. Diamond drillholes DDH1 and DDH2 are stored at the GSWA Kalgoorlie Core Library. Kilkenny Gold NL explored the northern Woodline Formation for gold and base metals during the 1990s (Kilkenny Gold NL, 1997). In 1989–91 Western Mining Corporation drilled a single diamond drillhole through the Woodline Formation during a nickel–gold exploration program, with the aim of assessing the groundwater potential of the area (Western Mining Corporation Ltd, 1992b).

Sedimentary — basin mineralization

Energy rock — lignite

Brown coal or lignite of Eocene age are found in the Eucla Basin and the drainage channel deposits overlying the crystalline rocks of the Albany–Fraser Orogen and the southeastern part of the Yilgarn Craton (Le Blanc Smith, 1990). Lignite typically forms a single seam, up to 12 m thick, within siltstone and claystone of the Lower Werrillup Formation (Cowan paleodrainage channel) and the Pindinga Formation (Lefroy paleodrainage channel) that have been recently grouped into the North Royal Formation (Clarke et al., 2003).

Exploration drilling by CRA Exploration Pty Ltd during the 1980s on southeastern YARDINA, and on YARDILLA, delineated a northerly trending lignite deposit with considerable variation in thickness and quality from east to west (CRA Exploration Pty Ltd, 1986a). An overall reserve of 480 Mt of lignite was determined and additional testing of the deposit indicated a bed moisture content of 60%, and high sodium, chlorine, sulphur, and ash contents, suggesting that the deposit has relatively low economic potential (CRA Exploration Pty Ltd, 1986b).

Further investigations by CRA Exploration for lignite on YARDINA were carried out along the eastern margin of Lake Cowan in the southwestern corner of YARDINA. Combined drilling and SIROTEM results gave inferred coal reserves of 110 and 18 Mt in two areas of lignite development. Tests on the quality of the lignite indicated lower moisture contents and a higher specific energy than other deposits in the region (CRA Exploration Pty Ltd, 1984).

Industrial rock — limestone

Western Mining Corporation Ltd (1976) reviewed the potential of a limestone unit of the Cenozoic Eundynie Group for use as a nickel smelter flux. The limestone, on the western margin of Lake Cowan (MGA 434683E 6510558N), is a well-indurated fossiliferous limestone with a sparry calcite matrix and unconformably overlies Archean rocks. Western Mining Corporation Ltd (1976) drilled nine percussion and three diamond drillholes that encountered limestone, clays, and ferruginous silcrete in the top 6–10 m, above a coquina in a muddy matrix. Geochemical sampling indicated an ore grade in the coquina in the top 2.63 m, with an average CaO value of 27% (Western Mining Corporation Ltd, 1976).

Hydrogeology

The hydrogeology of YARDINA has been discussed in a report on the WIDGIEMOOLTHA 1:250 000 sheet by Kern (1996). The groundwater on YARDINA is saline to hypersaline. Groundwater recharge is minimal, with most rainfall lost to evaporation or uptake by vegetation. Fresh water for pastoralists is almost entirely derived from surface waters, and most dams are located along drainages and alluvial flats. Kern (1996) identified the most prospective aquifers on WIDGIEMOOLTHA (1:250 000) as the Tertiary sandstone, carbonate, and spongolite units in the large paleochannels. Other prospective rock types include the Woodline Formation (Roberts and Moore, 1991) and the metasedimentary rocks of the Mount Belches Formation. Several water bores have been drilled in the Mount Belches Formation south of the Bald Hill mine, where yields ranging from 200 to 600 m³/day have been recorded (Rockwater Pty Ltd, 1989).

Acknowledgements

The author would like to acknowledge Fugro Airborne Surveys Pty Ltd for the permission to reproduce

aeromagnetic imagery over YARDINA in this publication (Fig. 4). Mincor Resources Ltd are thanked for access to drillcore results and petrography and aeromagnetic data.

References

- Anand, RR, and Paine, M, 2002, Regolith geology of the Yilgarn Craton, Western Australia: Implications for exploration: *Australian Journal of Earth Sciences*, v. 49, p. 3–162.
- Archibald, NJ, 1987, Geology of the Norseman–Kambalda area *in* Second Eastern Goldfields Geological Field Conference: Geological Society of Australia (WA Division), Extended Abstracts, p. 13–14.
- Archibald, NJ, Bettenay, LG, Binns, RA, Groves, DI, and Gunthorpe, RJ, 1978, The evolution of Archean greenstone terrains, Eastern Goldfields Province, Western Australia: *Precambrian Research*, v. 6, p. 103–131.
- Archibald, NJ, Bettenay, LG, Bickle, MJ, and Groves, DI, 1981, Evolution of Archean crust in the Eastern Goldfields Province of the Yilgarn Block: Geological Society of Australia, Special Publication, no. 7, p. 491–504.
- Asarco Limited, 1971, Woodline Project, Final report: Geological Survey of Western Australia, Statutory mineral exploration report, A3146 (unpublished).
- Barley, ME, Brown, SJ, Cas, RAF, Cassidy, KF, Champion, DC, Gardoll, SJ, and Krapez, B, 2003, An integrated geological and metallogenic framework for the eastern Yilgarn Craton: developing geodynamic models of highly mineralised Archean granite–greenstone terranes: AMIRA, Perth, Western Australia, Project no. P624, 192p (unpublished).
- Barley, ME, Brown, SJ, Krapez, B, and Cas, RAF, 2002, Tectono-stratigraphic analysis of the Eastern Yilgarn Craton: an improved geological framework for exploration in Archean terrains: AMIRA, Perth, Western Australia, Project P437A, final report, 200p (unpublished).
- Barley, ME, Eisenlohr, BN, Groves, DI, Perring, CS, and Vearncombe, JR, 1989, Late Archean convergent margin tectonics and gold mineralization: a new look at the Norseman–Wiluna Belt, Western Australia: *Geology*, v. 17, p. 826–829.
- Beard, JS, 1975, The vegetation of the Nullarbor area — Explanatory Notes to sheet 4, Vegetation Survey of Western Australia: University of Western Australia Press, Perth, 104p.
- Beard, JS, 1981, The vegetation of Western Australia at the 1:3 000 000 scale: Western Australia Forests Department, Explanatory Notes: University of Western Australia Press, Perth, 32p.
- Beard, JS, 1990, Plant life of Western Australia: Kangaroo Press, Kenthurst, NSW, 319p.
- Bettenay, LF, 1977, Regional geology and petrogenesis of Archean granitoids in the southeastern Yilgarn Block: University of Western Australia, PhD thesis (unpublished).
- Blewett, RS, Cassidy, KF, Champion, DC, Henson, PA, Goleby, BS, Jones, L, Groenewald, PB, 2004, The Wangkathaa Orogeny: an example of episodic regional ‘D₂’ in the late Archean Eastern Goldfields Province, Western Australia: *Precambrian Research*, v. 130, p. 139–159.
- Bordorkos, S, Love, GJ, Nelson, DR, and Wingate, MTD, 2006, 177917, metamorphosed tuffaceous sandstone, Round Hill; Geochronology dataset 624, *in* Compilation of geochronology data, June 2006 update: Geological Survey of Western Australia.
- Brown, SJA, Krapez, B, Beresford, S, Cassidy, KF, Champion, DC, Barley, ME, and Cas, RAF, 2001, Archean volcanic and sedimentary environments of the Eastern Goldfields Province, Western Australia — a field guide: Geological Survey of Western Australia, Record 2001/13, 66p.
- Burbidge, NT, 1960, The phytogeography of the Australian region: *Australian Journal of Ecology*, v. 8, p. 75–211.
- Campbell, IH, 1977, A study of macro-rhythmic layering and cumulate processes in the Jimberlana Intrusion, Western Australia. Part I: The upper layered series: *Journal of Petrology*, v. 18, part 2, p. 183–215.
- Campbell, IH, 1991, The Jimberlana Intrusion, *in* Mafic–ultramafic complexes of Western Australia *edited by* S J Barnes and RET Hill: Geological Society of Australia, Sixth International Platinum Symposium, Excursion Guidebook No. 3 p. 15–18.
- Campbell, IH, McCall, GJH, and Tyrwhitt, DS, 1970, The Jimberlana norite, Western Australia — a smaller analogue of the Great Dyke of Rhodesia: *Geological Magazine*, v. 107, p. 1–12.
- Cassidy, KF, and Champion, DC, 2002, Granitoids of the southeastern Yilgarn Craton: Distribution, geochronology, geochemistry, petrogenesis and relationships to mineralization, *in* The characterization and metallogenic significance of Archean granitoids of the Yilgarn Craton *edited by* KF Cassidy, DC Champion, NJ McNaughton, IR Fletcher, AJ Whitaker, IV Bastrakova, and AR Budd: MERIWA, Perth Western Australia, MERIWA Project M281/AMIRA Project P482, Chapter 3 (unpublished).
- Cassidy, KF, Champion, DC, Krapez, B, Barley, ME, Brown, SJA, Blewett, RS, Groenewald, PB, and Tyler, IM, 2006, A revised geological framework for the Yilgarn Craton, Western Australia: Geological Survey of Western Australia, Record 2006/8, 8p.
- Champion, DC, and Cassidy, KF, 2002, Granites in the Leonora–Laverton transect area, northeastern Yilgarn Craton, *in* Geology, geochronology and geophysics of the north eastern Yilgarn Craton, with an emphasis on the Leonora–Laverton transect area *edited by* KF Cassidy: Geoscience Australia, Canberra, Report 2002/18, p. 13–36.
- Champion, DC, and Sheraton, JW, 1993, Geochemistry of granitoids in the Leonora–Laverton region, Eastern Goldfields Province, *in* Kalgoorlie ’93 — an international conference on crustal evolution, metallogeny, and exploration of the Eastern Goldfields *compiled by* PR Williams and JA Haldane: Australian Geological Survey Organisation, Canberra, Record 1993/54, p. 39–46.
- Champion, DC, and Sheraton, JW, 1997, Geochemistry and Sm–Nd isotope systematics of Archean granitoids of the Eastern Goldfields Province, Yilgarn Craton, Australia: constraints on crustal growth: *Precambrian Research*, v. 83, p. 109–132.
- Chen, SF, Witt, WK, and Liu, S, 2001, Transpression and restraining jogs in the northeastern Yilgarn Craton, Western Australia: *Precambrian Research*, v. 106, p. 309–328.
- Clark, DJ, Hensen, BJ, and Kinny, PD, 2000, Geochronological constraints for a two-stage history of the Albany–Fraser Orogen, Western Australia: *Precambrian Research*, v. 102, p. 155–183.
- Clark, DJ, Kinny, PD, Post, NJ, and Hensen, BJ, 1999, Relationships between magmatism, metamorphism and deformation in the Fraser Complex, Western Australia: constraints from new SHRIMP U–Pb zircon geochronology: *Australian Journal of Earth Sciences*, v. 46, p. 923–932.

- Clarke, JDA, 1994, Evolution of the Lefroy and Cowan paleodrainage channels, Western Australia: Australian Journal of Earth Sciences, v. 41, p. 55–68.
- Clarke, JDA, Gammon, PR, Hou, B, and Gallagher, SJ, 2003, Middle to Upper Eocene stratigraphic nomenclature and deposition in the Eucla Basin: Australian Journal of Earth Sciences, v. 50, p. 231–248.
- Cockbain, AE, 1968, The stratigraphy of the Plantagenet Group, Western Australia: Geological Survey of Western Australia, Annual Report 1967, p. 61–63.
- CRA Exploration Pty Ltd, 1984, Annual report on E15/13 Heartbreak 9, Widgiemooltha, Western Australia: Geological Survey of Western Australia, Statutory mineral exploration report, A36162-1 (unpublished).
- CRA Exploration Pty Ltd, 1986a, Annual report on E63/30 Heartbreak 2 and E28/11 Heartbreak 3 Widgiemooltha, Western Australia; Report No. 13781: Geological Survey of Western Australia, Statutory mineral exploration report, A36154 (unpublished).
- CRA Exploration Pty Ltd, 1986b, Annual report for 1986 on E63/30 Heartbreak 2 and E28/11 Heartbreak 3 Widgiemooltha, Western Australia; Report No. 189381: Geological Survey of Western Australia, Statutory mineral exploration report, A46534 (unpublished).
- Dawson, GC, Krapez, B, Fletcher, IR, McNaughton, NJ, and Rasmussen, B, 2002, Did late Palaeoproterozoic assembly of proto-Australia involve collision between the Pilbara, Yilgarn and Gawler Cratons? Geochronological evidence from the Mount Barren Group in the Albany–Fraser Orogen of Western Australia: Precambrian Research, v. 118, p. 195–220.
- Dawson, GC, Krapez, B, Fletcher, IR, McNaughton, NJ, and Rasmussen, B, 2003, 1.2 Ga thermal metamorphism in the Albany–Fraser Orogen of Western Australia: consequence of collision or regional heating by dyke swarms?: Journal of the Geological Society, London, v. 160, p. 29–37.
- Diels, L, 1906, Die Pflanzenwelt von West-Australien südlich des Wendekreises: Vegetation der Erde 7, Leipzig, 326p.
- Evans, T, 1999, Extent and nature of the 1200 Ma Wheatbelt dyke swarm, southwestern Australia: University of Western Australia, BSc. (Hons) thesis (unpublished).
- Fetherston, JM, 2004, Tantalum in Western Australia: Geological Survey of Western Australia, Mineral Resources Bulletin 22, 162p.
- Fletcher, IR, Libby, WG, and Rosman, KJR, 1987, Sm–Nd dating of the 2411 Ma Jimberlana dyke, Yilgarn Block, Western Australia: Australian Journal of Earth Sciences, v. 34, p. 523–525.
- Fletcher, IR, and McNaughton, NJ, 2002, Granitoid geochronology: SHRIMP zircon and titanite data, in The characterization and metallogenic significance of Archaean granitoids of the Yilgarn Craton edited by KF Cassidy, DC Champion, NJ McNaughton, IR Fletcher, AJ Whitaker, IV Bastrakova, and AR Budd: MERIWA, Perth Western Australia, MERIWA Project M281/AMIRA Project P482, Chapter 6, (unpublished).
- Frey, RW, and Pemberton, SG, 1984, Trace fossil facies models, in Facies models (second edition) edited by RG Walker: Geoscience Canada, Reprint Series 1, p. 189–207.
- Geological Survey of Western Australia, 2005, Southeastern Yilgarn geological exploration package: Geological Survey of Western Australia, Record 2005/2.
- Geological Survey of Western Australia, 2007, East Yilgarn — 2006 update: Geological Survey of Western Australia, 1:100 000 Geological Information Series.
- Goleby, BR, Rattenbury, MS, Swager, CP, Drummond, BJ, Williams, PR, Sheraton, JE, and Heinrich, CA, 1993, Archean crustal structure from seismic reflection profiling, Eastern Goldfields, Western Australia: Australian Geological Survey Organisation, Canberra, Record 1993/15, 54p.
- Goscombe, BD, Passchier, CW, and Hand, M, 2004, Boudinage classification: end-member boudin types and modified boudin structures: Journal of Structural Geology, v. 26, p. 739–763.
- Gresham, JJ, and Loftus-Hills, GD, 1981, The geology of the Kambalda nickel field, Western Australia: Economic Geology, v. 76, p. 1373–1416.
- Griffin, TJ, 1988, Cowan, WA Sheet 3234: Geological Survey of Western Australia, 1:100 000 Geological Series.
- Griffin, TJ, 1989, Widgiemooltha, WA (2nd edition): Geological Survey of Western Australia, 1:250 000 Geological Series Explanatory Notes, 43p.
- Griffin, TJ, 1990, Geology of the granite–greenstone terrane of the Lake Lefroy and Cowan 1:100 000 sheets, Western Australia: Geological Survey of Western Australia, Report 32, 53p.
- Griffin, TJ, and Hickman, AH, 1988a, Widgiemooltha, WA Sheet SH 51-14 (2nd edition): Geological Survey of Western Australia, 1:250 000 Geological Series.
- Griffin, TJ, and Hickman, AH, 1988b, Lake Lefroy, WA Sheet 3235: Geological Survey of Western Australia, 1:100 000 Geological Series.
- Groenewald, PB, Doyle, MG, Brown, SJA, and Barnes, SJ, 2006, Stratigraphy and physical volcanology of the Archean Kurnalpi Terrane, Yilgarn Craton — a field guide: Geological Survey of Western Australia, Record 2006/11, 25p.
- Groenewald, PB, Morris, PA, and Champion, DC, 2002, Tectonic evolution of the Eastern Goldfields: an overview of postulated models: Geoscience Australia, Canberra, Special workshop notes for the Northeastern Yilgarn Seismic Workshop, p. 53–75 (unpublished).
- Groenewald, PB, Morris, PA, and Champion, DC, 2003, Geology of the Eastern Goldfields and an overview of tectonic models, in The 2001 Northeastern Yilgarn deep seismic reflection survey compiled by BR Goleby, RS Blewett, PB Groenewald, KF Cassidy, DC Champion, LEA Jones, RJ Korsch, S Shevchenko, and SN Apak: Geoscience Australia, Canberra, Record 2003/28, p. 63–84.
- Groenewald, PB, Painter, MGM, Roberts, FI, McCabe, M, and Fox, A, 2000, East Yilgarn Geoscience Database, 1:100 000 geology Menzies to Norseman — an explanatory note: Geological Survey of Western Australia, Report 78, 53p.
- Haddington Resources Limited, 2005, Initial resource of 136,000 tonnes at 390 ppm Ta₂O₅ for Creekside. A further 14 targets identified in soil sampling at Bald Hill: Report to Australian Stock Exchange, 23 May 2005, 5p.
- Hall, CE, 2007, The Mount Belches Formation – Black Flag Group, a late basin, or something else?: Geological Survey of Western Australia, Annual Review 2005–06, p. 77–80.
- Hall, CE, and Jones, SA, 2005, The Proterozoic Woodline Formation: new constraints from geochronology, sedimentology, and deformation studies: Geological Survey of Western Australia, Record 2005/5, p. 14–15.
- Hall, CE, Jones, SA, and Bodorkos, S, 2008, Sedimentology, structure and SHRIMP zircon provenance of the Woodline Formation, Western Australia: implications for the tectonic setting of the West Australian Craton during the Paleoproterozoic: Precambrian Research, v. 162, p. 577–598.
- Hallberg, JA, 1987, Postcratonization mafic and ultramafic dykes of the Yilgarn Block: Australian Journal of Earth Sciences, v. 34, p. 135–149.
- Hammond, RL, and Nisbet, BW, 1992, Towards a structural and tectonic framework for the Norseman–Wiluna greenstone belt, Western Australia, in The Archean: Terrains, processes and metallogeny edited by JE Glover and SE Ho: University of Western Australia, Geology Department and University Extension, Publication no. 22, p. 39–50.

- Hill, RI, Chappell, BW, and Campbell, IH, 1992, Late Archean granites of the southeastern Yilgarn Block, Western Australia: age, geochemistry, and origin: *Royal Society of Edinburgh, Transactions*, v. 83, p. 211–226.
- Hocking, RM, 1994, Subdivisions of Western Australian Neoproterozoic and Phanerozoic sedimentary basins: *Geological Survey of Western Australia, Record 1994/4*, 84p.
- Hocking, RM, and Cockbain, AE, 1990, Regolith, *in* *Geology and mineral resources of Western Australia: Geological Survey of Western Australia, Memoir 3*, p. 590–602.
- Hocking, RM, Langford, RL, Thorne, AM, Sanders, AJ, Morris, PA, Strong, CA, and Gozzard, JR, 2001, A classification system for regolith in Western Australia: *Geological Survey of Western Australia, Record 2001/4*, 22p.
- House, M, Dentith, M, Trench, A, Groves, D, and Miller, D, 1999, Structure of the highly mineralised late-Archean granitoid–greenstone terrain and the underlying crust in the Kambalda–Widgiemooltha areas, Western Australia, from the integration of geophysical datasets: *Exploration Geophysics*, v. 30, p. 50–67.
- Hunter, WM, 1993, The geology of the granite–greenstone terrane of the Kalgoorlie and Yilgarn 1:100 000 sheets, Western Australia: *Geological Survey of Western Australia, Report 35*, 80p.
- Jarosewich, E, Nelen, JA, and Norberg, JA, 1980, Reference samples for electron microprobe analysis: *Geostandards Newsletter*, v. 4, p. 43–47.
- Johnson, GI, 1991, The petrology, geochemistry and geochronology of the felsic alkaline suite of the eastern Yilgarn Block, Western Australia: University of Adelaide, PhD thesis (unpublished).
- Jones, SA, 2005, Geology of the Yardilla 1:100 000 sheet: *Geological Survey of Western Australia, 1:100 000 Geological Series Explanatory Notes*, 34p.
- Jones, SA, and Ross, AA, 2005, Yardilla, WA Sheet 3434: *Geological Survey of Western Australia, 1:100 000 Geological Series*.
- Jones, SA, 2006, Mesoproterozoic Albany–Fraser Orogen-related deformation along the southeastern margin of the Yilgarn: *Australian Journal of Earth Sciences*, v. 53, p. 213–234.
- Jones, SA, 2007, Geology of the Erayinia 1:100 000 sheet: *Geological Survey of Western Australia, 1:100 000 Geological Series Explanatory Notes*, 37p.
- Keays, RR, and Campbell, IH, 1981, Precious metals in the Jemberlana Intrusion, Western Australia: implications for the genesis of platiniferous ores in layered intrusions: *Economic Geology*, v. 76, p. 1118–1141.
- Kent, AJR, and McDougall, I, 1995, ^{40}Ar – ^{39}Ar and U–Pb age constraints on the timing of gold mineralization in the Kalgoorlie Gold Field, Western Australia: *Economic Geology*, v. 90, p. 845–859.
- Kern, AM, 1996, Widgiemooltha, WA: *Geological Survey of Western Australia, 1:250 000 Hydrogeological Series Explanatory Notes*, 16p.
- Kilkenny Gold NL, 1997, Madoonia Downs Project, Partial Surrender Report: *Geological Survey of Western Australia, Statutory mineral exploration report, A51681* (unpublished).
- Krapez, B, Brown, SJA, and Hand, J, 1997, Stratigraphic signatures of depositional basins in Archean volcanosedimentary successions of the Eastern Goldfields Province: *Australian Geological Survey Organisation, Canberra, Record 1997/41*, p. 33–38.
- Krapez, B, Brown, SJA, Hand, J, Barley, ME, and Cas, RAF, 2000, Age constraints on recycled crustal and supracrustal sources of Archean metasedimentary sequences, Eastern Goldfields Province, Western Australia: evidence from SHRIMP zircon dating: *Tectonophysics*, v. 322, p. 89–133.
- Leake, BE, 1978, Nomenclature of amphiboles: *American Mineralogist*, v. 63, p. 1023–1052.
- Le Blanc Smith, G, 1990, Coal, *in* *Geology and mineral resources of Western Australia: Geological Survey of Western Australia, Memoir 3*, p. 625–631.
- McCall, GJH, and Peers, R, 1971, Geology of the Binneringie Dyke, Western Australia: *Sondruck Geologische Rundschau*, v. 60, p. 1174–1263.
- Mikucki, EJ, and Roberts, FI, 2003, Metamorphic petrography of the Kalgoorlie region, Eastern Goldfields Granite–Greenstone Terrane: METPET database: *Geological Survey of Western Australia, Record 2003/12*, 40p.
- Morris, PA, 1993, Archean mafic and ultramafic volcanic rocks, Menzies to Norseman, Western Australia: *Geological Survey of Western Australia, Report 36*, 107p.
- Morris, PA, 1998, Archean felsic volcanism in parts of the Eastern Goldfields region, Western Australia: *Geological Survey of Western Australia, Report 55*, 80p.
- Myers, JS, 1990, Albany–Fraser Orogen, *in* *Geology and mineral resources of Western Australia: Geological Survey of Western Australia, Memoir 3*, p. 255–263.
- Myers, JS, 1995, The generation and assembly of an Archean supercontinent: evidence from the Yilgarn Craton, Western Australia, *in* *Early Precambrian processes edited by MP Coward and AC Ries: Geological Society of London, Special Publication no. 95*, p. 143–154.
- Myers, JS, 1997, Preface: Archean geology of the Eastern Goldfields of Western Australia — regional overview: *Precambrian Research*, v. 83, p. 1–10.
- Nelson, DR, 1995, Compilation of SHRIMP U–Pb zircon dates, 1994: *Geological Survey of Western Australia, Record 1995/03*, 244p.
- Nelson, DR, 1997, Evolution of the Archean granite–greenstone terranes of the Eastern Goldfields, Western Australia: SHRIMP U–Pb zircon constraints: *Precambrian Research*, v. 83, p. 57–81.
- Nelson, DR, Myers, JS, and Nutman, AP, 1995, Chronology and evolution of the middle Proterozoic Albany–Fraser Orogen, Western Australia: *Australian Journal of Earth Sciences*, v. 42, p. 481–495.
- Nemchin, AA, and Pidgeon, RT, 1998, Precise conventional and SHRIMP baddeleyite U–Pb age for the Binneringie Dyke, near Narrogin, Western Australia: *Australian Journal of Earth Sciences*, v. 45, p. 673–675.
- Northcote, KH, Isbell, RF, Webb, AA, Murtha, GG, Churchward, M, and Bettenay, E, 1968, Central Australia, *in* *Atlas of Australian Soils: CSIRO Australia*, 100p.
- Painter, MGM, and Groenewald, PB, 2001, Geology of the Mount Belches 1:100 000 sheet: *Geological Survey of Western Australia: 1:100 000 Geological Series Explanatory Notes*, 38p.
- Pan Australia Exploration Pty Ltd, 1997, Yilgarn extension project, Group 2, Buldania Project area, Annual report 1 January 1996 to 31 December 1996: *Geological Survey of Western Australia, Statutory mineral exploration report, A50258* (unpublished).
- Passchier, CW, 1994, Structural geology across a proposed Archean terrane boundary in the eastern Yilgarn Craton, Western Australia: *Precambrian Research*, v. 68, p. 43–64.
- Perring, CS, Barley, ME, Cassidy, KF, Groves, DI, McNaughton, NJ, Rock, NMS, Bettenay, LF, Golding, SD, and Hallberg, JA, 1989, The association of linear orogenic belts, mantle–crustal magmatism and Archean gold mineralization in the Eastern Yilgarn Block of Western Australia: *Economic Geology, Monograph 6*, p. 571–585.
- Red Back Mining NL, 1998, Annual Report 1998, 43p.
- Resource Information Unit, 2007, Register of Australian Mining 2005–06, p. 387.
- Ridley, JR, 1993, Implications of metamorphic patterns to tectonic models of the Eastern Goldfields, *in* *Kalgoorlie 93 — An international conference on crustal evolution, metallogeny, and exploration of*

- the Eastern Goldfields *compiled by* PR Williams and JA Haldane: Australian Geological Survey Organisation, Record 1993/54, p. 95–100.
- Roberts, P, and Moore, M, 1991, Groundwater exploration of the Woodline Beds area (groundwater well licence 31741): Western Mining Corporation (Kambalda Nickel Operations), Technical Report 190 (unpublished).
- Rockwater Pty Ltd, 1989, Bald Hill ground water investigations: Gwalia Minerals NL, Report (unpublished).
- Smithies, RH, and Champion, DC, 1999, Late Archean felsic alkaline igneous rocks in the Eastern Goldfields, Yilgarn Craton, Western Australia: a result of lower crustal delamination?: Geological Society of London, v. 156, p. 561–576.
- Sofoulis, J, 1966, Widgiemooltha, Western Australia.: Geological Survey of Western Australia, 1:250 000 Geological Series Explanatory Notes, 25p.
- Sofoulis, J, and Bock, WM, 1963, Boorabbin, WA: Geological Survey of Western Australia, 1:250 000 Geological Series Explanatory Notes.
- Sofoulis, J, Horwitz, RC, and Bock, WM, 1965, Widgiemooltha, WA Sheet SH 51-14: Geological Survey of Western Australia, 1:250 000 Geological Series.
- Swager, CP, 1989, Structure of the Kalgoorlie greenstones — regional deformation history and implications for the structural setting of the Golden Mile gold deposits: Geological Survey of Western Australia, Report 25, Professional Papers, p. 59–84.
- Swager, CP, 1997, Tectono-stratigraphy of late Archean greenstone terranes in the southern Eastern Goldfields, Western Australia: Precambrian Research, v. 83, p. 11–42.
- Swager, CP, Goleby, BR, Drummond, BJ, Rattenbury, MS, and Williams, PR, 1997, Crustal structure of granite–greenstone terranes in the Eastern Goldfields, Yilgarn Craton, as revealed by seismic reflection profiling: Precambrian Research, v. 83, p. 43–56.
- Swager, CP, and Griffin, TJ, 1990, An early thrust duplex in the Kalgoorlie–Kambalda greenstone belt, Eastern Goldfields Province, Western Australia: Precambrian Research, v. 48, p. 63–73.
- Swager, CP, Griffin, TJ, Witt, WK, Wyche, S, Ahmat, AL, Hunter, WM, and McGoldrick, PJ, 1995, Geology of the Archean Kalgoorlie Terrane — an explanatory note: Geological Survey of Western Australia, Report 48, 26p.
- Swager, CP, and Nelson, DR, 1997, Extensional emplacement of a high-grade granite gneiss complex into low-grade granite greenstones, Eastern Goldfields, Western Australia: Precambrian Research, v. 83, p. 203–219.
- Turek, A, 1966, Rb–Sr isotopic studies in the Kalgoorlie–Norseman area, Western Australia: Australian National University, Canberra, PhD thesis (unpublished).
- Tyler, IM, and Hocking, RM, 2001, Tectonic units of Western Australia (scale 1:2 500 000): Geological Survey of Western Australia.
- Weinberg, RF, Moresi, L, and Van Der Borgh, P, 2003, Timing of deformation in the Norseman–Wiluna Belt, Yilgarn Craton, Western Australia: Precambrian Research, v. 120, p. 219–239.
- Western Mining Corporation Ltd, 1972, Jimberlana Dyke Ni/Cu/platinum/chromium exploration, Final report: Geological Survey of Western Australia, Statutory mineral exploration report, A11407 (unpublished).
- Western Mining Corporation Ltd, 1976, Progress report: Binyarinyinna Mineral Claims, 1st July 1973 – 29th June 1976: Geological Survey of Western Australia, Statutory mineral exploration report, A6638 (unpublished).
- Western Mining Corporation Ltd, 1992b, Terminal Technical Report on Exploration Activities within E28/353 for the period 14/12/1989 – 12/7/1991: Geological Survey of Western Australia, Statutory mineral exploration report, A35107 (unpublished).
- Western Mining Corporation Ltd, 1992a, Sinclair Soak Project Terminal Technical Report, Relinquished part of Exploration licence 15/89: Geological Survey of Western Australia, Statutory mineral exploration report, A36402 (unpublished).
- Wingate, MTD, and Bordorkos, S, in prep., 183118: volcanoclastic sandstone: Geochronology dataset 715, *in* Compilation of geochronology data: Geological Survey of Western Australia.
- Wingate, MTD, Campbell, IH, and Harris, LB, 2000, SHRIMP baddeleyite age for the Fraser Dyke Swarm, southeast Yilgarn Craton, Western Australia: Australian Journal of Earth Sciences, v. 47, p. 309–313.
- Witt, WK, 1991, Regional metamorphic controls on alteration assemblages associated with gold mineralization in the Eastern Goldfields Province Western Australia: Implications for the timing and origin of Archean lode-gold deposits: Geology, v. 19, p. 982–985.
- Witt, WK, 1994, Geology of the Bardoc 1:100 000 sheet: Geological Survey of Western Australia, 1:100 000 Geological Series Explanatory Notes, 50p.
- Witt, WK, and Davy, R, 1993, Pre- and post-folding, I-type granitoid suites in the southwest Eastern Goldfields Province: an Archean syn-collisional plutonic event, *in* An international conference on Crustal Evolution, metallogeny and exploration of the Eastern Goldfields *edited by* PR Williams and JA Haldane: Australian Geological Survey Organisation, Record 1993/54, p. 39–46.
- Witt, WK, and Davy, R, 1997, Geology and geochemistry of granitoid rocks in the southwest Eastern Goldfields Province: Geological Survey of Western Australia, Report 49, 137p.
- Wyborn, LAI, 1993, Constraints on interpretations of lower crustal structure, tectonic setting and metallogeny of the Eastern Goldfields and Southern Cross Provinces provided by granite geochemistry: Ore Geology Reviews, v. 8, p. 125–140.

Appendix 1

Gazetteer of localities on YARDINA

<i>Locality</i>	<i>MGA coordinates</i>	
	<i>Easting</i>	<i>Northing</i>
Bald Hill tantalum mine	422000	6513000
Binneringie Homestead	414000	6508000
Binyarinyinna Rock	413500	6508000
Blue Dam	420500	6496500
Dog Lake	440000	6510000
Lake Cowan	414000	6500000
Jeffreys gold deposit	419800	6465300
Junction Lake	446500	6501500
Sinclair Soak	423000	6482000
Yardina Rock/Soak	426500	6494000

Appendix 2

Whole-rock geochemistry of metasedimentary, felsic volcanic, and granitic rocks from YARDINA

GSWA no. Rock code Rock type	Method	Detection limit	179015 Amha Para- amphibolite 413386 6458778	179016 Amha Para- amphibolite 413386 6458778	179607 Amha Para- amphibolite 415472 6460332	179608 Ant Meta- sandstone 413698 6460718	179609 Amha Para- amphibolite 413698 6460718	179610 Ant Psanmitite 412947 6459431	179611 Ant Psanmitite 412879 6459347	179612 Amhs Pelite 413303 6459340	179036 Abe-nh Psanmitite- pelite 423952 6212555	179604 Abe-nh Psanmitite- pelite 429870 6559114	179605 Abe-nh Psanmitite- pelite 421952 6512494	179606 Abe-nh Psanmitite- pelite 421952 6512494
Percentage														
SiO ₂	XRF	0.01	62.85	57.34	56.29	65.21	62.26	69.61	67.29	61.46	54.32	65.40	64.00	64.28
TiO ₂	XRF	0.005	0.480	0.464	0.523	0.652	0.438	0.318	0.341	0.166	1.136	0.492	0.548	0.585
Al ₂ O ₃	XRF	0.005	14.837	13.184	13.325	15.435	14.489	14.729	14.462	19.634	12.310	14.701	15.452	16.211
Fe ₂ O ₃ T	XRF	0.005	2.391	5.735	5.750	3.841	4.308	3.050	3.684	2.250	10.230	5.227	5.612	6.126
Fe ₂ O ₃	CALC	0.005	0.588	1.322	1.086	1.106	0.843	1.103	1.257	1.411	1.085	1.220	0.637	0.607
FeO	TITR	0.01	1.62	3.97	4.20	2.46	3.12	1.75	2.18	0.76	8.23	3.61	4.48	4.97
MnO	XRF	0.005	0.053	0.092	0.103	0.051	0.065	0.032	0.034	0.009	0.197	0.087	0.076	0.101
MgO	XRF	0.01	1.45	4.02	5.53	1.46	3.63	2.79	3.02	1.43	7.76	2.71	3.37	3.03
CaO	XRF	0.005	6.179	8.614	8.424	3.039	6.003	1.111	1.102	0.335	9.862	2.532	2.508	2.983
Na ₂ O	XRF	0.01	6.49	5.16	2.94	4.30	3.37	3.07	3.37	4.72	2.14	4.22	3.76	3.48
K ₂ O	XRF	0.005	0.356	0.504	2.621	3.068	3.653	3.880	3.817	6.993	0.777	1.889	2.186	2.001
P ₂ O ₅	XRF	0.005	0.233	0.186	0.154	0.386	0.159	0.053	0.043	0.097	0.699	0.154	0.165	0.197
SO ₃	XRF	0.005	0.190	0.109	0.134	0.153	0.043	0.036	0.050	0.090	0.038	0.053	0.124	0.572
LOI	GRAV	0.01	4.61	4.91	4.44	2.06	1.49	1.16	2.74	2.45	1.12	2.70	2.47	1.04
Total			100.12	100.30	100.23	99.65	99.91	99.84	99.96	99.63	100.58	100.15	100.26	100.62
Parts per million (unless otherwise indicated)														
Ag	ICP-MS	0.01	0.09	0.06	0.02	0.08	0.07	0.07	0.04	0.01	0.03	0.05	0.06	0.05
As	ICP-MS	0.5	5	3.7	2	2.6	8.1	10.8	7.5	21.7	1.8	1.2	1.1	0.9
Ba	ICP-MS	2	265	245	304	3133	1170	1150	805	2975	485	653	770	663
Be	ICP-MS	0.1	1.1	1.4	1.2	2.7	1.8	1.5	1.6	3.2	2	1.3	1.7	1.7
Bi	ICP-MS	0.1	0.2	0.2	0.3	0.4	0.7	0.4	0.3	0.4	0.2	0.2	0.2	0.3
Cd	ICP-MS	0.1	-0.1	-0.1	-0.1	-0.1	-0.1	-0.1	-0.1	-0.1	0.31	-0.1	-0.1	-0.1
Cr	XRF	2	122	200	306	25	212	150	173	47	235	195	173	177
Cs	ICP-MS	0.01	0.15	0.33	1.01	6.06	5.53	5.72	7.4	2.43	0.38	2.11	15.9	26.67
Cu	XRF	1	82	27	61	16	23	6	4	6	3	43	9	68
F	XRF	50	621	840	1079	1199	1062	967	1224	1487	1398	752	1288	1215
Ga	ICP-MS	0.2	13.7	18.3	16.4	18.5	19.5	20	19.8	33.2	18.1	17.9	19.3	20.3
Ge	ICP-MS	0.1	0.8	1.4	1.5	1	1.2	1.2	1.3	1.6	2.4	1	1.1	1.2
Hf	ICP-MS	0.1	4.8	3.7	3.3	5.3	3.6	3	2.8	3.7	5.8	2.9	3.3	3.4
Mo	ICP-MS	0.1	0.7	0.8	1.1	0.6	0.9	0.7	1.2	4.2	0.6	0.8	0.6	1
Nb	ICP-MS	0.1	5.2	4.4	4.8	6.1	5	4.8	4.3	12.6	8.9	4.6	5.5	5.6
Ni	XRF	2	54	83	147	11	126	41	55	6	141	78	71	61

Pb	ICP-MS	0.5	6.2	4.9	6.4	40.7	34.9	23.2	24.7	10.9	11.7	13.1	15.2	14.2
Rb	ICP-MS	1	10.1	16.5	88.3	81.5	105.4	121.2	128.6	131.8	23.8	54.5	81.5	81.5
Sb	ICP-MS	0.1	0.3	1	0.4	3.2	6	1.2	2.1	0.6	0.5	3	2.4	2.1
Sc	XRF	2	9	14	15	6	11	8	10	5	20	11	14	13
Sn	ICP-MS	0.5	1.2	1.6	2.1	1.6	2	1.4	1.2	3.1	3.2	1.3	1.3	1.4
Sr	ICP-MS	1	125.2	148.7	311.3	1 383	713.4	459.3	479.6	378.6	338.1	476.7	452.1	512.5
Ta	ICP-MS	0.1	0.4	0.4	0.4	0.3	0.4	0.4	0.4	1.2	0.5	0.3	0.3	0.3
Th	ICP-MS	0.1	13.2	7.6	6.7	19.7	9.8	12.4	12.5	28.4	7	4.8	5.8	5.7
U	ICP-MS	0.1	3.38	2.23	2.38	3.4	2.85	5.02	3.76	5.69	1.34	1.27	1.64	1.72
V	XRF	5	61	92	109	51	81	64	69	36	183	97	113	115
Y	ICP-MS	0.5	7	10.5	11	12.5	10.7	9.6	9.4	7.8	22.6	12.6	12.3	13.3
Zn	XRF	1	12	34	43	73	77	57	62	11	132	64	80	79
Zr	ICP-MS	1	155.9	120	104.3	209.3	114.3	91.9	87.2	94.5	189.4	108.3	111.7	122.7
La	ICP-MS	0.02	46.81	35.22	26.66	116.3	32.63	22.63	26.59	32.23	48.62	27.62	25.35	26.13
Ce	ICP-MS	0.1	96.85	72.48	52.63	235.2	68.5	44.52	50.34	57	112.5	52.91	54.54	55.52
Pr	ICP-MS	0.01	11.34	8.81	6.47	28.58	8.21	5.37	6.24	7.25	15.37	7.1	6.87	7.11
Nd	ICP-MS	0.01	43.28	34.97	25.3	109.2	31.01	19.54	23.32	27.77	67.72	28.56	26.59	28.72
Sm	ICP-MS	0.01	6.37	6.04	4.41	15.69	5.36	3.71	3.98	5.3	14.06	4.87	4.94	4.81
Eu (ppb)	ICP-MS	1	1 299	1 295	859	3 641	1 140	782	899	1 106	3 538	1 323	1 303	1 297
Gd	ICP-MS	0.01	3.4	4.08	3.33	7.42	3.7	2.31	2.5	2.95	10.3	3.23	3.28	3.62
Tb	ICP-MS	0.01	0.38	0.52	0.44	0.73	0.47	0.31	0.31	0.38	1.2	0.43	0.42	0.44
Dy	ICP-MS	0.01	1.92	2.81	2.48	3.14	2.52	1.72	1.59	1.81	6.23	2.28	2.41	2.49
Ho	ICP-MS	0.01	0.33	0.51	0.48	0.47	0.47	0.31	0.29	0.3	1.02	0.43	0.44	0.48
Er	ICP-MS	0.01	0.95	1.36	1.38	1.06	1.31	0.91	0.82	0.77	2.58	1.2	1.22	1.39
Yb	ICP-MS	0.01	0.85	1.2	1.18	0.79	1.22	0.89	0.82	0.79	2.11	1.11	1.17	1.22
Lu	ICP-MS	0.01	0.12	0.17	0.17	0.1	0.17	0.13	0.11	0.11	0.29	0.15	0.16	0.18

Appendix 2 (continued)

GSWA no. Rock code Rock type	Method	Detection limit	179043 Agvcs Clinopyroxene- bearing syenite 418908 6499363	179051 Afr Rhyolite 410563 6485535	179028 Afr Rhyolite 452596 6491826	179046 Agmb Monzo- granite 423360 6490981	179047 Agmb Monzo- granite 422436 6479824	179067 Agmb Monzo- granite 422436 6479824	179614 Agmb Monzo- granite 422436 6479824	179026 Agmb Monzo- granite 451720 6505893	179032 Agmb Monzo- granite 432014 6514457	179034 Agmb Granitic dyke 429681 6514128	179615 Agmb Leuco- granite 427910 6465094	179616 Agmb Monzo- granite 427837 6465174
<i>Existing</i>														
<i>Northing</i>														
SiO ₂	XRF	0.01	61.46	75.17	75.19	71.90	72.38	72.38	Percentage 69.54	72.27	72.49	72.09	75.33	69.90
TiO ₂	XRF	0.005	0.498	0.270	0.236	0.213	0.208	0.208	0.414	0.224	0.246	0.236	0.039	0.245
Al ₂ O ₃	XRF	0.005	17.263	14.288	11.732	15.235	15.015	15.015	15.205	15.317	14.840	15.736	13.475	15.418
Fe ₂ O ₃ T	XRF	0.005	3.807	0.547	2.297	1.157	0.795	0.795	2.111	0.572	0.600	0.321	0.603	1.507
Fe ₂ O ₃	CALC	0.005	2.092	0.418	0.932	0.459	0.298	0.298	1.021	0.572	0.092	0.178	0.511	0.405
FeO	TITR	0.01	1.54	0.12	1.23	0.63	0.45	0.45	0.98	0.00	0.46	0.13	0.08	0.99
MnO	XRF	0.005	0.105	-0.005	0.017	0.018	0.013	0.013	0.028	0.007	0.006	-0.005	0.009	0.021
MgO	XRF	0.01	1.08	0.26	0.48	0.44	0.26	0.26	0.67	0.23	0.21	0.16	0.09	0.81
CaO	XRF	0.005	2.541	1.848	0.032	1.564	1.348	1.348	1.746	0.947	1.095	1.060	0.630	1.804
Na ₂ O	XRF	0.01	6.06	5.68	2.75	5.24	5.44	5.44	4.88	4.99	4.76	5.05	4.66	5.47
K ₂ O	XRF	0.005	5.170	0.402	5.366	2.945	2.894	2.894	3.273	3.790	3.473	2.448	4.001	2.702
P ₂ O ₅	XRF	0.005	0.138	0.070	0.022	0.228	0.071	0.071	0.205	0.080	0.040	0.070	0.017	0.130
SO ₃	XRF	0.005	0.039	0.095	0.037	0.031	0.030	0.030	0.032	0.075	0.056	0.076	0.027	0.034
LOI	GRAV	0.01	1.18	1.28	1.78	0.72	1.34	1.34	1.56	1.17	1.81	2.45	1.04	1.28
Total			99.35	99.90	99.94	99.70	99.79	99.79	99.67	99.67	99.62	99.69	99.91	99.32
Ag	ICP-MS	0.01	0.07	0.08	0.07	0.04	0.06	0.06	0.02	0.04	0.03	0.07	0.04	0.06
As	ICP-MS	0.5	1.2	0.9	0.8	0.6	-0.5	-0.5	-0.5	0.8	3	0.7	-0.5	0.5
Ba	ICP-MS	2	3 254	190	1 118	1 435	1 107	1 107	1 702	1 556	2 413	1 453	128	2 154
Be	ICP-MS	0.1	3.4	1.2	1.9	1.4	2.4	2.4	2	2.6	2.5	2.1	2.2	2.7
Bi	ICP-MS	0.1	0.3	-0.1	-0.1	-0.1	-0.1	-0.1	-0.1	0.4	0.3	0.2	-0.1	-0.1
Cd	ICP-MS	0.1	-0.1	-0.1	-0.1	-0.1	-0.1	-0.1	-0.1	-0.1	-0.1	0.4	-0.1	0.53
Cr	XRF	2	29	25	8	6	4	4	4	11	8	7	3	7
Cs	ICP-MS	0.01	4.51	0.3	1.15	2.07	3.78	3.78	4.05	6.49	25.63	2.08	2.31	2.13
Cu	XRF	1	13	123	-1	2	-1	-1	4	2	-1	1	-1	4
F	XRF	50	560	262	362	702	587	587	1 005	662	694	426	167	1 313
Ga	ICP-MS	0.2	29.2	12.9	19.4	20.2	22.5	22.5	20.8	19.9	21.9	21.1	24.1	21.3
Ge	ICP-MS	0.1	1.2	1.4	0.6	0.6	0.7	0.7	0.7	0.7	0.7	0.6	1	0.6
Hf	ICP-MS	0.1	6.6	2.8	10.1	2.7	3.1	3	4	3.9	3.9	3	2.3	2.9
Mo	ICP-MS	0.1	0.5	0.7	0.8	0.4	0.6	0.6	0.5	0.4	0.5	0.6	0.5	0.6
Nb	ICP-MS	0.1	9.6	3.7	14.1	1.7	6.1	6.1	3.7	3.2	2.3	2.6	2.1	2.3
Ni	XRF	2	15	21	-2	-2	-2	-2	4	-2	-2	-2	-2	6
Pb	ICP-MS	0.5	34.5	9.5	6.4	35.1	38.5	38.5	36.9	50.5	60.2	45	46.3	130.3
Rb	ICP-MS	0.1	85.4	9.4	134.1	69.8	95.1	95.1	86	113.5	109.8	56.4	133	57.2
Sb	ICP-MS	0.1	4.5	3.6	1.1	0.1	3	3	0.5	1.9	0.1	3.3	3	3.5
Sc	XRF	2	3	3	-2	-2	-2	-2	3	-2	2	3	-2	2
Sn	ICP-MS	0.5	2.2	1.4	3.6	0.9	2.1	2.1	1.3	1.3	1.2	2.9	0.8	1.3

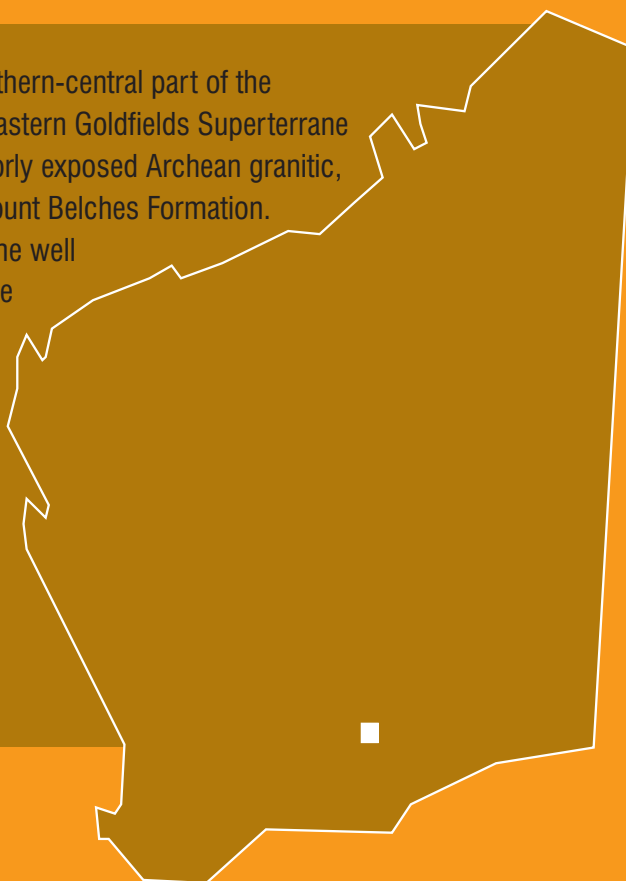
Sr	ICP-MS	0.1	2 341	295.3	26.9	904	863	608.1	867.3	1 011	891.4	1 082	160.4	1 361
Ta	ICP-MS	0.1	0.4	0.3	0.9	0.1	0.2	0.8	0.2	0.2	0.1	0.2	0.1	0.1
Th	ICP-MS	0.1	10.1	2.5	13.4	6	7	4.7	9.2	14	7	6.4	6.9	6
U	ICP-MS	0.1	1.68	0.81	3.66	2.09	2.37	2.36	7.12	3.18	1.46	2.23	1.66	0.95
V	XRF	5	70	23	-3	14	15	8	27	14	11	16	5	20
Y	ICP-MS	0.5	22.5	6.4	69.6	2.4	3.6	5.2	3.5	4.7	2.8	5.8	1.8	3.8
Zn	XRF	1	106	47	26	44	44	36	58	17	16	7	15	2 011
Zr	ICP-MS		260.8	104.6	362.8	96.8	114.4	90.7	138.3	116.1	140.1	102.7	39.6	99.3
La	ICP-MS	0.02	70.08	12.99	49.25	13.95	37.16	18.66	15.71	14.71	33.94	45.4	3.95	30.66
Ce	ICP-MS	0.1	170.8	25.91	95.16	42.7	65.65	40.76	65.28	37.22	82.94	77.88	7.69	65
Pr	ICP-MS	0.01	22.85	3.33	13.2	3.39	8.29	4.78	4.68	4.26	6.87	8.93	1.05	7.58
Nd	ICP-MS	0.01	87.94	12.56	52.86	12.56	28.66	18.05	18.16	17.42	23.42	30.85	4.12	29.06
Sm	ICP-MS	0.01	14.84	2.34	11	2.04	4.27	3.68	3.2	3.33	3.28	4.7	0.64	5.11
Eu (ppb)	ICP-MS	1	3 619	572	1 994	617	992	705	838	879	977	1 185	162	1 169
Gd	ICP-MS	0.01	8.25	1.71	9.94	1.02	1.78	2.59	1.56	1.96	1.48	2.35	0.42	2.56
Tb	ICP-MS	0.01	1.01	0.23	1.6	0.12	0.18	0.33	0.19	0.23	0.15	0.28	0.05	0.22
Dy	ICP-MS	0.01	5.05	1.12	10.17	0.51	0.65	1.32	0.82	0.99	0.65	1.34	0.23	0.93
Ho	ICP-MS	0.01	0.89	0.21	2.18	0.09	0.11	0.16	0.13	0.16	0.1	0.23	0.04	0.12
Er	ICP-MS	0.01	2.31	0.55	6.79	0.18	0.26	0.32	0.33	0.39	0.26	0.56	0.12	0.29
Yb	ICP-MS	0.01	1.91	0.55	6.86	0.18	0.23	0.19	0.29	0.36	0.24	0.49	0.13	0.22
Lu	ICP-MS	0.01	0.27	0.07	1.02	0.03	0.03	0.02	0.04	0.05	0.03	0.07	0.02	0.03

The YARDINA 1:100 000 map sheet covers the southern-central part of the WIDGIEMOOLTHA 1:250 000 sheet in the southern Eastern Goldfields Superterrane of the Yilgarn Craton. YARDINA is dominated by poorly exposed Archean granitic, and metasedimentary rocks, which include the Mount Belches Formation.

The Widgiemooltha Dyke Suite is represented by the well exposed Binneringie Dyke and to a lesser extent the

Jimberlana Dyke. Siliciclastic rocks of the Proterozoic Woodline Formation and flat-lying rocks of the Cenozoic Eundynie Group unconformably overlie the Archean basement.

Details are provided on the structural and metamorphic history, including deformation attributed to the Mesoproterozoic Albany–Fraser Orogeny. These notes also contain descriptions of mineralization and the Cenozoic regolith cover.

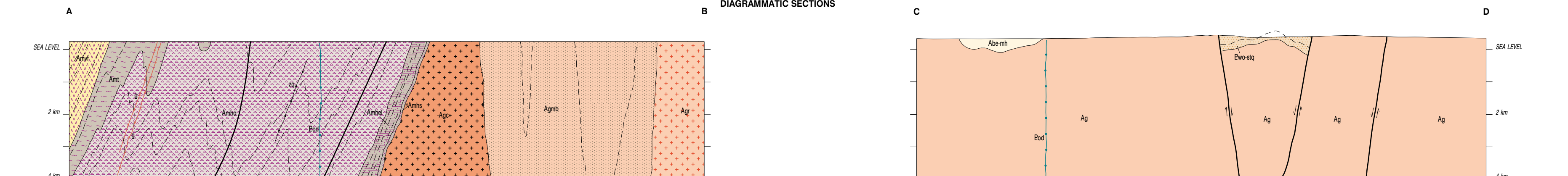
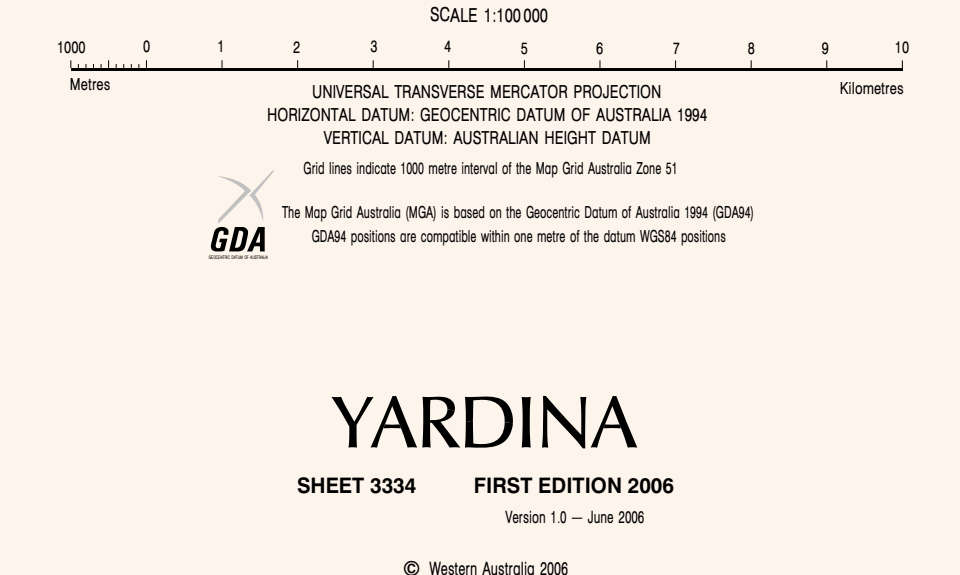
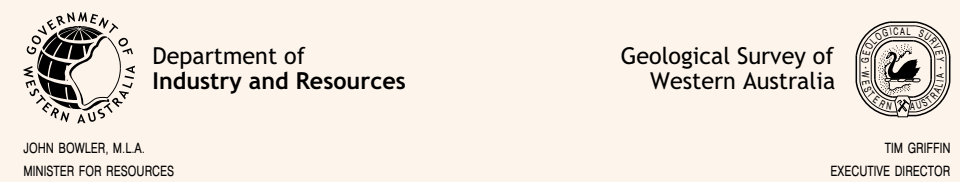
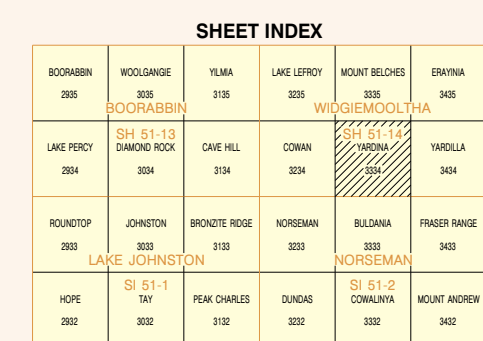
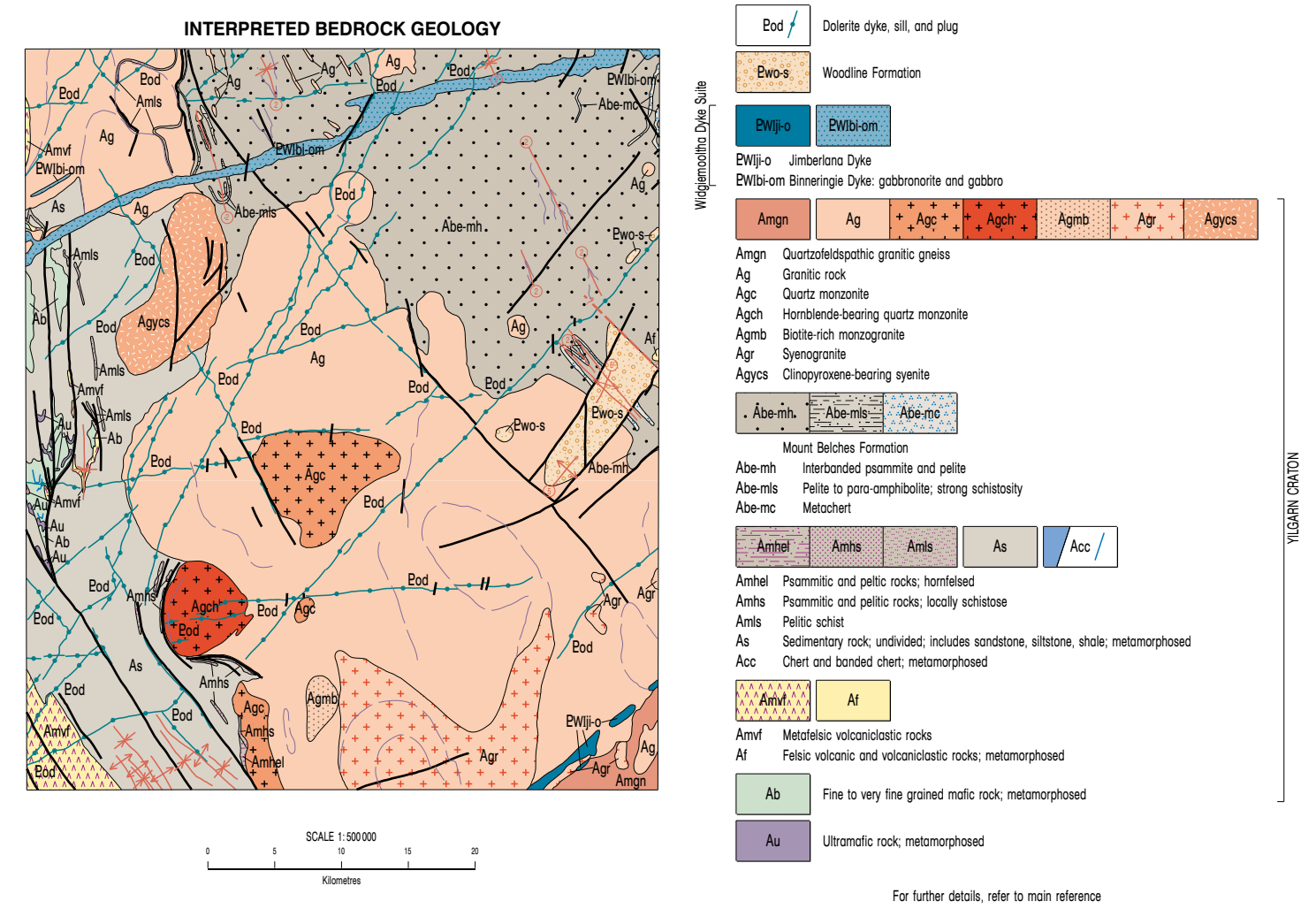
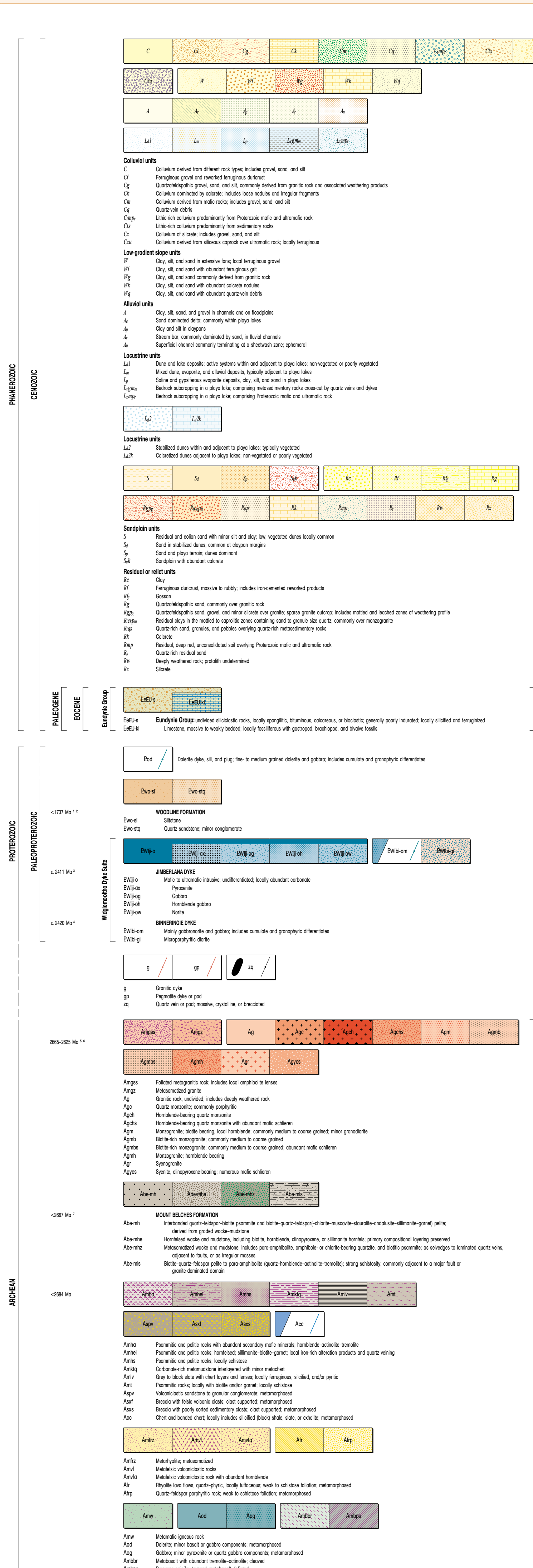


These Explanatory Notes are published in digital format (PDF) and are available online at: www.doir.wa.gov.au/GSWA/publications. Laser-printed copies can be ordered from the Information Centre for the cost of printing and binding.

Further details of geological publications and maps produced by the Geological Survey of Western Australia are available from:

**Information Centre
Department of Industry and Resources
100 Plain Street
East Perth, WA 6004
Phone: (08) 9222 3459 Fax: (08) 9222 3444**

[Www.doir.wa.gov.au/GSWA/publications](http://www.doir.wa.gov.au/GSWA/publications)



DATA DIRECTORY			
Theme	Date Source	Date Currency	Agency
Geology	GSRA	2005	Dept of Industry and Resources
Structural data	IMARCO	AUG 2005	Dept of Industry and Resources
Mineral occurrences (non-conflictual)	MINERDEX *	DEC 2005	Dept of Industry and Resources
	WAMIN	DEC 2005	Dept of Industry and Resources
Horizontal control	GSMAA	2002	Dept of Land Information
Topographic nomenclature	GEONAMA	2002	Dept of Land Information
Topography	DLI and GSMA field survey	2006	Dept of Land Information

Geoscience by C. E. Hall, S. A. Jones, and B. Goscombe 2005
Geoscience by:
(1) C. E. Hall, and S. A. Jones, 2005, *Western Australian Geological Survey Record*, 2005, p. 14-19
(2) A. Tuck, 1968, *Australian National University*, PhD thesis (unpublished)
(3) I. R. Fletcher et al., 1987, *Australian Journal of Earth Sciences*, v. 1, p. 523-556
(4) A. A. Nemchin and R. T. Pidgeon, 1998, *Australian Journal of Earth Sciences*, v. 45, p. 672-675
(5) R. Kozopchuk et al., 2000, *Tectonophysics*, v. 322, p. 89-133

Interpreted Geoscience by
(6) K. F. Cassidy and D. C. Chapman, 2002, *MEFRA Report No. 222*, p. 31-45
(7) I. R. Fletcher and N. J. McKnighton, 2002, *MEFRA Report No. 222*, p. 81-158

OSIRIS geological data are available online at www.darwin.gov.au/geoscience/index.cfm